5-2012

Evaluation of a Bisphosphonate Enriched Ultra-High Molecular Weight Polyethylene for Enhanced Total Joint Replacement Bearing Surface Functionality

Cassandra Wright-walker
Clemson University, cassanw@g.clemson.edu

EVALUATION OF A BISPHOSPHONATE ENRICHED ULTRA-HIGH
MOLECULAR WEIGHT POLYETHYLENE FOR ENHANCED TOTAL JOINT
REPLACEMENT BEARING SURFACE FUNCTIONALITY

―――――――――――――――――――――――――

A Dissertation
Presented to
the Graduate School of
Clemson University

―――――――――――――――――――――――――

In Partial Fulfillment
of the Requirements for the Degree
Doctor of Philosophy
Bioengineering

―――――――――――――――――――――――――

by
Cassandra Jane Wright-Walker
May 2012

―――――――――――――――――――――――――

Accepted by:
Dr. Martine LaBerge, Committee Chair
Dr. John DesJardins, Co-Committee Chair
Dr. Frank Alexis
Dr. Dan Simionescu
Dr. Ken Webb

ABSTRACT

Each year in the United States there is an increasing trend of patients receiving total joint replacement (TJR) procedures. Approximately a half million total knee replacements (TKRs) are performed annually in the United States with increasing prevalence attributed to baby-boomers, obesity, older, and younger patients. This trend is also seen for total hip replacements (THRs) as well. The use of ultra high molecular weight polyethylene (UHMWPE) inserts in TJRs results in wear particle-induced osteolysis, which is the predominant cause for prosthesis failure and revision surgery. Sub-micron size particle generation is inevitable despite the numerous efforts in improving this bearing material. Work by others has shown that the use of oral and intravenous systemic bisphosphonates (BP) can significantly minimize periprosthetic osteolysis. However, the systemic delivery and the high solubility of BPs results in a predominant portion of the drug being excreted via the kidney without reaching its target, bone.

This doctoral research project is focused on the development and evaluation of a novel method to administer BPs locally using the inherent wear of UHMWPE for possible use as an anti-osteolysis treatment. For new materials to be considered, they must be mechanically and tribologically comparable to the current gold standard, UHMWPE. In order to evaluate this material, mechanical, drug elution and tribological experiments were performed to allow assessment of material properties. Tensile tests

showed comparable yield stress and pin-on-disk testing showed comparable wear to standard virgin UHMWPE. Further, drug elution tests have shown that BP was released from the enriched material both in static and dynamic conditions. Additionally, an aggressive 2 million cycle total knee simulator experiment has shown statistically similar wear results for the two materials. Overall, this research has provided the groundwork for further characterization and development of a new potential material for total joint replacements as an enhancement to standard UHMWPE. This material shows significant potential as an alternative bearing material to indirectly increase TJR longevity by addressing osteolysis related issues.

DEDICATION

I dedicate this work to my family without whose love and support this journey would not have been possible. Particularly, to my husband, Burl, who encouraged me and provided moral support daily. And also to my parents who have provided sage counsel and taught me the pursuit of academic excellence from childhood onwards.

ACKNOWLEDGMENTS

First I would like to thank my advisor and mentor, Dr. Martine LaBerge, for all of her guidance, continual encouragement, and support throughout my Master's and Dissertation. Your passion for bioengineering and dedication to academia has been an inspiration to me. Thank you for giving me the privilege of being your teaching assistant and allowing me the opportunity to teach.

Thank you to Dr. John DesJardins, my co-advisor, for the insights and help with so many of my experiments along the way.

Thank you to my other committee members (Dr. Frank Alexis, Dr. Dan Simionescu, and Dr. Ken Webb) for your comments and suggestions throughout my project. I am also grateful for Drs. Gulya Korneva, Frank Alexis, and Jeoung Soo Lee for sharing their expertise in HPLC.

A special thanks to Dr. Delphine Dean. You have been a wonderful mentor and friend during my time at Clemson. I have been so privileged with the many late afternoon discussions of research, teaching, and life in general.

I would also like to recognize the many graduate and undergraduate students, both the LaBerge and the DesJardins lab, over the last 5 years who have provided support and suggestions throughout this process. I am appreciative of the staff of the Bioengineering Department as well as Machining and Technical Services (MTS), who crafted/modified many items I used in my research.

TABLE OF CONTENTS

Table of Contents (Continued)

LIST OF TABLES

LIST OF FIGURES

List of Figures (Continued)

List of Figures (Continued)

List of Figures (Continued)

Figure   Page

— CHAPTER ONE —

INTRODUCTION

1.1 Clinical Significance

There are approximately a half million total knee replacements (TKRs) performed in the United States annually[1]. By 2030, the number of TKRs may increase to over 3.48million/year due to baby-boomers, obesity, older & younger patients[1]. The use of ultra high molecular weight polyethylene (UHMWPE) inserts in total joint replacements (TJR) results in wear particle-caused osteolysis, which is the predominant cause for prosthesis failure and revision surgery. Sub-micron size particle generation is inevitable despite the numerous efforts in improving this bearing material. Work by others has shown that the use of oral systemic bisphosphonates (BP) can significantly contribute to minimize periprosthetic osteolysis[2, 3]. However, the systemic delivery and the high solubility of BPs results in a predominant portion of the drug being excreted via the kidney without reaching its target, bone. The goal of this research is to develop a novel method to administer BPs locally using the inherent wear of UHMWPE. This research aims to evaluate key material and tribological properties of this novel material (See Figure 1.1). It was hypothesized that optimum concentration of BP would not significantly affect the material properties and tribological performance of UHMWPE, and that BP would be released from the surface and thin films of the enriched UHMWPE.

1.2 Project Hypothesis

It is hypothesized that an UHMWPE based bearing material can be developed allowing the direct elution of BP through wear debris generation. This project is aimed at evaluating the effect of enriching UHMWPE with bisphosphonates to locally deliver bisphosphonate for possible use as an anti-osteolysis treatment. If bisphosphonate can be released in a controlled manner locally without significantly affecting the mechanical and tribological properties of the UHMWPE, it has the potential to effectively delay or slow the progression of osteolysis due to wear particle release. Further, the percentage of bisphosphonate that reaches its target (bone) is likely to increase as it now has a decreased distance to reach exposed hydroxyapatite onto which it binds than if taken orally or intravenously. However, the mechanical properties of the enriched UHMWPE must be comparable to that of the currently used UHMWPE in order to be considered as a viable approach.

1.3 Summarized Project Aims

Aim 1: Engineer Enriched UHMWPE Constructs and Evaluate Mechanical and Tribological Properties

A novel UHMWPE-bisphosphonate blend (PE-BP) was developed to administer bisphosphonates locally using the inherent wear of ultra-high molecular weight polyethylene (UHMWPE), a normal process occurring in total knee replacements, to manage periprosthetic osteolysis. It is hypothesized that particles worn off from a bisphosphonate-enriched UHMWPE tibial insert will act as a local delivery system for bisphosphonate. We evaluated of the effect of bisphosphonate (BP) additives on the mechanical and tribological properties of UHMWPE using a hydrophilic tag of similar molecular weight as BP and BP. The tag was initially used to assess properties via tensile testing and pin-on-disk test.

Aim 2: In vitro & Functional Drug Elution Testing

In order to further validate this material, assessment of the elution rate of BP from bisphosphonate-enriched UHMWPE, both in bulk as well as thin film forms, was performed in static conditions. Functional Drug Elution testing involving the assessment of the tribological properties as well as elution rate of BP from BP-enriched UHMWPE was completed to assess short term wear rates using a pin-on-disc. The experiment of BP-enriched UHMWPE was aimed at confirming the initial tag-enriched UHMWPE pin-on-disk studies by indicating the viability of this material for short term use. Further, this

experiment expanded the initial static elution to include the dynamic conditions of a pin-on-disk test in which BP was released both from the surface as well as from the pin tips as the pins were worn.

Aim 3: Knee Simulator Experiment

The expansion of previous wear testing protocols to allow assessment of the tribological properties over a longer term in order to assess potential clinical relevance was completed. This study used a Stanmore knee simulator to assess wear rates using a 2-million cycles, which is approximately 2 years *in vivo* in an older patient.

```
                    ┌─────────────────────────┐
                    │   Bisphosphonate-       │
                    │   Enriched UHMWPE       │
                    │      (PE-BP)            │
                    └─────────────────────────┘

┌──────────────────────┐              ┌──────────────────────┐
│  Aim 1:  Material    │              │   Aim 2: Drug        │
│     Properties       │              │   Elution (HPLC)     │
└──────────────────────┘              └──────────────────────┘
```

Bisphosphonate-Enriched UHMWPE (PE-BP)

Aim 1: Material Properties

Tensile Testing (Instron) →
▷Modulus of elasticity (E)
▷Strength
▷Elongation at break
▷Toughness

MAX-Shear Study

OrthoPod Study →
▷UHMWPE
▷ PE-BP

Aim 2: Drug Elution (HPLC)

Drug Elution from bulk PE-BP

Drug Elution from thin film PE-BP

Aim 2: Functional OrthoPod Study

Aim 3: Knee Simulator Study

Figure 1.1: Flowchart of experiments

1.4 Literature Review

1.4.1 Total Knee Replacements

History

Each year in the United States there is an increasing trend of patients receiving total joint replacement (TJR) procedures. As reported by the National Center for Health Statistics in 2004, total hip replacements (THRs) have risen to 234,000 per year and total knee replacements (TKRs) have risen to 478,000[4]. This is in part due to revision surgeries, but also due to patients receiving TJRs at younger ages. Additionally, surgeons have begun allowing patients in their 80s and later, even with co-morbid conditions, to receive TJR implants in order to increase quality of life, thus also increasing the total number of implants[5]. As arthroplasty age decreases, there is an increasing interest in longevity of the implant life to reduce the number of potential revisions a patient must undergo.

The first modern total knee replacements, excluding the Gluck's hinge arthroplasty of ivory created in the late 1800s, was the Walldius hinge in 1958 made of cobalt-chrome alloy. The first condylar total knee replacements were introduced by Gunston in 1971 as a cobalt chrome condyles articulating against a UHMWPE tibial insert, without metal backing[6]. This design is similar to those which are used today. The first TKRs were cemented in place using polymethylmethacrylate (PMMA). PMMA is a PMMA pre-polymerized polymer bead powder that is combined with the liquid monomer of methyl methacrylate that was then injected into the surgical site once it has achieved the proper paste consistency. The polymer completes polymerization *in situ* between the

implant and the prepared bone site creating a stable support for the implant. Advances in design to yield better patient outcomes and kinematics that more closely paralleled the natural knee started from the hinge designs and are still evolving today.

Advances in the 1970s included metal backing for the polyethylene tibial tray as well as the use of non-cemented components. Un-cemented implants allowed removal of less bone, however, many early non-cemented TKRs (up to 1/3) did not have bone ingrowth into the surface leading to revision[7]. The key for bone ingrowth is lack of micromotion between the prosthesis and the bone that is found via precise surgical skill and patient compliance to allow ingrowth. Significant research has been completed with different textures for porous ingrowth including sintered beads and fibers, meshes, and hydroxyapatite coatings. Outcomes have been variable with non-cemented knee implants, however, they have been successful in younger patients with better quality bone stock. In the 1980s advances included design of revision prostheses including longer stems, both with and without cement.

After development of the total knee replacement, unicompartmental knee replacements (UKR) were also developed using the same materials and design of the total knee at that time, however, only replacing either the medial or lateral section of the knee. In 1972, the Sledge prosthesis developed in Germany is one of the earliest reported UKRs with a CoCr femoral component bearing on a non-metal backed UHMWPE tibial tray. These were designed as a treatment for unilateral osteoarthritis or trauma to only the medial or lateral condyle/meniscus as an alternative to TKRs. UKRs are most often implanted on the medial side, though they may be used for the lateral compartment as

well. The disadvantage of UKRs is that they require surgical skill for alignment and thus are not used by all orthopaedic surgeons.

Total knee replacements, the focus of this research, are composed of four components: femoral component, tibial component, tibial insert, and patellar button (see Figure 1.2; patellar button not shown).
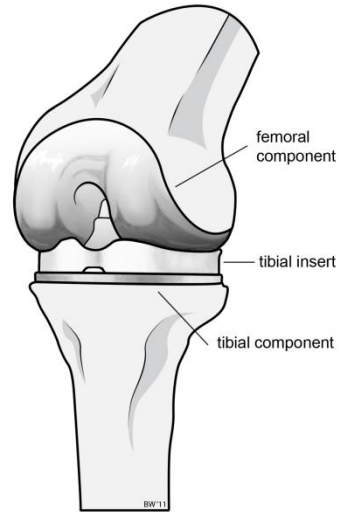
Figure 1.2: TKR components

The femoral and tibial components are made of CoCrMo alloy due to its biocompatibility. These two components are either press-fit or cemented over the associated bone (femur or tibia) once it has been surgically prepared. CoCrMo is an excellent metal for these components as the chromium adds wear resistance as well as allows for a passivating oxidation layer of chromium oxide to form on the surface. Further, the cast CoCrMo (ASTM F75) allows fabrication of a porous surface for bone ingrowth, which is necessary in non-cemented components; porous coating of the CoCrMo results in decreased overall strength of approximately 200MPa, which is significantly lower than the non-porous version of it[6]. The tibial insert is made of ultra high molecular weight polyethylene (UHMWPE), which serves as the sacrificial bearing surface for the joint. UHMWPE has been used for TJR bearing surfaces since the 1950s after polytetrafluroethylene's (PTFE) rapid failure as a sacrificial bearing surface. UHMWPE is either extruded and then machined into its final form or direct molded using

8

compression molding. Historically, sterilization was completed using gamma

sterilization in air but due to oxidative degradation this method was altered. Currently,

gamma sterilization is completed in an inert (low oxygen) environment. However, in

experimentation with UHMWPE and gamma sterilization, it was found that the gamma

radiation, which caused chain scission and crosslinking, could have a beneficial effect

with respect to wear by using high doses (100Mrad) of the radiation to increase cross-

linking; this increased wear resistance while decreasing the occurrence of pitting and

delamination[6,8,9]. More details on the use of high radiation doses to increase crosslinking

are provided in Section 1.4.4 (Effect of Gamma Sterilization on UHMWPE Wear). The

last component is optional, the patellar button. Many surgeons opt to keep the patient's

patella but sometimes it is necessary to replace it. It is a UHMWPE or metal-backed

UHMWPE button that is placed against the surgically refinished patella. Even with

advances in design as well as in material science and engineering, primary TKRs will fail

and need to be revised in approximately 10-20 years.

Failure

There are many factors that influence failure rate of a primary knee replacement.

Age as well as disease/condition causing the joint replacement both significantly

influence the service life of an implant (revision is considered the endpoint in this

review). As people age, they tend towards lower activity levels. This results in

decreased wear on artificial joints and typically longer implant service life. A

retrospective study of 11,606 primary knee replacements at Mayo Clinic showed that

survivorship at 10 years decreases with patient age at implantation[10]). Overall implant survivor rate over the 20 year time frame from the same study showed decreases as expected at 5, 10, 15, and 20 years. A more recent study at Mayo Clinic reported a survival rate of 95.9% of the living participants at 15 years (n=331 knees)[11]. Rand et al also separated the patients by gender and showed that women have a significantly higher implant survivorship at 10 years than men (93% vs. 88%)[10]. Rand and colleagues also divided the cause of primary arthroplasty by disease or condition which resulted in significantly higher survivorship of rheumatoid arthritis patients (95%) at 10 years compared to other diagnoses: osteoarthritis (90%), post-traumatic arthritis (86%), osteonecrosis (84%), and other diagnosis (76%). The authors suggested that patients with rheumatoid arthritis would have decreased physical activity compared to osteoarthritis patients.

Implant design also affects the implant service life. It was found that posterior stabilized designs had a significantly higher revision rate than posterior cruciate-retaining designs where at 10 years after surgery survivorship was 76% (n=2994) and 91% (n=8052) respectively[10]. Mahoney and Kinsey reported much higher survival rate of 95.8% of posterior stabilized implants at 5-9.5 years implantation among 1030 patients, however, this implantation time was shorter and implant failure increases with time[12]. Other TKR studies have also shown higher survival rates at 10 to 13 years (92% at 10 years, n=60[13]; 93% at 13 years, n=76[14]. The other studies had smaller group sizes, however, the lower survivalship may be due to early implant design, such as

impingement of the UHMWPE leading to additional wear and resulting in early failure as the Rand study contains cases starting in 1978.

A statistically increased survivalship of cemented knees (92%, n=11,166) was shown compared with uncemented (61%, n=259) and hybrid (84%, n=172)[10] at 10 years; the sample size however was small for those with cementless or hybrid fixation. Further, the survival rate of press-fit prostheses varies by study (81.5% at 15 years for n=15)[15]. Press-fit prostheses require healthy bone stock and are typically implanted in younger thus typically more active patients which may explain the decrease in survivorship. Further, significant surgical skill is required for the precise cuts used in cementless fixation and low frequency of implantation may also explain lower survivorship. Hybrid fixation has been shown to be 64% at 15 years (n=65)[16], much lower than overall 84% reported by Rand et al.

Other non-design related causes of failure include infection, stress-shielding, peri-prosthetic osteonecrosis or fracture, implant instability, polyethylene wear-through or fracture and allergy or hypersensitivity to one of the implant components[6]. Hypersensitivity to metal ions was found to increase after patients received implants as well as to be 4 times more likely in patients with previous metal hypersensitivities[17]. Infection results in 1-2% of all total knee failures[15, 18].

The most common cause of failure of an implant is implant loosening resultant of wear and osteolysis[6]. Failure rates vary drastically due to design, cemented, hybrid, or non-cemented, implantation time, as well as many other factors.

1.4.2 Wear

As previously stated, one of the most significant problems that leads to implant loosening andclinical failure is wear. This is true for all total joint replacements (TJRs), not just TKRs. Wear has been a known problem for several decades. Wear-induced osteolysis was first identified in the mid 1970s by Charnley (1975)[19] and Harris et al (1976)[20]. Harris et al reported large numbers of macrophages and cavities defining osteolysis in the proximal femur of a THR; additionally, PMMA particles were found in the retrieved tissue. Their findings were strengthened by a study by Willert and Semlitsch the following year that included samples from 123 failed implants. It also showed dense populations of macrophages and giant cells along with three particle types: polyethylene, metal, and PMMA[21]. In the 1970s, PMMA was thought to be the trigger for osteolysis as it was found in the osteolytic cavities and more readily visible than polyethylene (polyethylene is only visible using polarized light due to its birefringent properties), however with the invention of cementless implants and the continuation of the wear-induced osteolysis implant failures, the focus turned to polyethylene by the 1980s.

Howie et al (1988)[22] studied the effects of intraarticular injections of PE into rat knees in the presence of an acrylic bone plug showing resorption in the direct vicinity of the implant. Further they showed that the particles induced changes in the tissue surrounding the implant as well as the synovial membrane via an infiltration of macrophages, foreign body giant cells, fibrous tissue around the implant, and thickening of the synovial membrane. Their control group contained only an acrylic bone plug and

was sacrificed at 2 weeks instead of 8 weeks; but, it showed formation of new bone directly adjacent to the acrylic implant, suggesting that it is indeed the PE particles inducing negative changes in the tissue. Some researchers, notably Stuart B. Goodman and his collaborators, continued to study both PMMA and polyethylene debris as causes of osteolysis. Both PMMA and polyethylene debris induced osteolysis as well as infiltration of giant cells (not statistically different between the two groups) in a rabbit model; UHMWPE, however, resulted in increased thickening of the synovial membrane as well as higher numbers of histocytes and fibrocytes than PMMA indicating a more severe long term response to the particles. The PMMA samples showed more marrow cells indicating bone was attempting to refill the area[23].

Wear-induced osteolysis occurs due to a cascade of events that even after thirty years after its discovery is not yet fully understood. When a total joint replacement is implanted, the natural synovial membrane is destroyed due to the resurfacing of the joint. However, it has been shown that a pseudosynovial membrane is formed in its place that holds lubrication within the joint. Pizzoferrato et al[24] have suggested that this fibrous variable organized membrane formed is simply a part of the wound healing response of the body. It has also been indicated that it may take up to two years post-operation for this pseudo-capsule to completely form[25]. The natural synovial membrane is paper thin and filled with synoviocytes, while the pseudosynovial membrane resembles its thinness and lack of blood vessels[26]. This, however, changes with time as wear particles are released from the joint; many of them are trapped within the pseudosynovial membrane, as it forms a watertight boundary around the joint in order to hold in the lubricating fluid.

These foreign particles then evoke the body's natural response, which is to remove all foreign material from the body. UHMWPE, unlike bacteria, viruses, and small cellular parts, cannot be broken down by the macrophages, which are the first phagocytic cells to arrive at the site of foreign particles. Small particles will be ingested by the macrophages; however, due to their inability to break down the polyethylene cytokines are released (see Figure 1.3). Additionally, larger particles that the individual macrophages cannot break down on their own result in cytokine release causing the formation of multi-nucleated giant cells, which are simply multiple macrophages that have fused together in an effort to ingest larger debris. In general, particles less than 1 micron tend to be correlated with macrophages while giant cells form when particles exceed 10 microns[27]. Further, it has been shown that these macrophages and multi-nucleated giant cells are found within the pseudosynovial
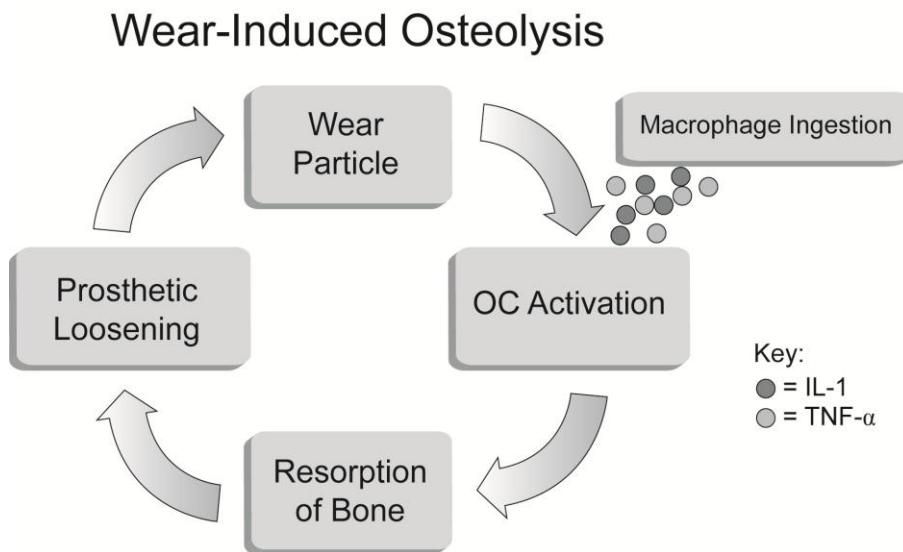

Figure 1.3: Simplified wear particle-induced osteolysis

membrane and change the histology of it drastically during the time period between implantation and explantation; the synovial membrane becomes thickened, and perfused with vascularization. This influx of inflammatory response cells releases a number of cytokines, which is upregulates osteoclast activation and thus bone resorption and prosthetic loosening (see Figure 1.3). Macrophage activation has been specifically associated with release of a number of cytokines: TNF-α [28], IL-1β[29], IL-6[30], IL-8[30], IL-11[31], and TGF-β[32].

Chiba et al showed that of these macrophage-released cytokines, there were three that were found in stronger concentrations in failed cementless THRs (cementless prostheses were used to eliminate potential macrophage activation in response to PMMA). Both THRs with and without osteolysis were tested so that a normal level in a failed joint replacement could be used as the control. They indicated that TNF-α, IL-1, and IL-6 were present in elevated amounts. All three of these cytokines (see Figure 1.4) are activators of osteoclasts thus increasing bone resorption in the area local to the macrophages. IL-1 and IL-6 are also activators of osteoblasts, however, it takes significantly more time to form bone than it does to resorb it (100 days vs. 20 days).

Adapted from Marcus et al[161]
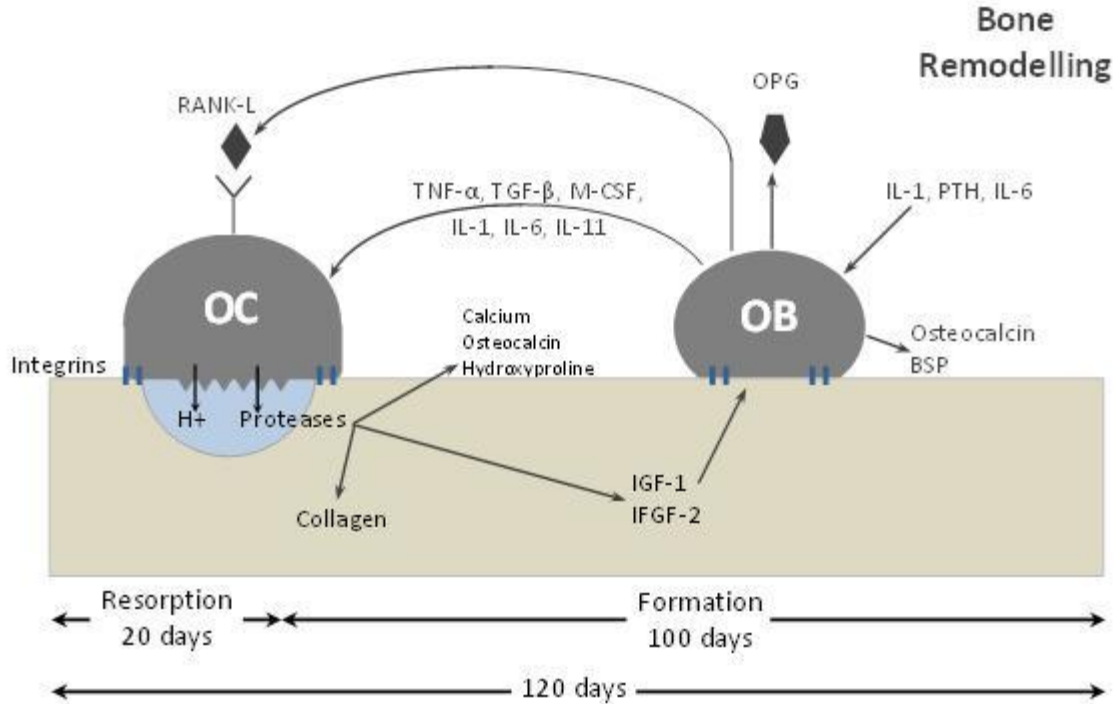
Figure 1.4: Bone Remodelling depicting cytokines that function as stimulators and inhibitors of both osteoblastic and osteoclastic activity as well as OB-OC relationship

Wear Mechanisms

In general there are three main wear modes observed in TJRs: abrasive wear, adhesive wear, and fatigue wear. Adhesion occurs when two parts bond under the exposed load; a portion of the material, one or both surfaces, is removed as relative motion between the two components occurs. Abrasion, on the other hand, is primarily due to asperities on the surface of one of the materials. These asperities scrape against the softer surface ultimately leading to scratches (thus material removal) in the material's surface[33]. Fatigue occurs when a materials is repetitively loaded. The material fails under loads that may be significantly lower than the ultimate tensile strength or even the yield strength of the material, due to the additive nature of the repetitive loading. Fatigue

failure begins with an initiation site, often a crack or crevice in the material that can also be termed a local stress concentration. This crack then begins to grow due to the repetitive loading, which ultimately leads to failure of the material. Predictions of how the material will perform can be estimated from the S-N curve (a graphical representation of stress with respect to number of cycles where a material will fatigue if the stress for a given number of cycles lies above the curve). Delamination wear is observed in tibial trays of total knee replacements. Often, though, wear is not one distinct wear mode, but a combination of one or more of the three types. So prediction of how a material will fail is most accurate retrospectively, though, educated analyses may provide similar predictions to what occurs in actuality.

Ultimately, thus, the goal is to reduce wear such that the service life of the implant may be lengthened. This, however, is highly complex as it deals with the interplay of a variety of variables including wear resistance, loading conditions, lubrication, surface roughness, design of the implant (conformity), surgical technique, etc. Furthermore, all of these variables will vary during the life of the implant based on accumulated wear to each surface.

Wear Resistance

Wear resistance includes the specific resin used to make the polyethylene. All polyethylenes are created from monomers through Ziegler-Natta catalyst reactions. But, the molecular weight, chain entanglement, and crystallinity may vary among different polyethylene types. Additionally, the manufacturing process may affect how the

polyethylene performs as the heat and pressure applied during different phases of compression molding have significant effects on a variety of mechanical properties, including stiffness, modulus and crystallinity[34].

Additionally, wear resistance may be affected by the sterilization method used; for example, gamma sterilization induces some cross-linking as well as free radicals within the material which affects the longterm wear properties. The effects of gamma sterilization are further addressed in a later section.

Loading Pattern and Contact Stress

In addition to polymer properties, wear varies due to the loads that a TJR experiences, which will vary based on the activity level and weight of the patient. However, research has shown the knee experiences loads up to approximately 2-4 times body weight during normal walking gait[35]. This load varies as a function of activities of daily living. Load data has been gathered in two ways: telemetry and modeling. Telemetry results have been more consistent in the hip than in the knee[35]. Telemetry, however, uses direct measurements taken via strain gauges or other pressure and load-sensitive devices that are then transmitted out of the joint. Measurements taken via telemetry have been variable between different groups which is largely due to small sample sizes (usually n=1 or 2) as the equipment is very expensive. Additionally, placing and securing the device require significant skill for the knee as well as any problem occurring while the device is implanted may result in total loss of data. Recently, though, there has been more telemetry research with cadavers as they are readily available and

easy to manipulate. Burny et al used a method in 2000 that consisted solely of strain gauges forming a Wheatstone bridge[36]. This was a test done *ex vivo*. With the percutaneous leads associated with this device, it will make it extremely challenging to gather longterm data as it must by definition cross the skin barrier thus risking potential infection and/or displacement of the device as the body attempts to close the wound.

The other option to using direct measurements is via modeling. Modeling requires assumptions to be made in the representation of the muscles, ligaments, and bones. Further, it requires significant skill as the human leg consists of 47 muscles and irregularly shaped joint surfaces. To deal with the complications of the knee joint, it is often approximated using six forces and torques representing the three rigid bodies of the knee (tibia, femur, and patella). Due to the complication of the system with numerous muscles and ligaments as well as the three rigid bodies, the system is an indeterminate one as there are not enough independent kinematics equations to define all of the movement at the knee; only 30 independent equations can be defined[37]. With an indeterminate system, it cannot be mathematically modeled without assumptions being made. Two techniques are currently used for it: reduction and optimization. Reduction as the name suggests reduces the number of muscles so that the number of equations of motion can equal the number of unknowns. This technique has been used since the 70s (See Table 1.1).

Table 1.1: Sample of results from different techniques to approximate the loads occurring at the knee joint.

Authors (Year)	Method Used	Activity	Load in terms of body weight (BW)
Morrison JB (1970)	Modeling (Reduction)	Walking	2.1 - 4.0 BW
Komistek RD et al (1998)	Modeling (Reduction)	Walking	1.7 - 2.3 BW
Wimmer MA & Andriacchi TP (1997)	Modeling (Reduction)	Walking	3.3 BW
Seireg et al. (1973)	Modeling (Optimization)	Walking	7.2 BW
Taylor SJG et al (1998)	Telemetry	Walking Stair Ascent Stair Descent One Leg Standing	2.2 - 2.5 BW 2.3 - 2.5 BW 2.6 - 2.8 BW 2.5 BW
Taylor SJG et Walker PS (2001)	Telemetry	Walking Stair Ascent Stair Descent Jogging	2.8 BW 2.8 BW 3.1 BW 3.6 BW
References: [37-42]			

The other modeling method, optimization, uses optimizing techniques to solve the motion equations. It has been employed since the early 70s as well. Optimization, however, yields higher resultant forces than reduction modeling or telemetry and has been questioned as to its validity, specifically whether the results may be legitimate mathematically however erroneous physiologically. Early results using optimization predicted load at the knee to be 7.1 times BW[40, 43]. As processing capabilities have increased with computers, the models as well have become more detailed and advanced thus allowing better potential for modeling the system. Additionally, electromyography data is being compared to the associated muscles to tweak and validate the newer models.

Recent models have focused on metabolic energy used to control the muscles or forces within the ligaments instead of load on the joint in terms of multiple body weights[44]. All of the work currently published in optimization modeling of the knee joint stems from the Pandy lab, including the work in Vail, CO which are former students from the Pandy lab. Reduction seems to be the more popular modeling method currently as well as the results of those studies more closely match the limited telemetry data.

The mechanical properties of UHMWPE have been widely reported and the approximate compressive yield stress is 23MPa, where a 0.2% plastic strain is used to define the offset yield stress. Given the increased loading resultant of stair climbing, jumping, running, or any activity beyond walking, exceeding the maximum yield stress becomes a concern[45]. If the tibial insert plastically deforms, this will alter the contact stresses at the interface as the joint will no longer be functioning the capacity that it which it was manufactured to perform. Past research has shown that thin tibial inserts will increase contact stress and thus wear rate resulting in failure[46]. This would make sense as increased contact and pressure will cause an increase in contact area and thus particle generation (aka wear). Additionally, the insert may flex if it is too thin thus changing the tension and compression within the molecular chains of the PE insert potentially resulting in fatigue of the material, which would generate fatigue cracking and thus delamination.

The exact kinematics of the knee joint has been difficult to elucidate. However, it is generally accepted that the loading pattern for a TKR is markedly different than that of a THR as the joints are very differently shaped. TKRs use a predominantly linear

motion, while THRs have multi-rotational movement. Kinematic studies have been

conducted using both subjects and TJRs labeled with reflective markers walking on force

plates recorded via motion analysis cameras. The kinematics of the TKRs however do

not mimic the natural knee exactly as TJRs are designed to balance range of motion with

low wear rates. Both cannot be simultaneously achieved because as conformity in a TKR

is increased, wear decreases[47]. On the contrary, however, increased conformity decreases

the patient's range of motion. Thus, a balance of the two qualities is reached for each

different TKR design allowing surgeons to select which of the two characteristics is more

important for a given patient based on their age, activity level, and desired outcome of the

surgery.

Additionally, a variety of motion patterns have been used in pin-on-disk wear

testing of orthopaedic components from a simple reciprocating motion to U-shaped

patterns to a variety of multi-axial motions. The simple reciprocating pattern has been

shown to produce inaccurate wear results in comparison with retrieved implant analysis.

Thus, it is not often used at present. Pin-on-disk testing predominately uses multi-

directional testing since motion of the joints is not completely limited to one-axis, even in

a TKR. The use of different testing protocols makes comparing results from pin-on-disk

tests challenging, however, many of the early tests may be overlooked as their testing

methodology (simple reciprocating motion) has been shown to be flawed in later tests

comparing their results to retrieval studies. Furthermore, pin-on-disk tests vary in length,

however one million cycles is the industry standard for the number of cycles an implant

will undergo in one year. Overall, while pin-on-disk testing may not accurately reflect

the kinematics of a TKR or THR, it provides a screening alternative for material

characterization prior to the use of more relevant knee or hip simulators, which many

laboratories cannot afford. Additionally, pin-on-disk systems provide a test to predict

wear results more quickly. Comparative information with respect to how various

polyethylenes (different sterilization methods or composites versus standard UHMWPE)

can be gathered from running the same size specimen under the same testing protocol for

an identical length of time in pin-on-disk tests; these results may be extrapolated as to

how the material may perform during longer tests, though, it is not completely accurate.

Cornwall et al tested a variety of three kinematic conditions for pin-on-disk testing

(sliding, rolling, gliding) in conjunction with variations in load and contact stress to

determine resultant wear factors. From this testing, it was shown that gliding under a

load of 190N and 3MPa contact stress resulted in the highest wear factor

$(k=24.0x10^6)$[48, 49].

For more information, McGloughlin and Kavanagh have provided a detailed

review of the wear studies conducted through 2000[49].

Surface Roughness and Lubrication

Wear resultant of the kinematic conditions and associated wear factors will also

vary based on surface roughness and lubrication. Initially, the surfaces of all components

in a TJR are polished prior to packaging. But, even polished CoCrMo will still present

asperities that will grind against the softer UHMWPE. Studies have shown that wear rate

increases with increased roughness of the CoCr alloy counterpart[50]. The change in

23

surface roughness, even when relatively small, can have a pronounced effect on the overall wear rate of the UHMWPE component. Cooper et al indicated that as roughness of the metal surface increases 300%, it will result in a significant increase (approximately 10x) in the UHMWPE particles generated[51]. Tests with various initial average surface roughnesses (R_a) of the femoral component have also been completed in bovine serum[51, 52]. These tests confirmed that as surface roughness increases, loss of polymer also increases drastically for rougher polished surfaces (R_a=2.0μm). On the contrary, smoother surfaces (R_a=0.06μm) were shown to have low initial wear followed by an increase. In addition to the wear testconditions (dry or wet), the type of lubrication has been shown to affect UHMWPE wear. In the early to mid-1990s, it was often considered that both the dry and wet-lubrication conditions were inadequate as many of the wear tests showed polymer film transferred onto the bearing surface that was not present in retrieval of failed specimens[52]. Kernick and Allen showed that as protein level (specifically the addition of synovial fluid) increased in saline in a wear test of zirconia on UHMWPE, the volume of wear decreased[53]. While TKRs are not constructed of zirconia, the same principle should still apply as far as lubrication against a bearing surface; however, the volume of wear will be higher with CoCrMo than the zirconia (or other ceramics) as CoCrMo has peak shaped asperities while zirconia has "valleys". At present, though, most research groups seem to use some form of protein-based lubrication, often bovine serum, for wear tests as it is readily available unlike synovial fluid which would be ideal as that is the environment the material will be ultimately tested in. Besong et al[54] also tested bovine serum in various dilution against distilled

water. It has been found that the distilled water condition alone yields polymer transfer thus harsher wear conditions. It was found that wear conditions were 14 times higher in distilled water (wear factor=2.73×10^{-6}) than 25% serum solution (wear factor=2.7×10^{-7}) as well as significantly larger stand-shaped particles formed in the distilled water condition[54].

Groups are continuously trying to search for alternative lubricant sources as the proteins in bovine serum are not stable during long-term wear tests. Ahlroos & Saikko[55] tested a variety of lecithin & soybean products as well as bovine serum and aspirate from a prosthetic joint that was undergoing revision, which contained some tissue shreds. The results of that study showed no transfer in the bovine serum (as expected) as well as none in the soy protein in salt solution. Additionally, both showed no visible debris in the supernatant, though, the authors did not use SEM so this result can be overlooked. The authors test of the prosthetic joint fluid showed the poorest results of all with heavy polyethylene transfer and large debris as well as grooves on the pin face such that the wear was as poor as that cause by distilled water lubrication tests; these results can be explained by the rapid wear and transfer causing surface roughening thus additional wear. Another group, though not as successful as the first, looked at gelatin in comparison with bovine serum[56]. Both were diluted to 25% in distilled water. Though the gelatin solution did not become contaminated with micro-organisms after 28 hours as the bovine serum did and maintained its stability, it did not produce physiologically sized particles and therefore is not relevant for use in joint simulators. Bovine serum, while having its shortcomings, does produce the most clinically relevant particle sizes, and therefore, it

has remained the industry standard. ISO Standard 14293-1.4[57] and 14293-3[58] (for force-controlled and displacement-controlled wear simulations respectively) specify 25±2% bovine serum in distilled water to be used as the lubricant. Further it says that the bovine serum should contain no less than 17g/l of protein and suggests adding sodium azide to reduce microbial contamination. The protocol, however, does not say how often the serum should be changed, which is interesting as the protein denatures rapidly during wear tests. The standards set by ISO are guidelines and thus a variety of concentrations are used by different research groups. Fisher's research group uses 25% bovine serum as a standard[54,56,59]. Joyce et al report using 30% bovine serum[60]. The highest mixture found is LaBerge's lab group at 50%[61-64]. Additionally, various concentrations of hyaluronic acid in bovine serum has been used in an attempt to closer replicate *in vivo* conditions[63,64]. DesJardins and collaborators showed a 7-fold increase in *in vitro* wear rate using the 50% bovine serum with 1.5g/L of hyaluronic acid as well as found pitting and delamination, both features of *in vivo* wear not previously seen in knee simulator experiments with bovine serum alone[64].

Third body wear also causes a dramatic increase in the wear rates. Third body wear may be a variety of materials in a TKR: metallic debris, PMMA, or bone. All of these materials have been found upon microscopic examination of failed components. As these debris migrate into the space between the bearing surfaces, they may transiently scratch the polished surface of the femoral component causing an increase in wear or may become imbedded into the polyethylene itself leading to increased damage to both the tibial tray as well as the femoral component. Wasielewski et al consider this to be the

leading cause of early implant failure[65]. Third body debris is a likely cause of early failure as it causes damage to one or both components leading to increased roughness and particle generation as well as the potential of pits gauged in the polyethylene. Joint replacements where significant third body wear is found may alter the contact mechanics and contact stress of the joint resulting in early failure.

1.4.3 Additives and Composites

As wear is one of the major limiting factors to the lifespan of a total joint replacement, many research groups have attempted a number of solutions to ameliorate the wear issue. Currently, though, none of these are clinically available.

Early UHMWPE Alternatives

In the 1950s and 60s, researchers were trying to find a viable bearing surface material. Charnley attempted polytetrafluoroethylene (PTFE) in 1957 to decrease friction between the surfaces, however, this was to fail due to high wear rate of the PTFE on the order of 835-2300mm^3/year. Silica-filled PTFE also failed due to high wear rates as the silica scratched the metal countersurface. In the 1960s polyethylene terephthalate (polyester) was introduced but clinically abandoned by the 1970s due to poor wear resistance and clinical outcomes[66]. High density polyethylene (HDPE) was used prior to the invention of UHMWPE for total joint replacement.

Carbon fiber-UHMWPE composite

Carbon fiber-polyethylene composites are the first group of polyethylene composites created for orthopaedic bearing surfaces. They were originally created in the early 1970s[67]. Initially, randomly oriented carbon fibers were used within the polyethylene matrix in an effort to yield better resistance to wear by increasing the modulus of elasticity and ultimate tensile strength[67] while decreasing creep in comparison to UHMWPE. It is understandable how increasing the mechanical properties to decrease wear and potential delamination would develop interest. Additionally, the carbon fibers had been shown to be relatively inert in the body. Early mechanical tests showed mixed results with respect to wear rates[67,68]. McKellop and collaborators showed results for carbon fiber composites that would be shown as similar to the latter *in vivo* testing. They found more wear in the carbon-fiber laden UHMWPE as well as abrasions to the femoral component bearing surface from carbon fibers exposed due to wear of the polyethylene[68]. Even with mixed *in vitro* results, Poly II[TM] was commercially released by Zimmer for total hip arthroplasties as well as total knee arthroplasties in the 1970s. Its success however was short lived as the *in vivo* testing did not prove as successful as any of the *in vitro* testing. In the mid-1980s analysis of the failed components began being published which indicated osteolysis as well as complete fracture of some of the implants. If McKellop's *in vitro* tests proved true *in vivo*, the protruding carbon fibers would have resulted in scratches on the surface of the femoral component thus increasing PE debris formation (see section on Roughness above for more information on mechanisms). Several of the implants had catastrophic failure and when revision surgery was

undergone, it was discovered that both the synovial tissue as well as periprosthetic tissue were laden with pyrolitic carbon debris, coloring the synovial tissue black[69-71]. Carbon, though harmless in its bulk form, will generate an inflammatory reaction in debris form as well as the debris may be carried into the lymph system, potentially leading to damage to it. Research was undertaken to understand why the material failed *in vivo*. It was shown that fatigue crack propagation was the primary cause of failure. The bond between the carbon fibers and the polyethylene was not as strong as between polyethylene and itself, which led to numerous sites where there was a mismatch of stress yielding stress concentrations. These stress concentrations became crack nucleation sites that combined with the material's low fatigue crack propagation resistance lead to the failure of the material *in vivo*. Due to the catastrophic failure as well as the carbon debris spreading from the implant, the use of carbon-fiber composites was abandoned by the mid-80s.

In the 1990s, however, with better control over machining, it has become possible to create nanotubes and nanofibers of carbon. One commercially available nanofiber that is often used is the Pyrograf III[TM] (Pygrograf Products, USA) which have outer diameters of 100-200nm with lengths of 30-100μm (aspect ratio: 150 to 1000). Over the last few years, several researchers are attempting to revive carbon-filled UHMWPE. Chowdhury et al tested two groups of nanocomposites: Kevlar fiber (10, 15, and 20 wt %) and carbon fibers (20 wt %). Their research showed that the carbon fibers had similar problems in wear to those tested in the 80s; the carbon fibers became exposed and the wear rate increased presumably due to the additional abrasive element of the carbon fibers. They,

however, are proposing that Kevlar fibers at 10 wt % maybe a viable biocompatible material as it performed better than the HDPE and UHMWPE in their pin-on-disk and hip simulator trials, though, they noted problems with increased wear in the UHMWPE in their trial presumably due to temperature errors during fabrication. While surface roughness and SEM were not looked at during the study, the 10 wt % Kevlar fibers showed increased modulus of elasticity and tensile strength in comparison to HDPE from tensile testing. Further wear testing showed wear volume similar to HDPE for both pin-on-disk and hip simulator testing under lubricated (carboxymethyl cellulose, 0.06 Pa-s) conditions with significantly lower hemolysis percentage than pure HDPE (2% compared to 7.5%)[72]. Chowdhury et al used the carboxymethyl cellulose instead of bovine serum as it had similar viscosity to synovial fluid, however, their tests showed some evidence of polymer transfer that would have been avoided with the bovine serum. It is for this reason that the wear tests may need to be repeated with the appropriate lubrication. Further the wear debris used for the hemolysis tests was not wear debris generated from the hip simulator but cut wear debris from the bulk; the test would have generated more reliable results had smaller more physiologically- sized particles been used for the test. These results show promise, however they are in their infancy stage and any *in vivo* testing (perhaps in a rabbit model with the Kevlar composite in one knee as the bearing surface (for *in vivo* particle generation) with the alternate knee serving as a control) will provide better information as to the usefulness of this proposed composite. Galetz et al has also worked with the carbon nanotube composite. This group reported increases in nanocomposite modulus and yield strength with a smooth surface while preserving a

similar ductility to extruded UHMWPE. Their pin on disk tests showed a reduced wear rate with 5 wt % of carbon nanofibers added while increased wear with 10 wt % under dry conditions. They attributed the increased wear rate to the non-homogenous distribution of the carbon within the PE matrix. Additionally, they reported no protruding carbon nanotubes and a relatively smooth surface even after the wear test[73]. Their wear studies however are non-indicative of *in vivo* wear as they were conducted under dry conditions instead of wet (preferably with bovine serum) as well as they were conducted at 25^0C instead of at 37^0C, where a change in mechanical properties has previously been shown between these two conditions. Additionally, there were agglomerates of the nanofibers within the matrix that may lead to stress concentrations within the material under longer more physiological wear testing resulting in failure of the material. Finally, no cell testing on the bulk or the nanofiber laden debris has been conducted. This needs to be undertaken before its viability as an enhanced polyethylene may be entertained; however, *in vivo* trials of the material are the ultimate deciding factor, as previously positive *in vitro* testing has led to poor *in vivo* results with carbon fiber containing UHMWPE.

While the publications concerning these new nanocomposites looks promising *in vitro*, the true test of *in vivo* compatibility remains. Further, while the initial carbon fibers are smaller this time, carbon particles will still be released with wear of the nanocomposite potentially causing systemic problems *in vivo*, if not simply a blackening of the synovial and periprosthetic tissue with high potential for an immune response even though bulk carbon is generally well tolerated by the body.

UHMWPE homocomposite

Another modification of UHMWPE included self-reinforced UHMWPE, also called

UHMWPE homocomposite. This is a composite that is made of UHMWPE in different

forms. This has been researched in an effort to create a composite with better interfacial

bonding strength along with better overall mechanical, wear, and fatigue properties as

carbon fiber reinforced UHMWPE had several shortcomings. Capiati and Porter were

the first to use this with polyethylene in 1975[74]; they were using high density

polyethylene, however, but the process is the same. It is a composite composed of

UHMWPE in fiber or fabric form along with the typical UHMWPE matrix that is

partially crystalline. The polyethylene fibers/fabrics are used to reinforce the matrix of

more amorphous polyethylene as fibers by definition are highly crystalline polymers.

The fibers or meshes of polyethylene are retained in the finished composite by

compression molding the mix at a temperature high enough to melt the amorphous

polyethylene, but low enough to retain the fibers as they typically have melting points 5-

9^0C above standard LDPE or UHMWPE. Increased tensile strength (24MPa for 40% by

volume fiber composition composite; approximately 3 times that of HDPE alone) was

found for the composite compared with simply the HDPE matrix as well as good

interfacial bonding leading to pullout strengths of 17MPa[76]. The tensile strength of the

composite was further enhanced by using irradiated HDPE fibers prior to compression

molding gaining tensile strengths approximately 9x higher than HDPE alone[77]. With the

advent of new fiber creation methods, namely gel/solution spinning, this opened the door

for a UHMWPE fiber-UHMWPE matrix composite. The gel/solution spun fibers had

higher crystallinity than their predecessors. Spectra fibers, UHMWPE solution spun

fibers, began being produced in the 1990s; there are currently three generations available:

Spectra 900 (the first generation), Spectra1000, and Spectra 2000 (US Patent 6,969,553 is

the most recent and 4,551,296 earliest).

Suh and Arinez' research group have continued research into the manufacture,

properties, and wear of this composite as a potential way to decrease overall wear and

specifically delamination in UHMWPE components[74,75]. They use Spectra 1000 fibers,

solution spun fibers of UHMWPE, for the fiber or fabric backbone of the composite with

particles of GUR415 used as the resin; both of these components are mixed or layered

and then compression molded to generate the composite. In early research of this

composite, it was found that compression molding needs to take place at 152.5^0C instead

of 162.5^0C as the higher temperature melted the fibers thus losing any potential

mechanical gain of the composite; composites created at 145^0C could not be tested as

mechanical bonding was insufficient. Initial wear testing for fabric and fiber composites

used 110,000 and 500,000 cycles respectively. Both groups showed reduced wear

compared to normal UHMWPE[74], however, the wear test was equivalent to six months or

less of cycles the material would experience *in vivo* so longer testing needs to be

completed. A second article by his group conducted wear testing using a cylinder shape

on a flat geometry (same shape as prior testing) as they felt it was most similar to the

geometry of the knee replacement. Both dry and lubricated (in bovine calf serum) wear

tests were conducted. Dry and lubricated testing showed similar results for coefficient of

friction for all materials tested: fiber homocomposites (all compositions), fabric

homocomposite, extruded UHMWPE, and molded UHMWPE. Wear, however, was

significantly lower for the homocomposite (though it doesn't specify which of the four

homocomposites tested) compared to "commercial" UHMWPE for the dry condition; the

lubricated condition did not however show significant differences. This is interesting to

note, however, that *in vivo* the two materials will be lubricated and are likely to depict

similar wear rates, Table 1.2[75].

Table 1.2: Comparison of UHMWPE homocomposite under various conditions

	Dry	Lubricated (bovine calf serum)
UHMWPE	0.15 (extruded) 0.18 (molded)	0.065 (unirradiated) 0.08 (irradiated)
0.25% volume fraction of fibers composite	0.10	
0.5% volume fraction of fibers composite	0.14	
0.75% volume fraction of fibers composite	0.18	
Fabric composite	0.1	**0.05**
	Note: These are approximate values from the graphs provided.	
Material from Suh NP et al[75]		

Additionally, Shalaby and Meng have developed a UHMWPE self-reinforced

composite as well (US Patent 5,824,411). This patent was followed by a second patent

for device, including biomedical implants such as replacement knees and hips and

applications varying as far as sporting equipment (US Patent 5,834,113). Their

composite was similar as it is also comprised of fibers oriented anisotropically within a

matrix of polyethylene, thus the material will be stronger in one direction than the other one. The composite was composed of UHMWPE (GUR 405) and Spectra 1000 fibers similar to the other composites while only containing approximately 5% (by weight) fibers. The mechanical and wear testing of the composites showed increased tensile properties, resistance to creep, and impact strength of the composite while wear rates were similar to that of UHMWPE[78]. This combination provides a potentially advantageous composite to standard UHMWPE for bearing surfaces as it could lengthen service life, but again *in vivo* tests are necessary for solid conclusions may be drawn.

Vitamin E doping

In addition to composites, additives have been attempted including Vitamin E, also known as α-Tocopherol. It is an antioxidant compound meaning that vitamin E removes the free radicals and will become oxidized itself in order to prevent oxidation of surrounding compounds. It has also been called lipophilic meaning it can dissolve in lipids and predominantly forms van der Waals bonds with other compounds (it is not capable of forming hydrogen bonds). Since one of the problems with UHMWPE is decreased fatigue strength which is associated with oxidation after gamma sterilization[79,80], Vitamin E doping has been researched as a potential way to lengthen the service life of the implant. Oxidation is particularly a problem with total knee joints as it speeds up the process of fatigue damage and delamination by weakening the UHMWPE. Tomita and collaborators showed that with the addition of Vitamin E prior to compression molding, the specimens tested exhibited little to no subsurface cracking thus

35

significantly less delamination using a "switched reciprocating" pattern (shape of a U) for 200,000 cycles at 196N. Additionally, the dynamic microhardness of the Vitamin E specimens more closely resembled that of virgin UHMWPE where gamma irradiated had a large difference in microhardness leading to stress concentrations and increasing the opportunity for fatigue crack propagation.   The microhardness is important as the differences in microhardness have been shown to lead to subsurface stress cracking that with time and repeated loading with result in flaking or delamination. The fatigue testing was much shorter than the service period of an implant and the sample size was relatively small (n=5 per group), however, their results suggested that delamination could be reduced with the addition of Vitamin E.   Additionally, these researchers had tested two different doping compositions, 0.1% and 0.3% Vitamin E; there was no statistical difference between the two for microhardness measurements or area of cracks (%), so the lower dose is recommended. Further, this research group showed that there is also a decreased surface roughness with the addition of the 0.1% Vitamin E. This research however, only looked at the first 60,000 repetitions, but it showed significantly decreased surface roughness (R_a) and no delamination in the Vitamin E specimens as compared to the gamma irradiated; additionally tests showed a significant decrease in R_a compared to virgin UHMWPE.   The dramatic increase in R_a of the gamma irradiated UHMWPE surfaces attributed to delamination defects; the Vitamin E-doped specimens were reported to not have such defects, but this is most likely due to the short cycle time. The surface roughness measurements presented were for cycle 50,000; however, there was no indication of why the 5th time point was used instead of the final time point and if the

results were less promising at the last time point. The reported results matched the shown

figures, but the question still persists of why the last time point was not used. This study

used n=5, however, there were 14 roughness measurement positions at each time point as

well as repetition to ensure accuracy of each measurement position (each position was

measured 10 times) which helps to ensure accuracy even with the small sample number[81].

The research of Tomita and others prompted other groups to begin investigating

the addition of Vitamin E as well and to further detail its effects on UHMWPE. Oral and

collabroators have looked at wear rates[82], fatigue resistance[83], migration stability[83], and

real-time aging of gamma-irradiated specimens in air[84]. Oral et al used cut specimens

UHMWPE bar stock that were irradiated at 100kGy and then doped them with Vitamin E

over a 16 hour period followed by a 27kGy irradiation for sterilization. Since Vitamin E

was not mixed into the sample then compression molded, it is necessary to show the

depth of Vitamin E penetration. The Vitamin E penetrated approximately 0.5mm;

beyond 5mm, no Vitamin E was detected. Additionally, a comparable wear rate was

shown in Vitamin E-doped specimens (1.9±.5 and 0.9±0.1 mg/million cycles for 65- and

100-kGy samples respectively) compared to 100 kGy gamma-sterilized UHMWPE

(1.1±0.7 mg/million cycles) after 2 million cycles post the accelerated ageing period (5

weeks at 80^0C in air). The oxidation index within the specimen were more constant

(0.48±0.25AU and 0.44±0.06AU decreasing to ~0.3AU 65- and 100-kGy samples

respectively) in doped samples than the dramatic decrease for the gamma-irradiated

(3.74±0.16AU at the surface to close to zero at 2.0mm deep). Further, the wear rates

(mg/million cycles) in both doped and aged specimens were shown to be similar to that

of unaged 100kGy irradiated/melted samples and significantly decreased from aged 105kGy irradiated/annealed as well as unaged or aged conventional 25kGy stored in nitrogen (only the wear rates of the doped specimens were from this experiment; the other results were from earlier reported data from the same research group under the same conditions). The fatigue resistance for the material was shown to be higher in doped than simply sterilized at the border region where Vitamin E was found; however, beyond 0.5mm (where no Vitamin E was detectable) there was a decrease in fatigue resistance. Penetration of Vitamin E could potentially be amended such that it the whole specimen was doped. This was not done, though, for consideration of manufacturing as well as a temperature limitation of $100^{0}C$, over which crystallinity of UHMWPE may be decreased. Overall, though, even without complete penetration, decreased oxidation and fatigue due to the crosslinking without embrittlement post-irradiation due to oxidation were shown for the specimens. As these specimens are a pilot study to gather more data about the optimal levels, pin on disk testing was used instead of hip or knee simulators; but, with more concrete data (and larger sample sizes: n=3 for this study), wear in joint simulators was proposed.

Since the doping of the bar stock proved to be a valid method, an elution test seemed to be the next step. Vitamin E is hydrophobic, however, it can be dissolved in isopropyl alcohol (IPA) – that which is used by orthopaedic companies to clean the samples prior to being bagged and sterilized. The elution tests included four conditions: control (not cleaned), 15-30 minute soak in IPA with subsequent wiping (industry standard), the industry standard repeated three times, and an eight hour soak in IPA

followed by wiping. Results showed no statistical differences between the four testing conditions, either on the surface or within the bulk, as measured by FTIR (n=3 for each group). Additionally, a wear test of 5 million cycles (approximately 5 years of service life) using a walking gait cycle with a max load of 3000N along with 37^0C circulating bovine serum in a hip simulator was performed. Two sets of liners were tested: control (cleaned and irradiated only) and vitamin E doped, cleaned, then irradiated. After the 5 million cycles was complete, the liners underwent an accelerated aging process (80^0C in air; 5 weeks). Results from this test showed that the oxidation index was significantly decreased both at the surface and in the bulk for the Vitamin E specimen (.3AU at surface; to virtually zero by 1mm depth) than the non-doped (2.5AU at surface to ~.3 at 2.5mm) as measured by FTIR. The results suggest long term stability of Vitamin E. It had been previously reported by Tomita et al that only .1% Vitamin E was necessary for effectiveness so starting with 1% allows for migration even though little was shown in this study. The authors concern, though, was that the lipids that exist in the synovial fluid may draw out the Vitamin E as they are hydrophobic like Vitamin E, where the synovial fluid itself has little draw due to its hydrophilic nature[83]. Additionally, Oral et al looked at free radical decay in real time to confirm that the results seen in the accelerated model were in fact truly mimicking what would happen in real time. A 7-month test was performed in air as well as a specimen that was packaged in inert gas for 13 months was examined via FTIR. The results confirmed the previous results from the accelerated aging studies that there is significantly more oxidation in non-doped specimens than Vitamin E-doped ones[84].

Further research has been conducted looking at the response of granulocytes, cells that with visible granules in their cytoplasm, to Vitamin E-doped UHMWPE. There are three types of granulocytes: neutrophils (most abundant making up ~70% of white blood cells), eosinophils (1-5% of white blood cells; activated in response to allergic reactions and parasites), and basophils (0.01-0.3%; store histamine & produces various cytokines). Granulocytes for this study were collected from human peripheral venous blood donated by six humans. First, they looked at the surface of both polyethylenes (doped and non-doped) to ensure the cellular reactions were similar to both surfaces and found that they were not significantly different in the number of plasma proteins that would adsorb to the surfaces. It was found that IgG was found adsorbed on both surfaces via Western Blot Analysis as would be expected so this was further explored. IgG, an immunoglobulin built of two heavy and two light chains, is the most abundant making up approximately 75% of the immunoglobulins in human serum. All of the proteins were desorbed from each of the polymer surfaces and run on a polyacrylamide gel to observe the specific types of IgG present. It was found that the doped polyethylene had less IgG adsorbed than the non-doped, which suggests that the doped surface may have reduced potential of long-term adhesion of macrophages as they have a difficult time adhering in comparison with normal UHMWPE[85]. The second paper by Reno et al was an opinion paper re-iterating the advantages that have been suggested in the literature for Vitamin E-doped polyethylene. It confirmed the only shortcoming that is visible in the research to this point is that no one has looked at the effects of wear on the polymer long-term including

the reaction elucidated *in vivo* to the bulk and particles once the surface begins to wear and age (no research has been published to date for animal or human models)[86].

As of Vitamin E-doped polyethylene for THRs were first clinically introduced in 2007 with TKRs introduced the following year (2008)[87]. Additionally, there are two modes of incorporation of Vitamin E to UHMWPE matrix: blending then molding or diffusion after the bar stock has been molded. Published Vitamin E content is always less than 1%, regardless of the manufacturer. Finally, as Vitamin-E doped UHMWPE has been clinically available for less than 5 years, there are no short or long-term clinical study results available to assess the *in vivo* performance of this material compared to highly crosslinked UHMWPE.

Carbon-Carbon composite

After interest in Carbon-UHMWPE composites, researchers looked at carbon-carbon composites as an alternative to eliminate the UHMWPE. Carbon-carbon composites have been researched for several years as a splint or artificial bone material. At its inception, it was not considered for bearing surfaces but simply as a material that had a modulus closer to bone for splinting. Early carbon-carbon composites when tested *in vivo* in a porcine model showed extensive chronic inflammatory reaction to both the implant and debris including large numbers of macrophages and giant cells. Additionally, when the lymph nodes were examined carbon debris was found there as well. The authors explained the poor results as caused by the wear of the material caused by the association of the screws with the plate. The results from this study were not

promising for a new bearing material[88]. Research, however, continued as to how to make

a viable bearing material. In 2003, Howling et al published on three carbon-carbon

composites formed using chemical vapor deposition (high modulus polyacrylonitrile

based carbon fiber (HMU), standard modulus version polyacrylonitrile based carbon fiber

(SMS), and P25, fibers constructed from the mesopitch phase) along with research on a

carbon fiber reinforced Polyetheretherketones (PEEK) to assess particle sizes generated

using pin-on-plate wear tester lubricated with bovine serum. Wear rates (determined

gravimetrically) as well as particle size and shape were examined for the 4 carbon-based

materials along with a UHMWPE (GUR 4120) control; all pins were worn against an

alumina countersurface. Three of the four carbon-based materials tested had lower wear

factors (K x 10^{-7} mm^{3}Nm) than metal on UHMWPE (2.00±0.5) including P25

(0.54±0.34), SMS (0.77±0.24), and CFR-PEEK (0.93±0.30). Mesophase-pitch based

P25, the carbon-based material with the lowest wear rate as well as the smallest average

particle size (most less than 100nm), was used for particle generation in a sterile

environment for cell studies. The P25 particles were then cultured with fibroblasts and

macrophage-like cells to assess cell viability and reaction compared to the carbon

particles, cobalt chrome metal particles (for comparison), and latex beads (used as a

negative control). Cell cultures were tested daily for 5 days; the cell cultures for both

fibroblasts and macrophages showed no cytotoxicity after five days compared with CoCr

and camtothecin (very cytotoxic chemical used as control)[89]. Howling et al continued

research into viable carbon-carbon composites for bearing materials with the positive

results of small particle generation (much smaller than that of UHMWPE) as well as

excellent resistance to cytotoxicity. One of the key reasons for carbon-carbon interest is the small particle size as macrophage activation has been shown to be caused via particles in the 0.1-0.5 micron range thus causing a release of TNF- α[90,91]. The smaller particle size generated from the carbon-carbon composites in wear is thought to potentially evoke a decreased macrophage reaction resulting in decreased TNF-α release thus decreased overall osteolysis around the prosthesis. The second study started with 22 different carbon-carbon composite materials that were placed under short term wear conditions (330,000, the equivalent of 13.2km) and then the resultant worn pins were looked at gravimetrically to determine the composites that had the best short-term wear resistance. The three composites selected were high modulus untreated (HMU) carbon fibers (polyacrylonitrile based) in a pitch matrix (HMU-PP), HMU polyacyrlonitrile-based fibers with a primary matrix of resin coke and a secondary matrix of pitch (HMU-RC-P) and the third was the standard modulus surface treated polyacrylonitrile-based fibers with a primary matrix of resin coke and a secondary matrix of pitch (SMS-RC-P) These composites with were then used for long-term wear testing of one million cycles under lubricated (bovine serum) conditions. Additionally, the lowest wearing of the three materials, SMS-RC-P, was used for cell culture to test the reaction of fibroblasts and peripheral blood mononuclear cells to bulk material and debris. Fibroblasts results showed a non-toxic response to SMS-RC-P. Additionally, mononuclear cells did not stimulate TNF-α production, even at a 80:1 μm^3/cell particle volume to monocyte cell ratio, thus the material may elicit a reduced osteolytic response *in vivo*. The average size of the particles generated by SMS-RC-P wear was approximately 50nm, thus it shouldn't

stimulate the macrophage response[92]. This research looks good, however, the presence of carbon particles in the surrounding tissue and lymph nodes from early studies will most likely still be a problem *in vivo* as the particles are small and therefore may get washed into the lymphatic system and trapped in the lymph nodes. This causes a potential for tumor and cyst formation due to response of the particles at distances far from the prosthesis. While this material may elicit a decreased osteolytic response, the balance of increased risk of reaction to the particles that are small enough to travel throughout the body may overcome the potential benefit of the material.

Other composites

Additionally, several composites of UHMWPE have been concocted that are not applicable to orthopaedic and/or weight bearing devices including UHMWPE/polyurethane (PU) composite[93,94] developed for cardiovascular applications to try to delay calcification; this composite has not been proven to be very successful compared to PU alone with respect to calcification as by day 28 the calcification level of the composite was nearing that of PU alone.

Additionally, a hydroxyapatite (HA)-doped HDPE[95-98] as well as a HA-doped UHMWPE[99-101] have been developed. This composite was designed for orthopaedic implants (e.g. replacement bone), however, due to the nature of polyethylene with its multiphases already, adding a hard additive into the matrix will lead to poor wear properties due to the additional stress concentrations via the mismatch of properties between the HA and UHMWPE if placed in a load-bearing situation. Tests using this

composite suggest it may be useful in a non-load bearing capacity as it has good fracture toughness and a Young's modulus within the range of cortical bone based on percent HA added (up to 9x that of virgin UHMWPE)[100].

1.4.4 Effect of Gamma Sterilization on UHMWPE Wear

Even with all the composites attempted, UHMWPE alone has proven to be the most viable sacrificial bearing surface. For UHMWPE, sterilization was standard for the industry from the mid-1960s when Charnley invented the hip until the mid-1990s. Sterilization by all orthopaedic manufacturers for polyethylene components was completed via gamma sterilization, also called gamma irradiation, in air. Gamma sterilization is achieved by use of a gamma ray emitting isotope, Cobalt-60 is most commonly for medical applications[102]. The emitted gamma rays (energy of 1.1732 and 1.3325MeV) then sterilize the object as gamma rays penetrate deep within the objects[102]; the gamma rays produce ionization that damages the organism's DNA and chemical structures.

In 1996, though, the manufacturers began using diversified sterilization methods as research had revealed problems with gamma sterilization in air. Additionally, it was discovered that gamma sterilization in air allows free radicals generated by the sterilization process to cause
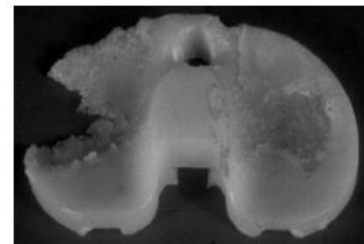
Figure 1.5: Oxidative degradation of tibial insert

chain scission resulting in shorter UHMWPE chains. These free radicals may then attack other chains and result in oxidation of the polyethylene, thus reduced mechanical

properties including toughness, ductility, and fatigue strength [49, 67, 102]. Further, the oxidation of the PE was exacerbated by long shelf life times as the implant is exposed to higher levels of oxygen within the air-filled sterilized package than it would be once implanted within the body[102]. Chain scission and oxidation leads to weaker bonds in polyethylene that gives way to delamination when under high stress loads in non-conforming devices, such as a TKR[103]. Fisher et al[104] suggest that if delamination is going to occur then oxidative degradation must precede it; an example of a failed tibial insert exhibiting oxidative degradation is shown in Figure 1.5. It has been found that aged gamma sterilization in air results in significantly higher wear rates than both non-aged (about 50% higher) and non-sterilized polyethylene (approximately 300%)[105]. As of 1998, gamma sterilization in air was no longer a sterilization method used by major orthopaedic companies in the United States and it had been replaced by a number of techniques attempting to reduce the wear rate of PE including gamma sterilization in a low O_2 or nitrogen environment, ethylene oxide, gas plasma, and supercritical CO_2 (see Table 1.3). While gamma sterilization in air was no longer a technique used for sterilization by the orthopaedic companies, the implants themselves were not recalled and surgeons continued implanting them post-sterilization changes. Urban et al[106] noted that the packaging on the implants did not specify what type of sterilization process the implant had undergone so unless the surgeon contacted the company, sterilization method was an unknown variable other than by date of manufacture after 1998 (or earlier for some manufacturers). Additionally, Urban et al pointed out a logical association that

hadn't been previously published, which was implant shelf life is inversely proportional

to the frequency of use (based on size and thickness of insert for a given design)[106].

Table 1.3: Sterilization methods used by US manufacturers as of Spring 1998

Manufacturer	Sterilization Method Used
Biomet	Gamma radiation in a low oxygen package
DePuy	Low temperature peracetic acid gas plasma Gamma radiation in nitrogen
Howmedica	Gamma radiation in nitrogen, followed by annealing in the sterile package below the melt temperature
Johnson & Johnson Professional	Gamma radiation in vacuum foil package
Stryker Osteonics	Gamma radiation in nitrogen
Smith & Nephew	Ethylene oxide gas
Sulzer Orthopaedics	Gamma radiation in a low oxygen package
Wright Medical	Ethylene oxide gas
Zimmer	Ethylene oxide gas Gamma radiation in nitrogen
	Gamma radiation in a low oxygen package
Table reproduced from Kurtz et al 1999[67]	

Gamma radiation in a low O_2 environment is typically indicative of an argon- or

nitrogen-based environment with little to no oxygen present. The rationale for this is that

if limited oxygen is available in the storage environment, oxidative degradation can be

postponed until the device is implanted thus significantly reducing the overall oxidative

degradation that will occur compared to gamma sterilization in air. This idea was

previously published by Premnath et al in 1996[102] who stated oxidative degradation

occurs *in vivo*; however, the amount of dissolved oxygen within the body is significantly

lower thus the conditions are much less harsh signifying less oxidative degradation in the polyethylene.

A beneficial effect of the gamma irradiation, which is not produced via other sterilization methods, is the production of crosslinks within the polyethylene. These crosslinks reduce the wear rate as they increase Young's modulus of the material. Crosslinking may be chemically created (via silane chemistry). A one-step process (gamma irradiation at higher levels), however, is advantageous as it allows a reduction in the overall number of steps the product must go through for manufacturing.

Additionally, Shen and McKellop[107] showed that as oxidation is decreased, crosslinking is increased with respect to depth from the surface of UHMWPE. This is due to oxygen binding to the end of the free radical instead of the free radical joining two polyethylene chains together to form a crosslink. So, if the polyethylene is irradiated in a low oxygen environment, it will have increased number of crosslinks formed in the surface regions thus it should have better wear resistance due to increased stiffness. Different manufacturers use different radiation doses between 50 and 105kGy). Some of the highly-crosslinked polymers available currently on the market include Prolong (knees, Zimmer), Durasul (knees, Zimmer), Longevity (hips, Zimmer), X3 (knees & hips, Stryker Orthopaedics), and Crossfire (hips, Stryker Orthopaedics). The goal of these highly-crosslinked polymers is to reduce particle generation.

1.4.5 Bone & Osteolysis

Osteolysis – Basic Science

Even with advances in sterilization and other factors affecting wear, wear particles are unavoidable. The particles generated (typically polyethylene, but may also be metal debris or corrosion products) that are released into the synovial fluid. This elicits the body's natural defense mechanism to remove foreign material. Macrophages respond to phagocytose the debris. They, however, cannot break down the particles as they are not biological in nature (i.e. bacteria, viruses, etc.) and thus they secrete cytokines that result in osteoclast maturation and activation. Once osteoclasts mature, they function to resorb bone in the regions surrounding the prosthesis. When bone is resorbed around the prosthesis, this results in loosening. Migration of particles to the bearing surface allows for third-body wear that will drastically increase the overall wear of the joint. As the prosthesis loosens, the result is an increase in particles being generated, inducing more bone resorption, and thus the result is a destructive positive feedback loop. This destruction of bone is called osteolysis or periprosthetic bone loss (see Figure 1.3).

The average particle size generated for THRs and TKRs is shown in Table 1.4. The average particle size ranges from approximately a half micron in THRs to just over a micron in TKRs. TKRs tend to produce larger particles due to oxidative embrittlement and delamination. The particle size is important as it determines the biological response. In a murine model, particles from 0.24-1.71µm have been shown to result in activated macrophages and thus bone resorption. Larger particles (7.6 - 88 µm) did not activate

49

macrophages[91]. An earlier study by Green et al looked at the cytokine response to particles and found that particles in the range of 0.49-4.3 μm, which includes most particles generated by TJRs, elicit significant elevation of cytokines[90]. Secreted cytokines include tumor necrosis factor – alpha (TNF-α), interleukins (IL-1, IL-6, and IL-10) as well as prostaglandins[108].

Table 1.4: Average particle size for THR & TKRs

Average Particle Size	
Hip	0.43μm[109], 0.53 μm[110], 0.694μm[112]
Knee	0.52μm[109], 1.190μm[112]

Osteoclast precursors do not resorb bone until they are signaled to become active, which is a key step in osteolysis. The transcription factor nuclear factor kappa B (NF-κB) must be stimulated to activate the NF-κB pathway, which results in differentiation and maturation of the precursor cells. The two main components of NF-κB pathway are receptor activator of NF-κB (RANK, found on osteoclast progenitors) and RANK ligand (RANK-L, molecule secreted by stromal cells that binds and activates the NF-κB pathway). Osteoprotegerin (OPG), a natural downregulation mechanism of this pathway, however, has been discovered. OPG is a molecule secreted by osteoblasts that competitively binds to RANK thus inhibiting osteoclast maturation. TNF-α and IL-1, two of the previously mentioned cytokines released by macrophages in response to wear particles, are particularly of interest as they upregulate RANK-L secretion[111, 112].

50

Treatment of osteolysis has used a variety of methodologies as the osteolytic cascade has not been fully elucidated at this point. The goal of these treatments is to target molecules known to be involved in osteolysis in an attempt to derail the osteolytic cascade before osteoclasts are activated. These methodologies can be divided into the two branches of the osteolytic cascade: osteoblastic and osteoclastic. The osteoblastic limb of the cascade includes application of growth factors (TGF-β and BMP-2). The osteoclastic limb of the cascade has been more deeply researched and includes treatments such as injection of osteoprotegerin (OPG), TNF-α inhibitors (Etanercept), and bisphosphonates.

Osteoblastic Limb of Osteolytic Cascade

The osteoblastic limb of the osteolytic cascade has involved application of growth factors, notably TGF-β and BMP-2, to enhance the osteoblastic response in non-cemented implants to enhance the stability. TGF-β is a cytokine that functions in many musculoskeletal tissues but specific to bone it stimulates osteoblast proliferation as well as bone/cartilage formation. It has been shown to improve bone density when injected into a localized area of polyethylene induced osteolysis in a lapine model[113]. TGF-β has also been shown to slightly improve osseointegration when used embedded within hydroxyapatite coating on titanium rods[114]. BMP-2, which is from the same family of cytokines, functions in fracture healing and osteoblast recruitment. BMP-2 has also been used in animal models to improve osseointegration of non-cemented implants via embedding it within a degradable polymer matrix. The use of BMP-2 has not been

elucidated yet with respect to osteolysis. The use of these growth factors to increase

osseointegration may postpone osteolysis as a stable prosthesis results in less wear.

However, using growth factors is not currently a viable solution as implants must be able

to have a lengthy shelf life. Further, even with recombinant human forms of these BMPs

being developed, they are still expensive, which may prohibit their widespread use.

Osteoclastic Limb of Osteolytic Cascade

The osteoclastic limb of the cascade has been more widely explored and includes

injection of osteoprotegerin (OPG), TNF-α inhibitors (Etanercept), and bisphosphonates.

Osteoprotegerin is a naturally occurring molecule synthesized by osteoblasts that

competitively binds to RANK on the osteoclast precursor thereby inhibiting maturation

and activation. OPG has been administered via two routes: antibody and via

subcutaneous injections. In the antibody method, an antibody was used against RANK

protein containing a Fc on the opposite end; it was shown to decrease Ti-particle-induced

osteolysis in a mouse model[115]. In another mouse model, Von Knoch et al administered

OPG via a subcutaneous injection in a calvarial murine model in the presence of

polyethylene particles. These OPG injections were shown to significantly decrease the

bone resorption when administered starting at Day 0 and Day 5[116]. Intravenous OPG

injections have been briefly used in clinical trials for other conditions such as Paget's

disease, however, no data to date on its effect on osteolysis.

Another osteoclast-related method is TNF-α antagonists. Since TNF-α is released

via activated macrophages that have ingested/attempted to ingest particulate debris, it is

also a logical choice for a method to prevent osteolysis. Anti-TNF-α agents are designed

to bind to TNF-α such that it cannot signal osteoclastogenesis. Etanercept, a FDA-

approved therapy (1998) that contains TNF-α receptor bound to the Fc portion of human

immunoglobulin (IgG-1), has been used successfully with rheumatoid arthritis as well as

in murine models[117].   In 2003, however, a second study on osteolysis was published by

this group using a small human clinical trial that showed no statistical difference between

patients awaiting that had osteolytic lesions at 6 or 12 months using computer

tomography[118]. The authors noted that a larger sample size would be needed due to

variability among humans. The authors used one of the more sensitive methods for

evaluating osteolysis (CT scan) and the length of the study was reasonable (12 months).

However, this method is not likely to become a routine method for prevention of

osteolysis as it has a yearly estimated cost of over ten thousand dollars[108].

1.4.6 Bisphosphonates

General Information

The third group contains bisphosphonates (also called diphosphonates), which

belong to a class of drugs that inhibit bone resorption. While bisphosphonates are

synthetic, they are structurally similar to a naturally occurring compound called

pyrophosphate, which also contains a P-C-P backbone. As the name diphosphonates

suggests, the backbone of this compound contains two phosphonate groups (PO_3)

covalently bonded to a carbon atom (see Figure 1.6a). The carbon atom is also bound to

the two side chains that define the chemical properties (potency, pharmokinetics, etc.),

and thus the differences between the multitude of commonly available bisphosphonates (Figure 1.6b).

Predominantly, though, one of the side chains is a hydroxide (-OH) group. These hydroxide groups are key to the high solubility of bisphosphonates. Bisphosphonates may be divided into two classes based on whether they contain nitrogen atoms in the side chains: nitrogenous and non-nitrogenous.
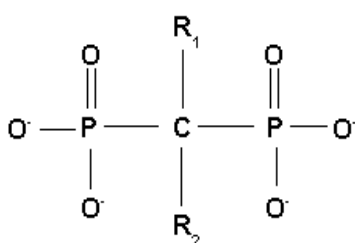
Figure 1.6a:

Agent	R_1 side chain	R_2 side chain
Etidronate	-OH	$-CH_3$
Clodronate	-Cl	-Cl
Tiludronate	-H	-S-〈◯〉-Cl
Pamidronate	-OH	$-CH_2-CH_2-NH_2$
Neridronate	-OH	$-(CH_2)_5-NH_2$
Olpadronate	-OH	$-(CH_2)_2N(CH_3)_2$
Alendronate	-OH	$-(CH_2)_3-NH_2$
Ibandronate	-OH	$-CH_2-CH_2N$ 〈 CH_3 / $(CH_2)_4-CH_3$
Risedronate	-OH	
Zoledronate	-OH	

Figure 1.6b:

Figure 1.6: Structure of bisphosphonates (a) backbone (P-C-P) and side chains of bisphosphonate (b) Side chain variations of different bisphosphonates.

Like many other pharmaceuticals, bisphosphonates have gone through several generations of evolution to resolve a variety of problems discovered during clinical trials. First generation bisphosphonates, including etidronate and clodronate, were originally

developed in the 1960s as a means to slow bone resorption[119-121]. This generation only included non-nitrogenous side groups (hydroxide, chorine, and methyl groups).

Table 1.5: FDA approved bisphosphonates (www.fda.gov)

	Brand Name
Alendronate	Fosamax, Fosamax Plus D
Etidronate	Didronel
Ibandronate	Boniva
Pamidronate	Aredia
Risedronate	Actonel, Actonel W/Calcium
Tiludronate	Skelid
Zoledronate	Reclast, Zometa

As techniques improved and their mechanisms of action became better, second and third generation bisphosphonates began to utilize hydroxide groups for R_1 and nitrogenous side chains for R_2 (see Figure 1.6b above). Pamidronate was a second generation bisphosphonate. Third generation drugs included alendronate and risedronate drugs. Both of these generations are fairly similar, however, the major distinction is that the 3rd generation bisphosphonates have been shown to be significantly more potent. Alendronate (Fosamax), risedronate (Actonel), and zoledronate (Zometa) are examples of 3rd generation bisphosphonates that are currently clinically available. Currently, there are 7 FDA approved bisphosphonates available (Table 1.5, www.fda.gov).

Mechanism of Action

In order for bisphosphonates to function, they need to bind to bone so that they are not excreted by the kidney. Specifically, they must bind to the exposed hydroxyapatite sites where bone has already been resorbed in order to function most efficiently. The first step for all bisphosphonates is "ingestion." By this process, the osteoclasts take in the drug along with the HA to which it is bound. However, after ingestion, non-nitrogenous and nitrogenous bisphosphonates have been shown to use different mechanisms to inhibit bone resorption. Non-nitrogenous bisphosphonates are broken down within the osteoclast yielding a chemical compound that interferes with the cell's adenosine triphosphate (ATP) pathway causing the cell to commence apoptosis, since ATP is necessary as an energy source for osteoclast function. As increased particles of bisphosphonate are bound to bone, the number of osteoclasts committing 'cell-suicide' leads to a decrease in the overall number of osteoclasts present and therefore a decrease in the amount of bone that can be resorbed. With a decrease in bone resorption and assuming normal osteoblast function, more bone will then be laid down with respect to that being resorbed thus increasing the overall amount of bone with time.

The second group, nitrogenous bisphosphonates, acts through the HMG-CoA reductase pathway, a metabolic pathway. The bisphosphonates disrupt the pathway as they are used in place of the normal pathway chemical, pyridoxal-phosphate (PPi). The disturbance occurs since both contain phosphate groups, and PPi's functions within the pathway as a phosphate group donor. This disruption of the pathway results in minimal rho protein expression. This lack of rho protein detrimentally affects the osteoclast's

cytoskeleton such that the osteoclast will lose its 'ruffled border.' Rho protein controls the attachment of the cell membrane to the cytoskeleton, and a lack in its expression leads to the same outcome, osteoclast apoptosis, simply via different mechanisms and pathways.

Clinical Applications

Bisphosphonates have been used in a variety of clinical applications. Most bone-related diseases, including those where bone turnover or bone metabolism is non-optimal, have been tested in conjunction with bisphosphonates. Initially, bisphosphonates were used to treat Paget's disease, a disease in which bones have become enlarged and fragile typically from deformity or injury. In addition, bisphosphonates are now prescribed for diseases such as post-menopausal osteoporosis and hypercalcemia of malignancy, a condition typically associated with cancer patients in which there is an abundance of parathyroid hormone-related peptide (PT-HRP). In addition to these three current clinical usages, bisphosphonates are being experimented with to test for beneficial effects on a variety of other diseases: inflammation-related bone loss [122, 123], fibrous dysplasia[124, 125], osteogenesis imperfecta[126-128], osteoarthritis[129], and rheumatoid arthritis[130].

Typical characteristics of bisphosphonates could be represented by that of alendronate, clinically known as Fosamax. Merck, its manufacturer, has published detailed information pertaining to the drug's use and effects in both animals and humans. Alendronate's absorption, which is representative of many of the bisphosphonates, is only 0.59% when the patient has fasted overnight and the dose occurs two hours before a

standard breakfast. If the patient takes the pill within an hour prior to breakfast,

absorption is reduced by 40% and it is negligible if dosing is two hours after breakfast.

Merck has also shown that alendronate may exist transiently in soft tissues; however, it

will become redistributed into the bones or excreted after a short period of time. It has

not been shown that alendronate can be metabolized in any way by humans or animals.

Further, the company shows that at least 50% of the drug (using ^{14}C labeling) was

excreted within 72 hours via the urine. The drug is expected to have a terminal half-life

of more than 10 years in the human skeleton if it can become bound before being

excreted. However, while the drug is bound to bone, it is inactive. The drug does not

become active until both the drug and a small amount of the bone (specifically the

hydroxyapatite) have been ingested by an osteoclast. The most prominent

contraindication for the drug is those who have renal insufficiency as their kidneys will

not excrete the drug thus leading to an increased but unknown drug concentration in the

body[131].

Systemic Bisphosphonate Delivery

Delivery of bisphosphonates to the body is currently limited to systemic delivery

systems. There are two delivery systems in use: oral and intravenous. These two

methods are very similar as to advantages and disadvantages. Both systems, due to their

systemic nature, require high dosages since more than 80% of the administered drug is

excreted unaltered via the kidney. Oral administration is advantageous as no needles are

involved; however, a pill must be taken either daily or weekly. Furthermore, most

bisphosphonates must be taken without food and after fasting overnight due to their high solubility. On the other hand, intravenous administration can occur much less frequently (every 3-6months) and has similar clinical and absorption results.

Injection-based bisphosphonate research

Several groups have researched the effects of bisphosphonates as ways to reduce wear particle-caused osteolysis. Typically lapine or canine models have been used. It has been shown that bisphosphonate (specifically alendronate) may inhibit bone lysis even in the presence of wear particles (combination of UHMWPE, titanium alloy, and cobalt chrome alloy) in a canine total hip replacement model[132]. Using this model, three groups of canines were tested: Group I (control), Group 2 ($1x10^9$ mixed particles), and Group 3 ($1x10^9$ mixed particles+ 5mg alendronate/day). It was shown that after 24 weeks, Group 3 that had been treated with bisphosphonate had little bone lysis in comparison with Group 2; both groups, however, did continue to show macrophage infiltration, which is common in chronic inflammation conditions.

Another injection-based trial that has been recently published (2007)[3] to study the effect of bisphosphonates on the bone adjacent to an implant. This study employs the implantation of titanium alloy (TiAlV) rods into both femurs of New Zealand rabbits (n=36) with rods in the left knee of each rabbit covered with approximately $2x10^8$ particles of polyethylene of clinically relevant size for THRs (2.3±0.5μm). The right knees were used as controls and had only the TiAlV rod. The three groups (n=12 each) of rabbits were divided as follows: control (no bisphosphonate dosing), zolendronate

(dosed once intraoperatively), and alendronate (subcutaneous injections weekly starting intraoperatively). The rabbits were sacrificed at 6 and 12 weeks to assess the thickness of the cortical bone surrounding the implant. It was found that both bisphosphonate groups significantly increased the thickness of the cortical bone at both six and twelve weeks over the non-dosed rabbits. Additionally, no statistical difference was found between the knees containing particles versus no particles as well as no osteolytic lesions were present in any of the bisphosphonate-dosed rabbits. Further, osteoid thickness and osteoid volume per bone volume was statistically higher in all implants in the bisphosphonate-dosed groups (with and without particles) at six weeks, however, these results were not statistically different by the twelve week time point. This indicates that the bisphosphonate dosing may help overcome the body's natural reaction towards osteolysis with proper dosing as the bisphosphonate downregulates the osteoclast activity as the drug was intended. Additionally, bone measurements were made at the sixth lumbar vertebrae to assess any systemic effects of the drug treatment. It was found using microcomputer tomography (μCT) that the vertebrae of the dosed rabbits (both groups) had an increase in cancellous bone volume, cortical bone volume, and trabecular thickness with respect to the controls. These results indicate that bisphosphonate may be advantageous in conjunction with TJRs to combat the macrophage activation in response to generated debris, as the generation of debris can never be completely halted with any UHMWPE or composite created.

Localized Bisphosphonate Delivery

In addition to injection-based delivery, a more localized approach has been undertaken. Microspheres have been researched for drug delivery in the pharmaceutical as well as tissue engineering field as early as the 1980s and 90s. Microparticles were researched first as delivery options for proteins & peptides[133, 134] as well as DNA[135]. However, this method was potentially problematic for use with bisphosphonates as they are relatively low molecular weight drugs and very hydrophilic. Two groups have published on microencapsulation for lower molecular weight drugs[136, 137] but until recently no one had attempted bisphosphonate encapsulation. Kissel and his group at Marburg, Germany have been trying to encapsulate bisphosphonates (specifically pamidronate) for the last few years[138, 139]. Their group has tried several different methods in order to achieve a 30% (wet weight) target drug loading in the microspheres using Poly(D,L-lactide-co-glycolide-D-glucose) abbreviated PLG-GLU. In 2003, the group presented three different methods of encapsulation that they had used with the best results from suspension of bisphosphonate in organic solvents (SOO). SOO combined methodology for previous methods for encapsulation of hydrophilic drugs as well as gaining high yield; the best results achieved were 71-99% yield with about a quarter of the drug being lost in the initial 24-hour burst. This technique involved using paraffin instead of water as pamidronate is almost insoluble in paraffin and this helped to slow the initial release of the highly soluble drug. Furthermore, dichloromethane (DCM) was added to the mixture in order to maximize both initial drug release and encapsulation efficiency; it was found that 50% DCM in the PLG-GLU mix resulted in the best

compromise of the two characteristics. This resulted in more desirable microsphere

characteristics, however, the microspheres still did not result in continuous drug

release[138]. Their 2004 paper[139] continued work creating the microspheres, however, the

microspheres had increased drug release during the first 24 hours (almost 100%). The

idea of the microspheres is highly advantageous over the systemic dosing as it is local

and would need much lower dosages if the burst problem could be overcome. However,

significantly better drug release profiles must be attained which may mean

experimentation with block copolymers using hydrophobic external blocks or a

hydrophobic surface eroding polymer that could retain the drug.

— CHAPTER TWO —

AIM 1: Engineer Enriched UHMWPE Constructs and Evaluate Mechanical and Tribological Properties

2.1 Introduction

The use of ultra high molecular weight polyethylene (UHMWPE) inserts in total joint replacements (TJR) results in wear particle-caused osteolysis, which is the predominant cause for prosthesis failure and revision surgery[132]. The particles generated are released into the synovial fluid; this elicits the body's natural defense mechanism to remove foreign material. Ultimately this process ends in wear particle induced osteolysis and implant loosening.

Numerous efforts have been made to reduce UHMWPE particle generation such as the use of highly crosslinked UHMWPE (XLPE)[140] or use of alternative polymers. While new materials have been successful at reducing the number of particles generated, wear particles are still unavoidable.

A number of studies, both in vitro and in animal models have investigated whether the use of an intravenous family of drugs called bisphosphonates (BP) could help mitigate the effects of osteolysis. BPs have been shown to be effective for use in patients with osteoporosis as well as other bone metabolism diseases. These drugs function by apoptosing osteoclasts after they ingest the BP bound to bone. Work by others has shown that the use of bisphosphonates can decrease osteoclast activity as well as increase osteoblast activity in vitro[141]. Further, intravenous systemic bisphosphonates (BP) can

significantly contribute to minimize periprosthetic osteolysis[2, 3]. However, the systemic delivery and the high solubility of BPs results in a predominant portion of the drug being excreted via the kidney without reaching its target, bone[142]. Therefore, a local delivery system would allow for more of the bisphosphonate to reach its target prior to being removed from the system. Previous groups have attempted to microencapsulate bisphosphonates but have encountered problems with burst release due to the hydrophillicity and small size of the drug[138, 139].

The goal of this study is to develop a novel method to locally administer BPs using the inherent wear of UHMWPE as a drug release mechanism. If bisphosphonate can be released in a controlled manner locally, it has the potential to effectively delay or slow the progression of osteolysis due to wear particle release. This study is aimed at prooving the concept that bisphosphonates can be effectively added to UHMWPE without significantly affecting the material properties. However, the mechanical properties of the enriched UHMWPE must be comparable to that of the currently used UHMWPE in order to be considered as a viable approach. The mechanical properties are paramount to the success of a load-bearing material. Thus, material characterization for the UHMWPE-BP blend is essential. As the biocompability of both materials (UHMWPE and BP) has been demonstrated elsewhere, it is expected that the UHMPE-BP blend material will exhibit a of similar level of biocompatibility as its individual components. Therefore, the first step in development of this novel material consisted in the examination of the resultant mechanical and tribological properties. It is hypothesized that an UHMWPE based bearing material can be developed containing two

percent bisphosphonate (or similarly sized compound) that would not perform similarly in laboratory trials. It was also hypothesized that optimum concentration of BP would not significantly affect the material properties and tribological performance of UHMWPE, and that BP would be released from the surface and generated particulate of the enriched UHMWPE. Local delivery of bisphosphonates would be advantageous as an anti-osteolysis treatment. If bisphosphonate can be released in a controlled manner locally, it has the potential to effectively delay or slow the progression of osteolysis due to wear particle release.

2.2 Materials and Methods

Two types of proof of concept studies were conducted to assess the mechanical and tribological properties of the enriched UHMWPE: tensile testing and pin-on-disk tribological testing.

Compression Molding

All UHMWPE and UHMWPE-blend specimens were compression molded to reduce variability among the specimens as each specimen had undergone a similar compression molding process. Compression molding using a Carver press was completed using methods published by Parasnis & Ramani[34]. Briefly, Table 2.1 details the times and pressures used in the compression molding process.

For tensile testing, a custom mold was used with a molding area of 4580 mm^2 (4.4g PE powder/mm thickness). For pin-on-disk tests, a larger custom mold was used

containing a molding area of 7960 mm^2 (7.4g PE/mm thickness). For this mold,

approximately 187g of PE was used to achieve 1" thick block from which pins were

machined. All pin specimens for a given material (PE or PE-tag) were machined from

the same block. This helped control for inter-specimen variability within a given

material.

Table 2.1: Carver Press Molding Times (Reproduced from Parasnis et al[34])

Step	Time (min)	Stage Duration (min)	Force (Mpa)	Temperature (degC)		Temp Rate deg/min
				Top	Bottom	
1	0		38.9	29	29	---
2	5	5	7.8	29	29	0
3	20	15	7.8	177	215	9.9
4	30	10	7.8	177	215	0
5	57	27	38.9	93	140	-3.1
6	87	30	38.9	93	140	0
7	107	20	0	29	29	-3.2

UHMWPE + 2% Tag Preparation

Blocks of enriched UHMWPE (PE-tag) were prepared using 2% (by weight)

8-Anilino-1-naphthalenesulfonic acid hemimagnesium salt hydrate (Sigma) blended with

GUR 4150 UHMWPE powder (Ticona). Hemimagnesium salt hydrate (Sigma) was

selected as it contains a fluorescent tag (naphthalene) which would aid in visually inspecting the blocks to ensure evenness in tag distribution. Additionally, it is hydrophilic and of similar size (MW=310) to alendronate sodium (MW=325.12), commonly referred to as Fosamax (Merck, Inc.). Thus, it provided a cost-effective alternative to using alendronate, which was still under patent in 2007, for initial studies to determine whether blending BP into PE was feasible. The powder material was blended using dry mixing via a vortexer (VWR Standard Mini Vortexer; speed=10) for 10 minutes. Initial mixing followed by compression molding of blends that were vortexed for 6 minutes or less yielded uneven distributions of the tag within the PE using visual inspection post-molding. Tag distribution was determined by visual inspection of the green particles (tag) within the translucent PE matrix (See Figure 2.1). A mixing time of 10 minutes ensured even distribution of the tag within the material. The mixture was then compression molded using the Carver press as previously described. The amount of PE powder added was calculated based on the selected mold and specimen thickness.
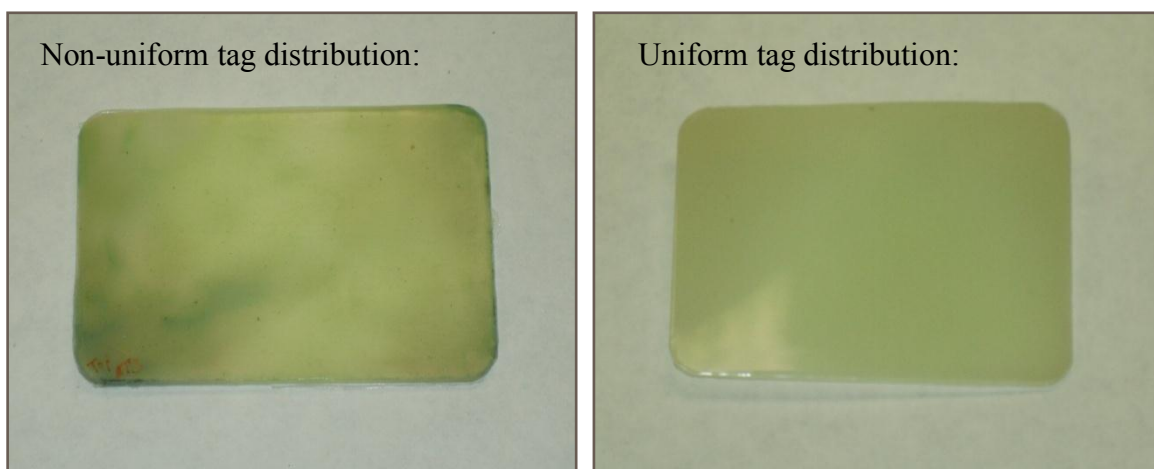
Figure 2.1: Representative samples of non-uniform and uniform tag distribution of hemimagnesium salt hydrate (tag) within the UHMWPE matrix

A 2% by weight of tag/BP was selected as the targeted BP amount. This concentration was derived by assuming the size and number of UHMWPE particles that would be generated in a typical TJR, and BP concentration shown to be effective for cell proliferation control. It was also assumed that BP would be equally dispersed throughout each wear particle, and that the wear particles would be small enough that the drug would elute from within the particle. According to Bartel and collaborators, an average of $20mm^3$ UHMWPE particles are released per million cycles (approximately 1 year) of TKR implantation life and approximately 1 billion wear particles generated per year[143], resulting ina calculated average particle diameter (from wear debris volume and approximate numbers) is 3.4 microns. Moreau and colleagues reported that an alendronate concentration of 10^{-4}M inhibits cell proliferation and induce apoptosis in murine macrophage-like cells (J774 A.1)[144]. Im and colleagues have shown an increase in cell proliferation in osteoblasts (MG-63 osteoblast-like cell line) occurred with BP concentration between 10^{-7} and 10^{-8}M[141]. Therefore, a 2% by weight was selected in this studyAs the addition of BP within the UHMWPE matrix can lead to formation of stress risers that would result in crack initition, this low concentration will minimize this incidence.

The effect of molding on the fluorescent tag has been investigated as the literature from the distributor (Sigma) does not provide its melting point. Digital scanning calorimetery (DSC) was performed using the following protocol. The sample was first heated in a Mettler Toledo DSC823e system (Columbus, Ohio) to 25°C and held for 2 minutes. Then, it was heated at 10°C /minute to 200°C and held there for 2

minutes. DSC showed that the melting temperature of the 2% w/w tagged UHMWPE

(PE-tag) has a lower melting temperature ($T_M = 134.1 \pm 1.2°C$) compared to UHMWPE

alone (TM=135°C). As this was lower, a preliminary test of only the tag was completed

demonstrating the tag had a $T_M = 102°C$.

Tensile Test

In order to assess the mechanical properties of the 2% w/w 8-Anilino-1-

naphthalenesulfonic acid hemimagnesium salt hydrate (Sigma) by weight enriched

UHMWPE (PE-tag), a uniaxial tensile test was performed. Two millimeter thick blocks

of UHMWPE (PE) and UHMWPE-tag (PE-tag) were prepared and compression molded

as detailed above. Dogbone-shaped specimens (20mm gage length & 4.9mm width) were

cut from each block (n=7-8) using a die (Figure 2.2).   After specimens were cut, all

specimens were then cleaned using ASTM F1715 protocol followed by ethylene oxide

sterilization. A total of specimens 86 specimens were used for the tensile test (n=43 for

PE and n=43 for PE-tag). Specimens were tested at room temperature in air to failure at a

constant strain rate of 5mm/sec using a servohydraulic testing system with a 25kN load

cell (Instron 8874, Instron Corporation, Canton, MA). Stress-strain curves were plotted

using the results of the tensile test; from these curves several material properties were

determined including elastic modulus, yield stress, ultimate stress, and toughness. Yield

stress was calculated at 0.3% strain. A Student t-test was used to assess the statistical

differences between the material properties of both groups ($\alpha=0.05$).

Figure 2.2: Dogbone die and sample blocks from which specimens were cut for tensile testing

Pin-on-Disk Testing

Preliminary pin-on-disk wear tests were conducted using the OrthoPod machine, which is a six station pin-on-disk machine (AMTI, Figure 2.3).[64] Blocks of PE and PE-tag were molded using compression molding as previously described in the larger custom mold. Half inch thick blocks of both PE and PE-tag were fabricated and then 9.5mm diameter pins with 3mm flat tip (n=12) were cut from each block of PE and PE-tag (Figure 2.4). Each tribosystem was lubricated with 25mL of 50% bovine serum (Hyclone) diluted with deionized water + 0.2% w/v sodium azide (NaN_3, Sigma) as an anti-microbial agent per station. During the trial, lubrication levels were checked and deionized water was added as necessary to maintain appropriate serum levels. Soak controls were used for these experiments and maintained in an environmental chamber at 37°C. The portion of the pin that was in fluid was controlled to be similar to that in the OrthoPod due to the hydrophilic nature of the tag.
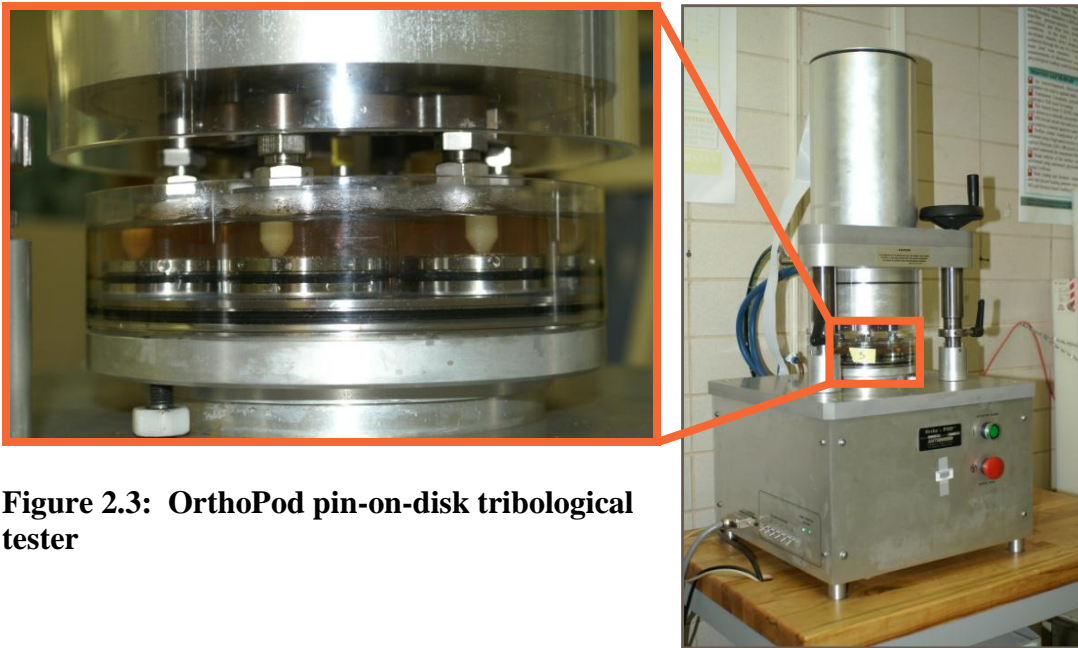
Figure 2.3: OrthoPod pin-on-disk tribological tester

For this experiment, diamond-coated CoCrMo specimens ($R_a = 22.4 \pm 1.8$ nm) were used as the countersurface (Figure 2.4). These were mounted in custom OrthoPod fixtures. A circle-shaped wear pattern (19mm Ø) was selected as it has the highest wear factor; a speed of 1Hz was selected yielding a velocity of 60mm/sec, which is within pin-on-disk ASTM standard (F732). Applied loads of 21.2N and 42.4N (3MPa and 6MPa pin tip pressure, respectively) were used in 2 separate experiments. Data from the experiment was recorded every ½ km over the 40km. Every 10km, the experiment was stopped, disassembled, and cleaned using ASTM F1715 method; additionally the soak controls were removed from the environmental chamber and cleaned via the same methodology. Each of the specimens (experimental as well as soak controls) were dried

in a vacuum oven maintained at 37°C for a minimum of 30 minutes and then weighed

(Mettler Toledo, d=.01mg). The use of a vacuum oven allowed a control for the

temperature as well as humidity in lieu of simply humidity as stated in ASTM F1715

methodology. Additionally, at each 10km interval, the tips of the pins were imaged using

non-contact surface profilometry (Wyko). Once gravitational weights and imaging was

complete, the OrthoPod was reassembled with application of new bovine serum. A two-

tailed t-test (α=.05) was used to analyze the results for significance.
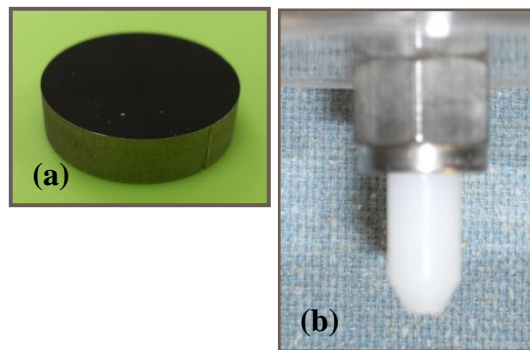
Figure 2.4: (a) Diamond-coated CoCrMo countersureface and (b) UHMWPE pin in OrthoPOD holder

2.3 Results

Tensile Test

Results showed that the yield stress of the enriched material (PE-tag) was not

significantly different from that of PE (Table 2.2). Other material properties were

however significantly different including elastic modulus (p=.004), ultimate stress

(p=.002), and toughness (p<.001). Additional graphs are shown in Appendix B, Figures B-1 and B-2.

Table 2.2: Summary of results of tensile test for virgin UHMWPE (PE) and UHMWPE enriched with a 2% tag (PE-tag) (n=43 for each material)

		PE	PE-tag	p-values
Elastic Modulus	*MPa*	529±38*	509±37*	0.004
Yield Stress	*MPa*	20±0.7	20±0.8	0.091
Ultimate Stress	*MPa*	38±2.0*	36±2.0*	0.002
Max Load	*N*	391±21*	375±20*	0.002
Ultimate Strain	*%*	403±67*	347±47*	<0.001
Toughness	*MPa*	125±24*	105±18*	<0.001

* denotes significance (p<0.05)

OrthoPod Pin-On-Disk Testing

A preliminary trial using 3MPa of pressure (n=3 for PE and PE-tag) at pin tip using a circle wear pattern did not generate measurable wear over the 40km. The force was increased to 42.4N to generate a clinically relevant pin tip pressure of 6MPa. UHMWPE manufacturers suggest no more than 10MPa compressive stresses for UHMWPE and recommend less than 5MPa[145]. However, it has been reported that peak stresses may exceed 15MPa in some TKR designs[143, 146]. Two experiments using the previously described protocol (including soak controls) and n=3 of each material type were completed. The 6MPa pressure did generate sufficient wear over the 40km trial (Figure 2.5). However, there was no significant difference in the gravimetric weight loss

between the two material types at 40km (p=0.78). All pin results with an overlay of the

averages are shown in Appendix B, Figure B-3.
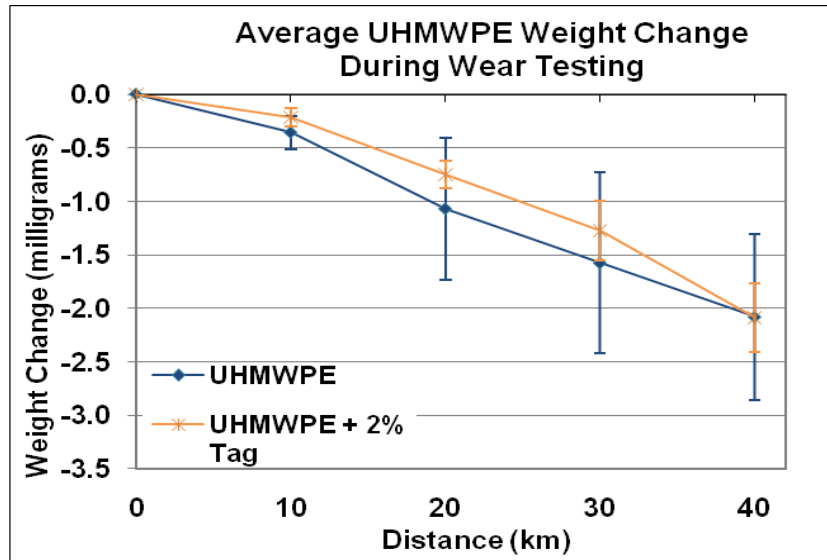
Figure 2.5: Average change in gravimetric weights over 40km OrthoPod trial (6MPa contact pressure)

From these preliminary studies, it can be concluded that the BP-UHMWPE blend is a

viable bearing material for the application targeted in this study.

2.4 Discussion

Tensile Test

There are a number of properties shown that differ from those of standard PE. The

modulus of elasticity and the yield strength are of a particular interest. The lower elastic

modulus of PE-tag may be advantageousas it may yield better lubrication when used *in*

vivo[147, 148]. While the ultimate stress of PE-tag was shown to be significantly lower than

that PE, the material will likely never experience stresses comparable to its ultimate

stress. Research has shown that during walking the knee experiences loads up to approximately 2-4 times body weight during normal walking gait [35]. The yield stress, however, was critical to the mechanical properties of this material as the material will be frequently challenged at its yield stress. Yield stress was shown to have non-significant differences for the two materials.

OrthoPod Pin-On-Disk Testing

Though initial 3MPa trials did not generate adequate wear for measurement over the 40km trial, measureable wear was achieved by increasing the applied force. The force was increased to 42.4N to generate a clinically relevant pin tip pressure of 6MPa. UHMWPE manufacturers suggests no more than 10MPa compressive stresses for UHMWPE and recommend less than 5MPa[145]. However, it has been reported that peak stresses may exceed 15MPa in some TKR designs[143, 146] thus this experiment does not attempt to fully describe wear that would occur even over a short trial. The 6MPa trial showed non-significant differences between the two materials (PE and PE-tag), which indicates that this material should be further investigated using a bisphosphonate to determine if the same tribological properties are seen. It is likely that as the tag and bisphosphonates are similar in size (thus the 'defect' in the PE matrix) and hydrophilicity, that they will in fact act similarly. For this reason, one of the two mechanical experiments should be replicated with bisphosphonate substitution to confirm these early results.

2.5 Conclusion

These initial studies indicate that it may be feasible to incorporate bisphosphonate

into the UHMWPE matrix for total joint replacement based upon the results of these

preliminary tag-based studies. Future studies should incorporate the actual

bisphosphonate to confirm the tribological results obtained in this preliminary study.

— CHAPTER THREE —

AIM 2: in vitro & Functional Drug Elution Testing

3.1 Introduction

Several experimental studies have focused on the effects of both particles as well as treatment with bisphosphonate on cell and tissue response *in vitro* (osteoblasts[141, 149], osteoclasts[150], macrophages[151, 152]) and *in vivo* using animal models[2, 3, 132, 153-155]. For approximately two decades, osteoclasts (OCs) have been investigated as one of the primary cause of osteolysis leading to implant failure. Initially, researchers assessed the inhibitory effect of BPs on osteoclastic activity in an attempt to mitigate early failure as osteolysis is the most common cause of failure in TJRs. *In vitro* research confirmed *in vivo* has shown that BPs induce OC apoptosis and thus reduce overall osteoclastic activity. Work by others has shown that the IC50 (concentration required for 50% inhibition *in vivo*) of alendronate is 50nM[150]. The goal of BP-loaded UHMWPE is to be in the range to down-regulate OC activity thus functioning as a local drug delivery system.

The scope of this study was not to reproduce well known therapeutic and prophylactic effects of BPs on OBs and OCs, but a brief overview of the results from the literature will be discussed. However, It has been shown that BPs affect the maturation and proliferation of OBs *in vitro*; this has been shown via increases in number of cells, as well as increased alkaline phosphatase activity and gene expression of OB markers (BMP-2, type I collagen, osteocalcin)[141, 149]. Im and colleagues indicated that a

concentration between 10^{-7} and 10^{-8}M increases OB proliferation with peak levels of OB proliferation at 10^{-8}M[141]. Further, research has also shown that in high concentrations, bisphosphonates may also have an effect on macrophages; Moreau and colleagues reported that an alendronate concentration of 10^{-4}M significantly decreases the number of macrophages *in vitro*[144]. These authors found that more potent bisphosphonates such as zolendronate require a lower concentration for apoptotic evidence (10^{-5}M - 10^{-6}M)

Based on the 10^{-6} and 10^{-8}M targeted BP concentration to inhibit OC proliferation with a neutral effect on OBs and estimated wear debris average size, a concentration of 2% w/v of BP in UHMWPE has been determined to provide optimal effect (see earlier calculations in UHMWPE + 2% Tag Preparation section).

The purpose of this study was to characterize the release of alendronate from bulk and thin film samples of enriched UHMWPE in a constantly moving water solution. The results of the study were aimed at elucidating whether the alendronate migrates out of the PE, if the release is from the exterior only, or if there is migration occurring from slightly below the surface (e.g. first 10 microns). This study will be useful as proof of concept that bisphosphonate does in fact elute from the surface of the PE to confirm the utility of enriching with bisphosphonate. Further, this will be useful to confirm specifically which published experiments show what would happen if the enriched material was placed into contact with them.

From previous studies, we know that the polyethylene (PE) enriched with a fluorescent tag (PE-tag) had similar yield strength and wear rates from 40km pin-on-disk studies to virgin PE. Additionally, the aim of this study is to investigate whether PE-BP

performs similarly to PE-tag in 40km pin-on-disk wear tests to confirm earlier pilot study results. In addition, to confirm static drug elution results, we will attempt to measure the BP released into the lubricant during the wear study. It is our hypothesis that the PE-BP will in fact perform similarly to PE-tag and that BP will be released into the lubricant.

3.2 Materials and Methods

This aim consists of three drug elution experiments. The first two are performed under static conditions (thin film and bulk) while the third is performed on samples that have undergone wear in the OrthoPOD.

Static Thin Film Elution

Drug elution tests were performed using small blocks (1.0cm x 1.0cm x 1.0cm) of PE (n=6) and PE-BP (2% w/w of bisphosphonate, n=6) molded using a custom mold. Each PE specimen was molded using 950±0. 5mg GUR 4150 UHMWPE. Each PE-BP specimen was molded using the same amount of PE (950±0.5mg GUR 4150 UHMWPE) with the addition of 19.4±0.2mg alendronate sodium (ALN), a bisphosphonate (BP). All specimens were compression molded as previously described. Dimensions of each specimen as well as gravimetric weights were obtained prior to the experiment as some material was lost in the compression molding process due to flashing. Data allowed for estimations of actual alendronate content in each block for drug elution calculations. Specimens were not washed prior to drug elution tests to ensure that alendronate would be in a measurable range. Dimensions of each specimen as well as gravimetric weights

were obtained prior to the experiment as some material was lost in the compression molding process due to flashing. Measurements and weights allowed for estimations of actual alendronate content in each block and therefore slices from each block for drug elution calculations. Specimens were not washed prior to drug elution tests to ensure that alendronate would be in a measurable range.

In vitro alendronate release study was performed in an environmental chamber maintained at $35° \pm 2°C$; for the duration of the experiment, the specimens undergo shaking using a VWR mini shaker at 300rpm.

Thin film drug elution tests were performed using thin slices (15μm x 1.0cm x 1.0cm) of PE and PE-BP (2% w/w) cut (PolycutE, Leica) from 1cm^3 blocks molded using the same mold as bulk elution drug elution tests. Thin films for pilot studies were cut from either the top or the center of blocks of PE and PE-BP (see Figure 3.1). For the experimental studies, 1 slice (0-15um) was cut from the outside of 15 separate blocks and placed in a centrifuge tube. A second slice (15-30um) was cut from the outside of the 15 blocks and placed in a second centrifuge tube. This pattern was repeated for a total of 8 sample tubes (0 – 120um surface depth) of PE-BP (see Figure 3.2).
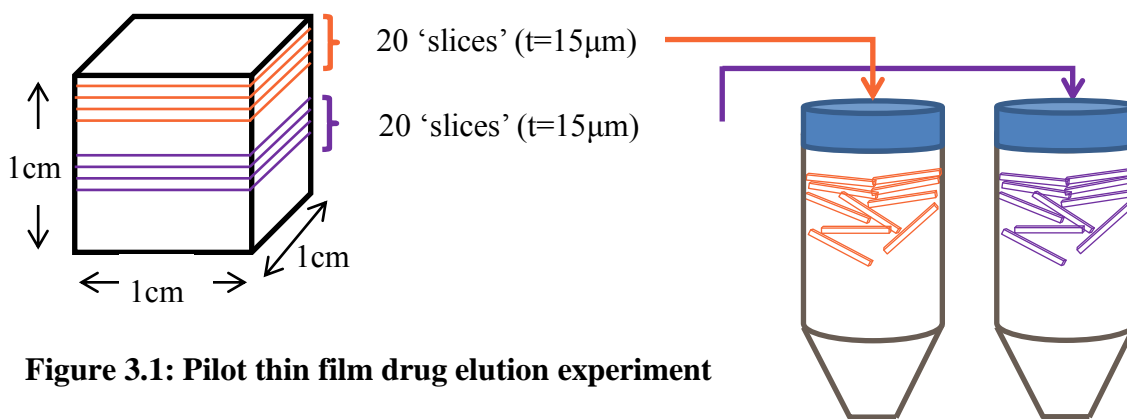
Figure 3.1: Pilot thin film drug elution experiment
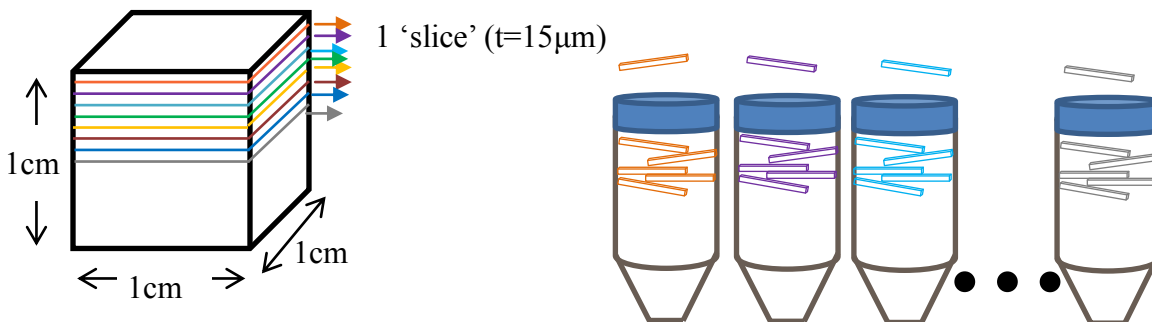
Figure 3.2: Thin film drug elution experiment

The thin film samples were maintained in 10 mL of HPLC-grade water (Fisher) on a shaker at 37°C. Aliquots of 1mL was collected at the indicated time intervals (1,2,3,5, and 7 days for the pilot study) with equal amounts of HPLC-grade water being re-added. For the experimental study, aliquots of 1mL were taken over the course of 28 days with equal amounts of water re-added for (time points in hours): 1, 2, 4, 8, 12, 24, 48 (2 days), 72 (3 days), 120 (5 days), 168 (7 days), 336 (14 days), 404 (21 days), 572 (28 days) with equal fluid amounts being re-added for pilot studies. Samples (n=4; triplicate) were analyzed using high pressure liquid chromatography (HPLC, Waters, Milford, MA).

Several methods for measuring alendronate sodium using HPLC have been reported in the literature. However, many of these methods either require time-intensive ion complexing as alendronate lacks a chromophore or methodology that requires perchloric acid, which is undesirable as it is flammable, corrosive, and explosive. Ion chromatography with refractive index detection methods previously published by Han &

Qin[156] were used for pilot experiments; however, the needed sensitivity was not achieved. Thus, another method[157] that uses in-line complexation of copper II nitrate with the bisphosphonate and detection via the UV detector was used. A Waters HPLC (Milford, MA) with an anion-exchange column (Waters IC-Pak anion HR column) packed with polymethacrylate resin with a quaternary ammonium functional group (6μm particles size, 4.6x75mm ID) was used. The following parameters replicated those previously published by others[157]: column temperature of 25°C, 0.85mL/minute flow rate, and injection volume of 50μL. It should be noted that for our experiment a flow rate of 0.85ml/min was used instead of 1.0mL/min as published due to maximum recommended flow rate for our column of 1.0mL/min and our slightly lower value was selected to insure we remained below that desired limit. Dilute nitric acid (Fluka) at a concentration of 6mM with copper II nitrate (0.5mM, Alfa Aesar) will be used for the mobile phase as that concentration yielded the sharpest peak and shortest retention time of alendronate within the column[157]. A calibration curve was generated prior to beginning any elution experiments. The same HPLC column was used throughout the duration of the elution experiments; further, the column was equilibrated via injection of the standard alendronate solution till reproducible retention times & peak shapes are generated. A 0.4mg/mL standard alendronate solution was produced by dispersing 2mg of alendronate sodium in 5mL of deionized water and stirring for 30 minutes. Then, the solution is passed through a 0.2μm filter (Nalgene) for HPLC use. Each individual sample was filtered using 0.45 μm polypropylene syringe filters (National Scientific) prior to injection in an HPLC vial (Waters). From our experiments, it has been found that the

alendronate peak had a retention time of approximately 4 min with a detection level of 0.4μg/mL. This was similar to published values reporting a detection limit of 0.3μg/mL[157].

Static Bulk Elution

Drug elution tests were performed using small blocks (1.0cm x 1.0cm x 1.0cm) of PE (n=6) and PE-BP (2% w/w of bisphosphonate, n=6) compression molded using a custom mold as previously described. Each PE specimen was molded using 950±0.5mg GUR 4150 UHMWPE. Each PE-BP specimen was molded using the same amount of PE (950±0.5mg GUR 4150 UHMWPE) with the addition of 019.4±0.2mg alendronate sodium (ALN), a bisphosphonate (BP).

In vitro alendronate release study was performed in an environmental chamber maintained at 35° ± 2°C; for the duration of the experiment, the specimens undergo shaking using a VWR mini shaker at 300rpm. A 1cm^3 block of PE or PE-BP is placed into 10mL of HPLC-grade water. Measurements were found using the HPLC methodology described above. HPLC measurements were repeated in triplicate.

Aliquots of 1ml were taken over the course of 28 days (time points in hours): 1, 2, 4, 8, 12, 24, 48 (2 days), 72 (3 days), 120 (5 days), 168 (7 days), 336 (14 days), 404 (21 days), 572 (28 days). At the end of 28 days, the percent of drug eluted was calculated as determined by HPLC. The latter time points will show whether or not BP is migrating towards the surface of the PE-BP or remaining locked within the bulk region if no additional drug is released at later time points. Samples (n=6; triplicate) were analyzed

using high pressure liquid chromatography (HPLC, Waters, Milford, MA) anion

exchange using in-line complexation[3]. A 6mM nitric acid (Fluka) + 1.5mM copper II

nitrate (Alfa Aesar) mobile phase were used at a flow rate of 0.85mL/min using a Waters

IC-Pak Anion HR column as previously described in the Static Thin Film Elution section.

Dynamic Elution Using the OrthoPOD

      Pin-on-disk wear tests were conducted using the OrthoPod machine (AMTI).

This experiment was completed as before with the PE versus PE-tag. Briefly, [64]12.7mm

thick blocks of PE and PE-ALN (alendronate, 2% w/w) were molded using compression

molding as previously described. Pins (9.5mm diameter, 3mm flat tip, n=12) were

machined from two 12.7mm thick blocks. Three pins of each material as well as 2 soak

controls were used in individual trials with a total of 6 pins of each material

experimentally tested. Each tribosystem was lubricated with 25mL of 50% bovine serum

diluted with deionized water; lubrication levels were monitored during the trial and

deionized water was added as necessary to maintain appropriate serum levels. Soak

controls were used as previously described. Six diamond-coated CoCrMo specimens (R_a

= 22.4 ± 1.8 nm) mounted in custom fixtures were used as the countersurface. A 40-km

were test was used (circle-shaped wear pattern 19mm Ø wear pattern; 1Hz), which is

within ASTM standard F732 for pin-on-disk testing. Applied pin tip pressure was 6MPa.

Every 10km, all specimens (experimental and soak controls) were cleaned (ASTM F1715

method). Additionally, the bovine serum was collected and frozen from each of the

tribosystem for later HPLC analysis. Pins were imaged using non-contact surface

profilometery (NT-2000 Non-Contacting Surface Profilometer; Wyko, Tucson, AZ). Additionally, gross images at 12X and 25X of the pin tips were recorded using a stereomicroscope (Model K400P, Motic Inc, Xiamen, China) with attachments for image acquisition including a fluorescent ring lamp illuminator and a color digital camera (Model Inifinity 2-1C, Lumenera Corp., Ottawa, Ontario, Canada) with 1392x1040 pixel resolution.

Each of the specimens were dried in a vacuum oven maintained at 37°C for a minimum of 30 minutes and then weighed (Mettler Toledo, d=.01mg). Once gravitational weights and imaging was complete, the OrthoPod was reassembled with application of new bovine serum.   A two-tailed t-test (α=.05) was used to analyze the results for significance.

Bovine serum samples that were collected at the end of each 10km segment were thawed at room temperature for 4 hours. Bovine serum from six stations containing PE-ALN pins were used for this experiment with bovine serum thawed for each 10km segment (24 total samples). In order to remove the proteins from the bovine serum so that it could be analyzed using HPLC, Microsep 3k filters (Pall Life Sciences) were used. These filters contain Omega (modified polyethersuflone membranes); further, they are designed for filtering HPLC samples and are reported to have over 90% recovery of sample. The 3kDa filter was selected as it was larger than the drug we are trying to measure as well as significantly smaller than bovine serum albumin (66-69kDa), which would damage the anion column used in the HPLC methodology. Samples were placed in the Microsep filters and then centrifuged at 3000g for 180min (in two 90 minute

increments) using an Eppendorf Centrifuge 5702R. Ninety minute increments were used

as they were the maximum time for the centrifuge.   The 1mL of the resultant filtrate was

removed using a syringe and filtered through a 0.45 μm polypropylene syringe filters

(National Scientific) prior to injection in an HPLC vial (Waters). Samples were then

analyzed as previously reported in Static Thin Film Elution section above.

3.3 Results

Static Thin Film Elution

Pilot 7-day drug elution tests showed ALN being eluted from the PE-BP thin

films predominantly between day 0 and day 1 (Figure 3.3). After Day 1, the graph

remained flat indicating that there was negligible continued release from the 15μm thick

thin film samples. Control (PE) thin films showed no measurable peak at the ALN peak

time (data not shown).
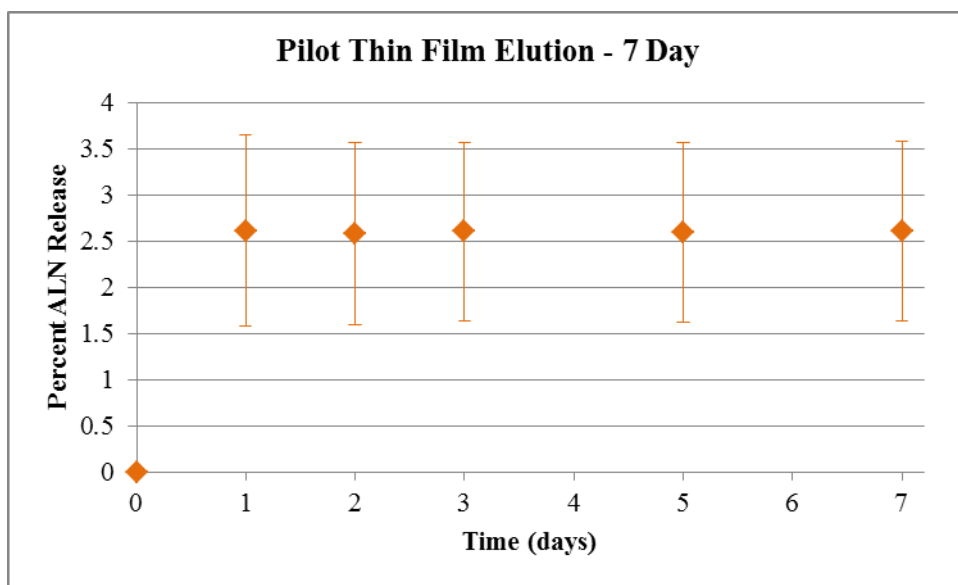
Figure 3.3: Pilot 7-day drug elution results from thin films

Static Thin Film Elution

Longer studies (28-days) confirmed that most of the ALN that would elute is eluted within the first 24 hours. The 28-day thin film elution studies showed that the predominant portion of ALN eluting was within the first 4 hours and after 4 hours little to no ALN was eluting from these 15μm thick thin films (Figure 3.4). Total release was approximately 6% release from PE-BP thin films (60.5 ± 2.2μg) Using ANOVA, there was a significant difference between the ALN released at different depths over the experiment (p=0.000) as shown in Figure 3.5. Samples show approximately 5-7% release regardless of whether they were cut from the exterior or 120um into the sample blocks.
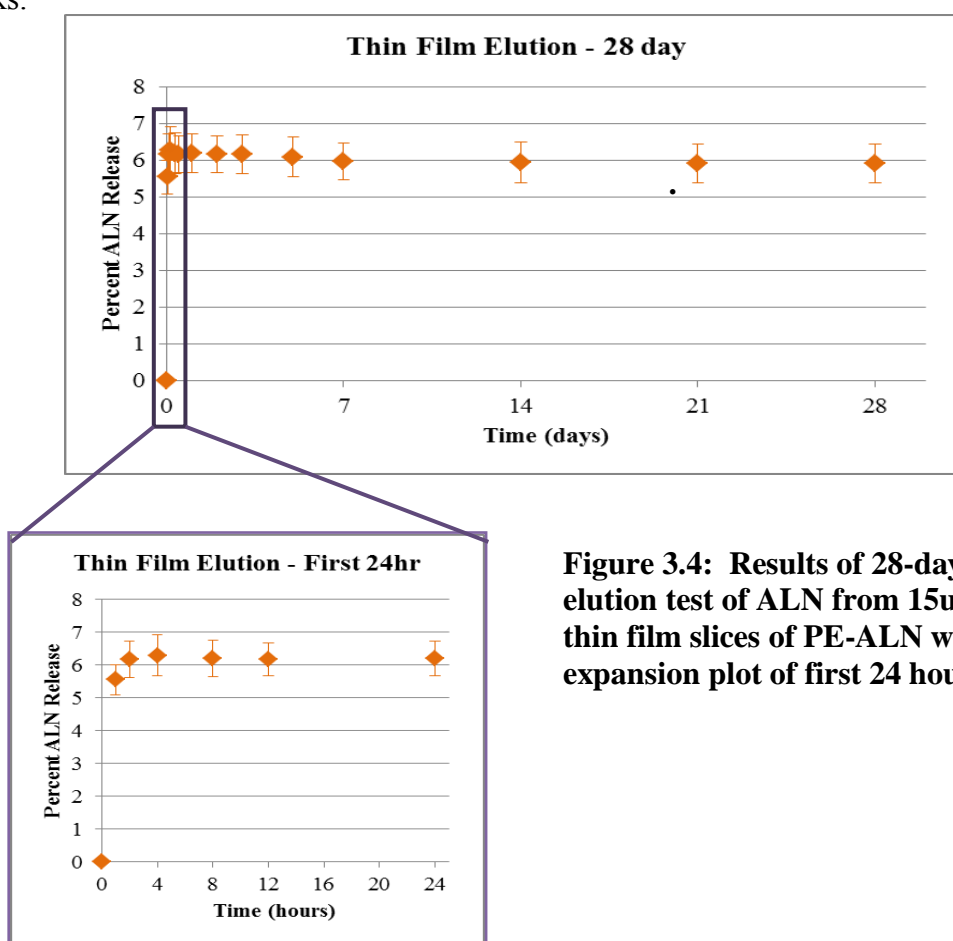
Figure 3.4: Results of 28-day elution test of ALN from 15um thin film slices of PE-ALN with expansion plot of first 24 hours.
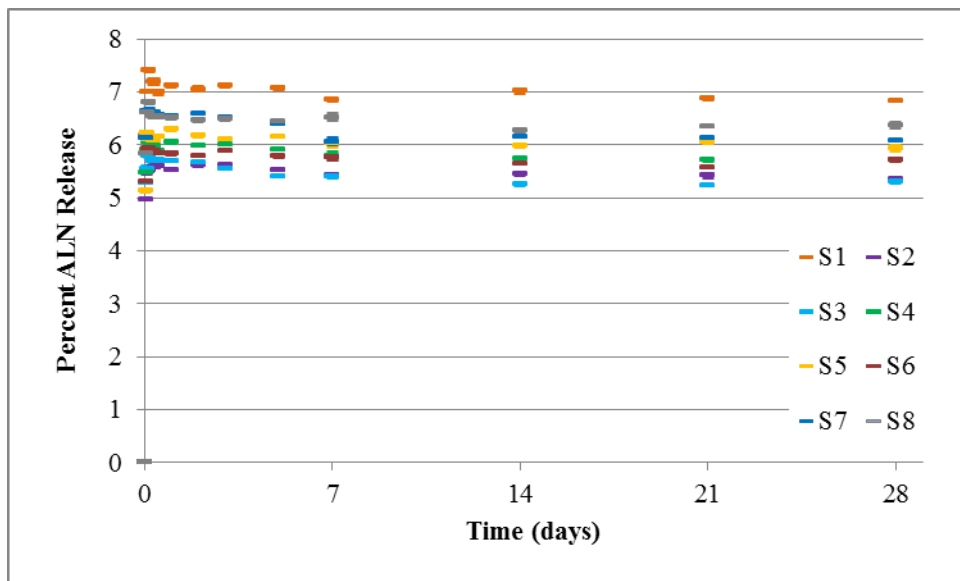
Figure 3.5: Results of 28-day elution test of ALN from 15um thin film slices – Data separated by individual depth of slices (S1 represents 0-15um, S2 = 16-30um, S3=31-45um, etc.; Refer to Figure 3.2 for complete diagrammed list)

Static Bulk Elution

Elution from the bulk samples showed similar results with the majority of ALN being eluted within the first 24-hour time period (Figure 3.6). After day 14, little to no ALN continued to be released from the PE-ALN blocks. After 28 days, approximately $0.14 \pm 0.04\%$ of the ALN had eluted from the bulk specimens ($82.0 \pm 33.4\mu g$ ALN). Again, no ALN peaks were evident in the control samples (data not shown).
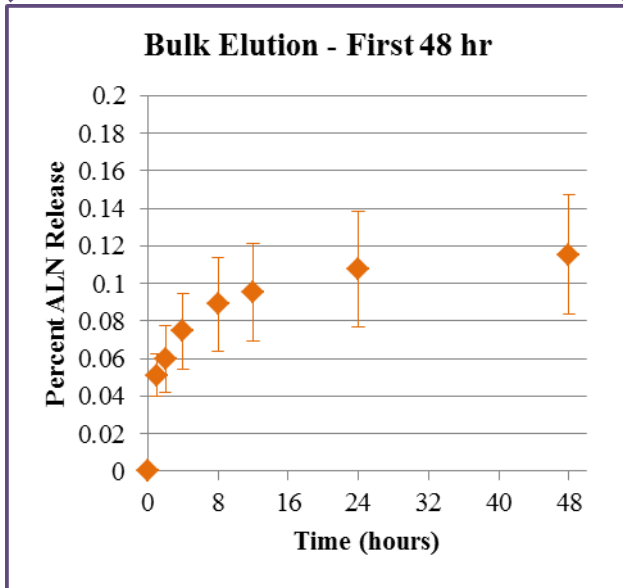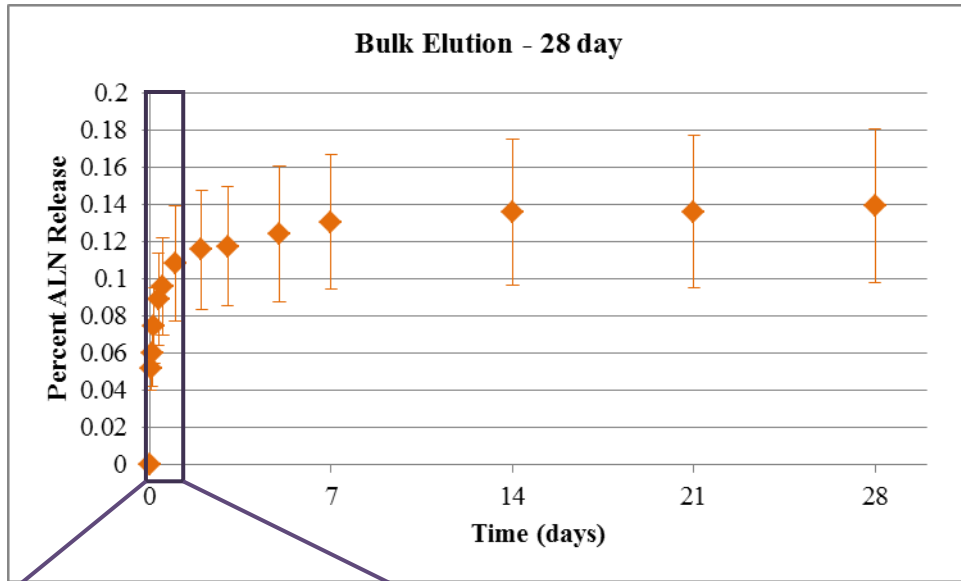
Figure 3.6: Results of 28-day elution test of ALN from bulk PE-ALN blocks with expansion plot of first 48 hours.

Dynamic Elution Using the OrthoPOD

Results of the gravitational weight loss over the 40km time period showed non-significant differences (p=0.26) for the PE-ALN and control pins. Data for each segment of the 40km wear test is shown in Figure 3.7.

Average UHMWPE Weight Change During Wear Testing
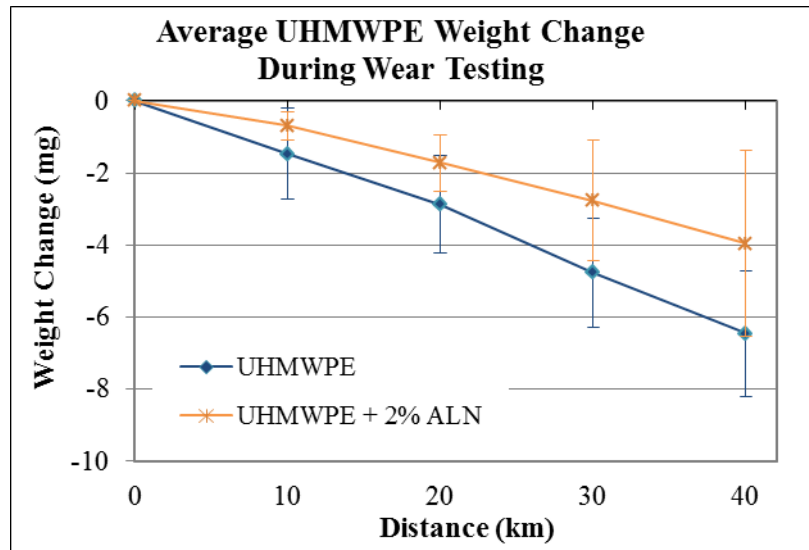
Figure 3.7: Gravitational weight loss over 40km OrthoPOD trial for PE and PE-ALN pins

There was no significant difference (p=0.53) between the average roughness of the two material types over the 40km trial as shown in Table . Both materials showed a decrease in average roughness over time as the materials burnished and initial machining marks worn off. The diamond-coated CoCrMo countersurfaces had an average roughness (Ra) of 20.28±2.92nm at 0km and 13.12 ± 2.06nm at 40km. The crystalline surface is shown in the profilometry image (Figure)
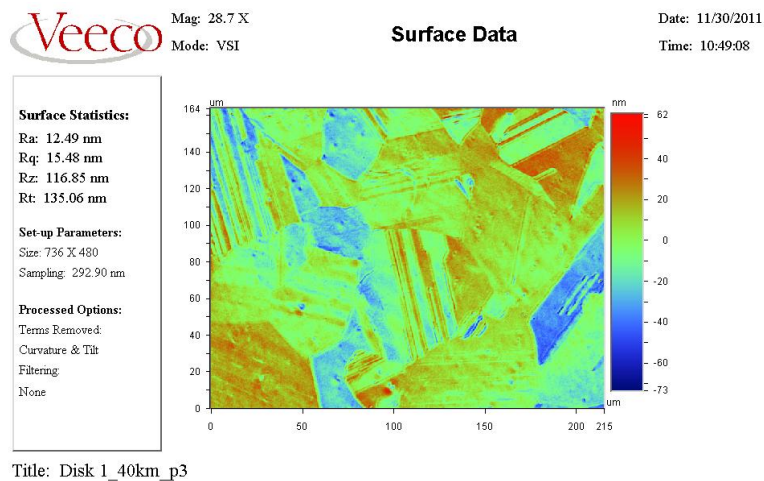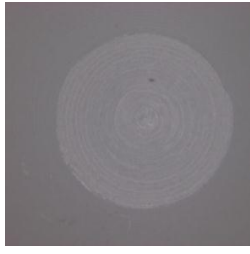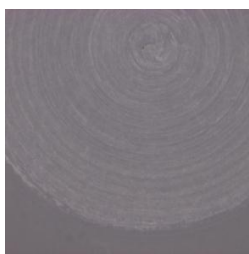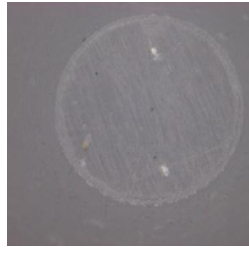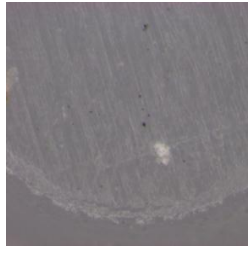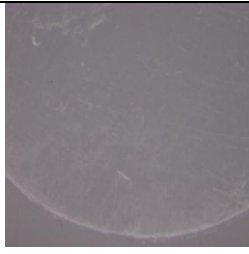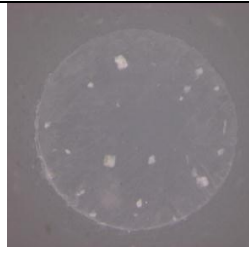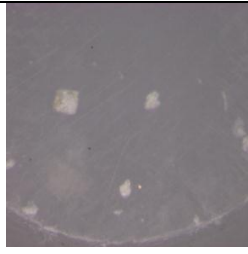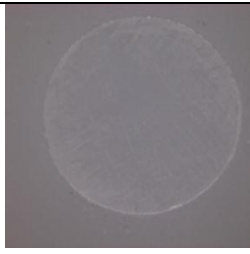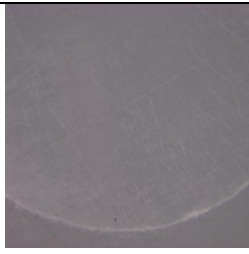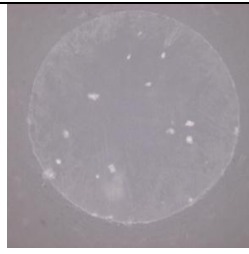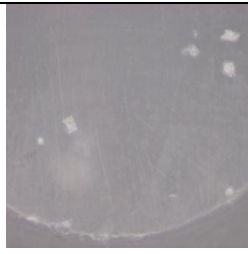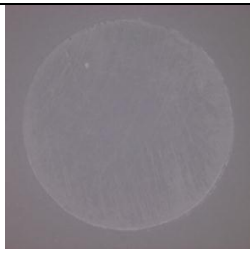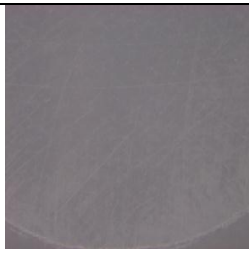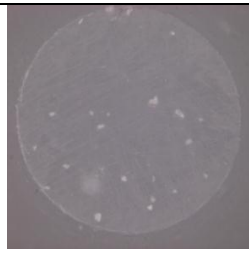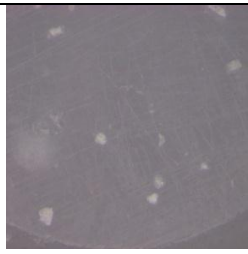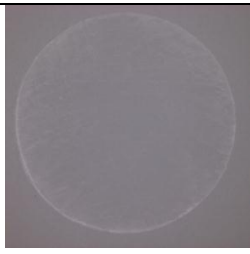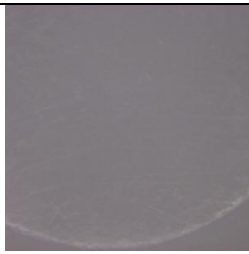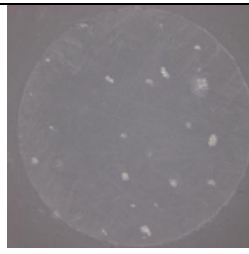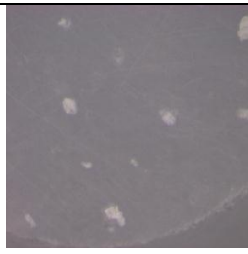
Figure 3.8: Representative topographical image of diamond-coated CoCrMo disks (28.7X)

Table 3.1: Summary of mean roughness (nm) of PE bearing surfaces cycled against diamond-coated CoCrMo over 40km trial

	PE (nm)	PE-ALN (nm)
0km	3940 ± 2667	1069 ± 568
10km	367 ± 436	810 ± 723
20km	188 ± 115	354 ± 346
30km	220 ± 152	346 ± 89
40km	118 ± 47	157 ± 48

Analysis of startup friction showed no-significant differences between the two materials at both timepoints. At start-up, coefficient of friction was found to be 0.15±0.05 for PE and 0.14±0.06 for PE-ALN (p=0.76). For mid-cycle, it was 0.17±0.06 for PE and 0.13±0.05 for PE-ALN (p=0.28).

Gross microscopy showed that all pins at 0km had machining marks on the surface. The concentric circle pattern was more evident on the PE-only pins. PE pins showed burnishing over the wear period and very few surface scratches were evident under gross microscopy at later distances. Additionally, the BP was clearly evident on the surfaces both in the initial 0km images as well as throughout the experiment. BP was evident as bright white spots on the grey-toned PE surface. It should be noted that no BP can be seen on the PE only images. PE-ALN pins also showed burnishing and fewer scratch marks as the experiment progressed (See Figure 3.9). Additionally, some of the PE-ALN pins showed voids where the ALN had eluted out during the last 10km segment of the wear test. An example of this is shown below in Figure 3.10. For microscopy of diamond-coated CoCrMo counter surface and all pins from this experiment (0, 10, 20, 30, and 40km), see Appendix C.

	PE Only		PE - ALN	
	12X	25X	12X	25X
0km				
10km				
20km				
30km				
40km				

Figure 3.9: Representative images of PE and PE-ALN pins during 40km OrthoPOD wear test

	12X	25X	25X
0km			
10km			
20km			
30km			
40km			
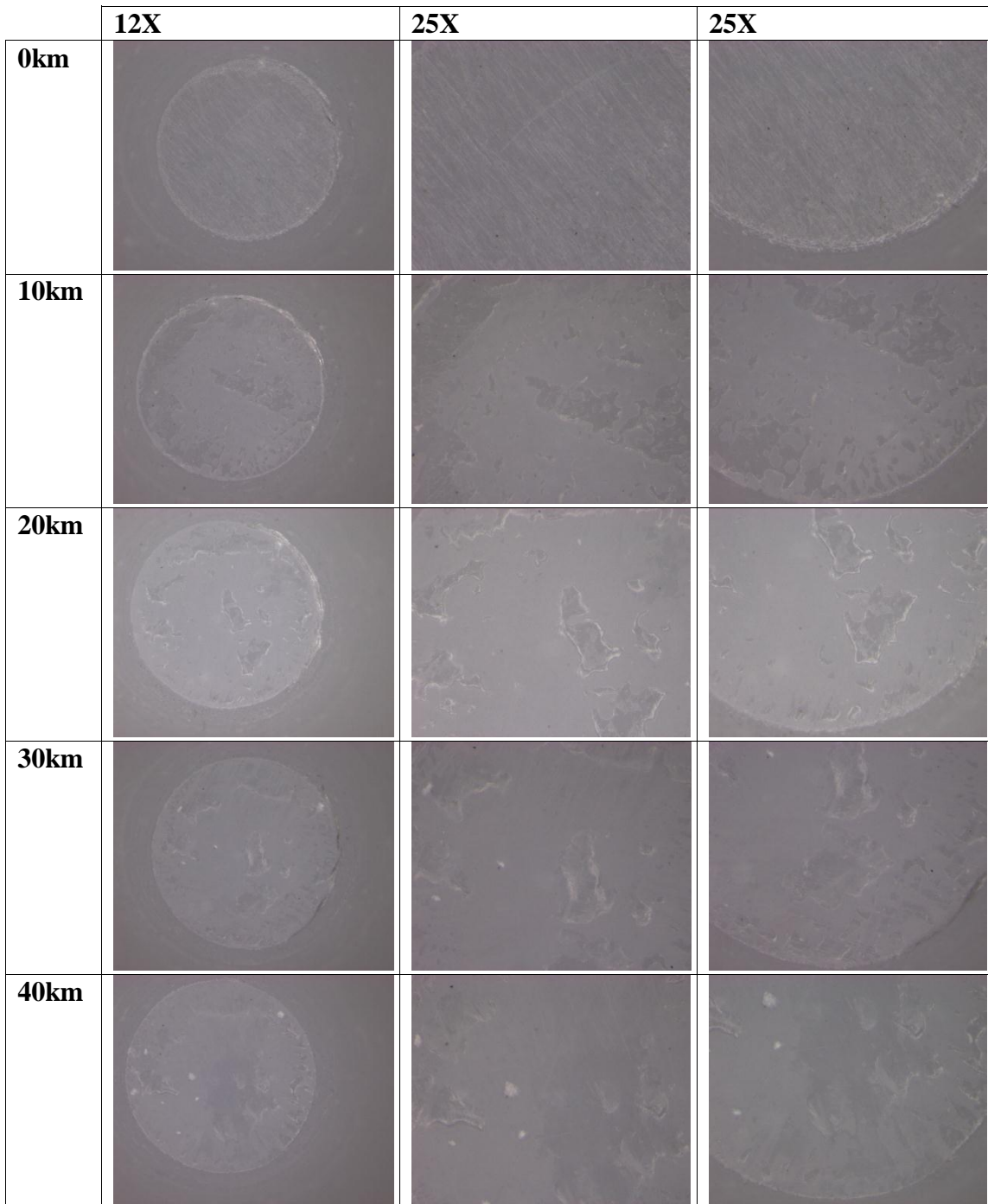
Figure 3.10: Example of a PE-ALN pin showing drug elution pits on pin tip

HPLC results for the functional drug elution were not as clean as previous results as these results are in filtered bovine serum instead of water. There are several unknown peaks in the bovine serum that are small (<3kDa) unidentified biomolecules that were not filtered out. Further, there are small peaks within the filtered ALN in bovine serum that were not shown in the filtered bovine serum only (Figure 3.12). A peak was identified at the same time point (t=1.6min) as the alendronate standards (See Figure 3.11), however, it is not the only peak in the area around the alendronate peak. Below are representative chromatograms from the experiment (Figure 3.13).
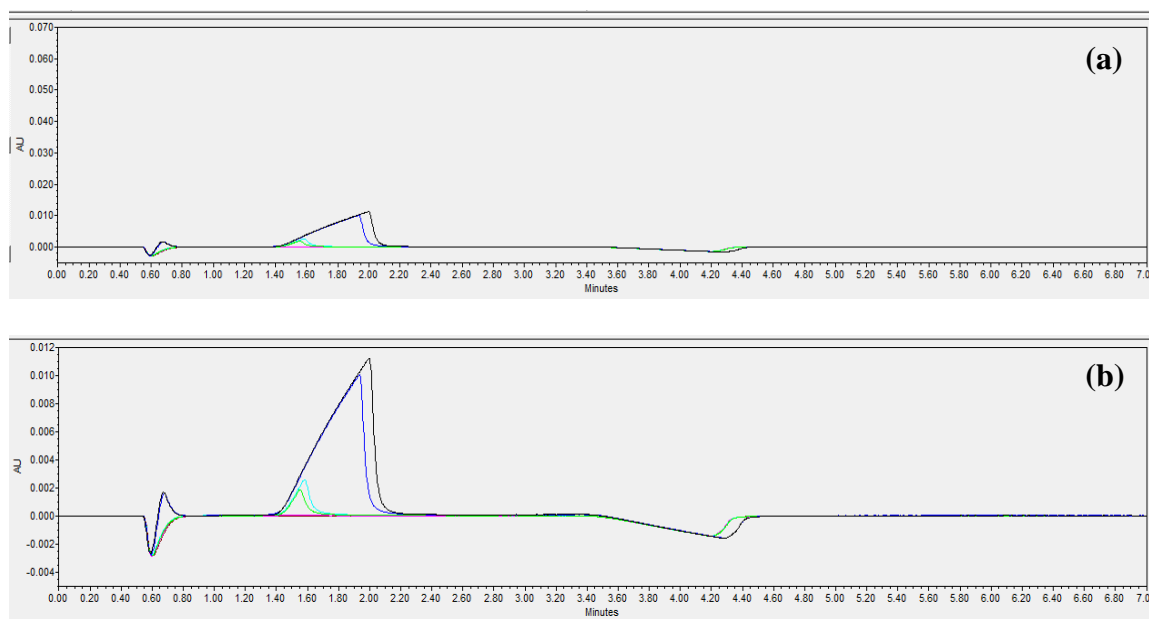
Figure 3.11: HPLC results for alendronate standards (0.4, 0.2, 0.08, 0.04, 0.004) in water (a) full view and (b) expanded view
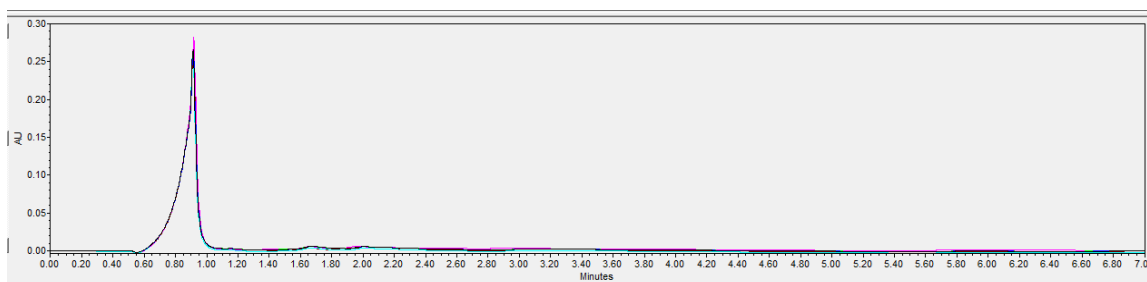
Figure 3.12: HPLC results for filtered 50% bovine serum
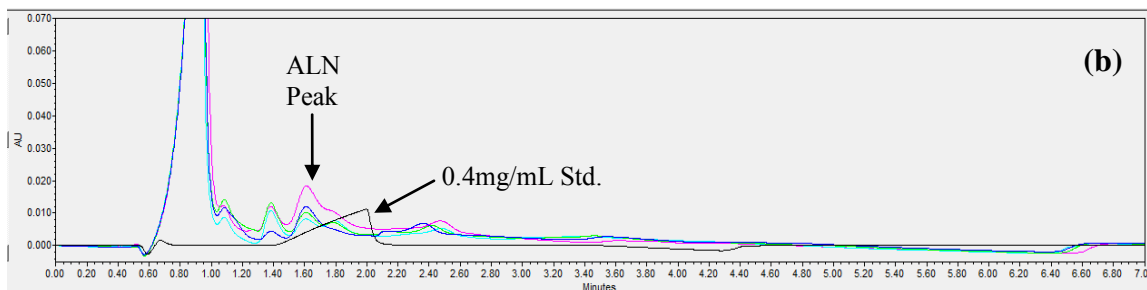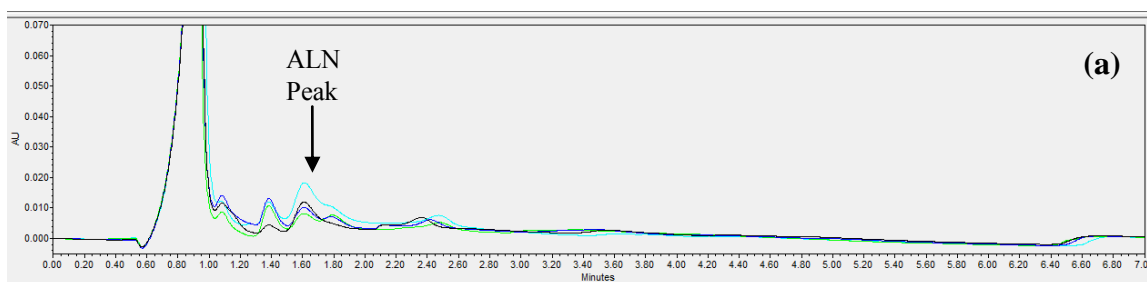
Figure 3.13: ALN release from a representative pin at 10km, 20km, 30km, and 40km (a) time points only and (b) time points with ALN curve from standards overlaid (shown in black)

From the analysis of the ALN standards, the ALN peak is shown at 1.6 minutes. The

ALN peak is still visible in the filtered bovine serum samples from the OrthoPOD,

however the chromatographs are not as precised. These graphs clearly show that there is

ALN released from the pins, however, with multiple peaks within the analysis region, it

makes quantifying those peaks challenging. From the data, if looking at the sole ALN

peak only and ignoring all other peaks, we find that there is an average percent ALN

release of $0.56 \pm 0.12\%$ over each of the 10km intervals. Figure 3.14 shows the

cumulative ALN release over the 40km trial.
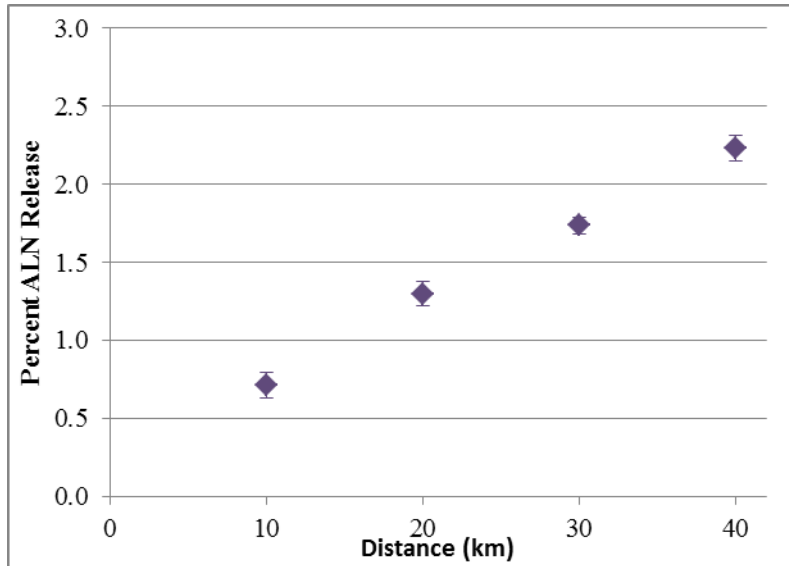
Figure 3.14: Cumulative ALN release over 40km

3.4 Discussion

Both the short and long-term thin film elution studies showed a majority release during the first 24 hours after the material comes in contact with water. This indicates that the thin films will begin releasing ALN immediately upon generation. Further, it should be re-iterated that average particle size from failed total joint arthroplasties is 0.53μm for the hip and 1.190μm for the knee[158]. Therefore, with the particles being much smaller, they will have a larger surface area to volume ratio and thus should release a much higher percentage of the drug contained within the particle. While 1.0cm x 1.0cm x 15μm thick particles are not representative of the most frequent particles generated, the 15μm size is representative of particulate generated via delamination, which is common in TKRs[159]. The size for the thin films used in this experiment was selected as it was the smallest 'particle' we could consistently compression mold and then generate to allow for standardization of our trials.

While the results showed that there was a significant difference between ALN released from thin film slices at different depths, this is due to the extremely small standard deviation for each point as 3 injections were taken from each sample vial. Regardless of whether the sample was cut from the shallowest depth (0-15um) or the deepest (106-120um), there was 5-7% ALN release. Further, there was not a clear gradient of release where the higher release came from the exterior or the interior indicating that it is small inconsistencies of the mixing of the ALN within the material that is attributing to the variation. It should be noted however that these are in fact small differences and there is ALN present and being released at all 8 depths showing that the

drug did not accumulate at the bottom or top surface during molding. This is important as it allows for a continuous pool of ALN present within the PE-ALN components of a total joint replacement allowing extended release of the drug over an extended period of time. It has been reported that the linear wear rate for total hip replacements (THRs) is 0.18mm/year for the first 5 years and then it drops to 0.10mm/yr for years 5-10 in a 10-year study[160]. Therefore, looking at linear wear rate alone, we have shown that there is ALN in the first 120μm (or 0.12mm) and therefore there would be ALN present for at least 8months of implantation. It is likely that the concentration of ALN within the UHMWPE construct is similar deeper into the blocks, however, only the first 120μm superficial thickness was studied.

Additionally, the total concentration of ALN released after 40km was 0.08mg/mL. Moreau and colleagues have previously reported that an alendronate concentration of 10^{-4}M significantly decreases the number of macrophages *in vitro*[144] and this concentration is well above that value. Additionally, Research has shown that the IC50 of alendronate is 50nM[150] and our values are also well above this. However, not all of the ALN released into the synovial capsule will make its way to bone so a higher value of ALN is acceptable and should still decrease the number of macrophages as well as osteoclasts in the bone surrounding the implant.

From the results, it is evident that the ALN exhibits little migration as the bulk elution reached its maximum release over the 28 days by day 14 and then was constant afterwards. This gives credit to the concept that the ALN will remain in the PE once it is

placed *in vivo*. Using the known surface area, volume, and density of each cube the

depth of release can be calculated using

$$\frac{Total\ Release\ [\mu g]}{mm^2} = \frac{Release\ [\mu g]}{Surface\ Area\ [mm^2]}$$

$$Depth\ of\ release\ [\mu m] = 1000 * \frac{\frac{Total\ Release\ [\mu g]}{mm^2}}{\rho\ [\frac{\mu g}{mm^3}]}$$

Using each block's respective drug elution at day 14, the calculated drug elution only

occurs from the outer 0.05±0.01 micron of the blocks. These results are in strong

contrast to previous studies where BPs were encapsulated into Poly(D,L-lactide-co-

glycolide-D-glucose) microspheres (abbreviated PLG-GLU) [138, 139], this UHMWPE

appears to have a high enough hydrophobicity as well as a tight enough matrix that the

100% release within the first 24 hours seen with those microspheres. The highly

hydrophobic UHMWPE, even though it is known to absorb some liquid in aqueous

environments, appears to maintain the ALN within its matrix even though ALN is highly

hydrophilic.

For the pin-on-disk experiment, as expected, the pins at 0km were rougher than at

completion of the trial after 40km. This is expected due to machining marks present on

the surface of the pins at the beginning of the trial that are removed by 20km distance.

Further, the PE-ALN had a lower initial roughness as the pin tip of one of these pins was

1 of these pins did not have a machined edge but had the compression molded edge from

the edge of the block. While all pins were machined at the same time by the same

machinist, there still exists variability between the pins. Further, each pin had 5 points where the average roughness was measured. This is a small percentage of the overall area and these measurements are indicators only and not the penultimate surface roughness.

Over the course of the 40km trial, it can be observed that the bisphosphonate is eluting out of the pin tips as voids are present in the pin tips when viewed using light microscopy. These voids do have the potential for increasing the wear of the surface as they decrease the contact area thus increasing the pin tip contact stress. However, short term wear studies have not shown this to increase wear rates rates. This may be attributed to the lower modulus of elasticity shown in earlier experiments leading to better elastohydrodynamic lubrication [147, 148]. It should be noted that the BP is not as evenly distributed as was in the earlier PE-tag experiments. No clumps could be visually seen in the PE-tag experiment however, early PE-BP components had clear evidence of clumping. Attempts to separate the drug were completed by grinding using a mortar and pestle for 10minutes followed by immediate measurement then mixing with PE using the vortexer. This achieved non-visible at the gross level clumping of the drug. However, during the pin-on-disk experiment, it was noticed that there was still non-uniformity of the drug dispersion within the pin tips as shown in the images. Mixing using high shear rates available in commercial equipment may help alleviate this problem.

The HPLC studies do show that there is some release of the drug at each of the 10km time points along the 40km trial. There are a number of small peaks within the normal area that the ALN peak is found that are not found in the filtered bovine serum

alone. These may be other biomolecules or degraded drug that is bound to other biomolecules within the filtered bovine serum. The peak data doses show a small release which mimics that of the earlier drug elution experiments. In contrast to previous studies where BPs were encapsulated into Poly(D,L-lactide-co-glycolide-D-glucose) microspheres (abbreviated PLG-GLU) [138, 139], this UHMWPE appears to have a high enough hydrophobicity as well as a tight enough matrix that the 100% release within the first 24 hours seen with those microspheres has not been shown with the current material. Further, the continuous release over the 40km experiment shows that the drug is in fact present in the pin tips and is eluting as the surfaces are wearing. It should be noted that the apparent percentage released is lower for pin-on-disk testing as only the pin tips were in lubricant, not the entire pins from which percent released is calculated.

3.5 Conclusion

Pin-on-disk tests showed no significant differences between the wear of these two materials for short test duration. Further, BP can be seen in the wear pins over the course of experiment indicating that there is in fact drug remaining in the pins throughout these experiments. Additionally, HPLC results indicated that there are small amounts of BP release over the course of the trial. However, a more aggressive and in-depth experiment such as a knee simulator test is needed to validate whether a difference exists between the wear rates of these two materials.

— CHAPTER FOUR —

AIM 3: Knee Simulator Experiment

4.1 Introduction

Currently, ultra-high molecular weight polyethylene (UHMWPE) is the bearing

countersurface used in all total knee replacements. This UHMWPE undergoes high

repetitive stresses both compressive as well as shear that leads to wear particle generation

and possible delamination. Ultimately the body's reaction to these particles results in

osteolysis and failure of the implant. Therefore the driving force in development of new

UHMWPEs and sacrificial bearing surfaces is the reduction of osteolysis.

High doses of gamma radiation as well as gamma radiation + vitamin E doping

have previously been used to reduce the generated particulate. However, even if wear

rates are reduced, there is still particulate generated and therefore osteolysis is still a

potential problem. This research approaches the problem differently in that it is not

attempting to decrease the amount of wear generated but using the wear generated for a

positive outcome.

Previously in this research, we showed that bisphosphonate (BP) could be blended

into UHMWPE; this methodology has also been used for integrating Vitamin E into

UHMWPE[87]. Then, pin-on-disk tests gave us an initial idea as to whether the material

would be successful in the short term. While pin-on-disk tests are good for initial

examination of the tribological properties of a material, a deeper understanding using a

more robust experiment set-up is needed. A knee joint simulator with full-scale

components that could be used *in vivo* was used to examine longer term tribological properties. The goal of this study was to show that bisphosphonate-enriched UHMWPE tibial inserts are tribologically comparable to virgin UHMWPE tibial inserts. Ultimately, the goal of these inserts is not to reduce the wear of the material but rather to use the particles as local drug delivery systems to manage the effects of the particles on the surrounding tissue.

4.2 Materials and Methods

A total knee simulator experiment was conducted as a more rigorous wear test and generic right tibial plateau and femoral component. This design was selected to use already existent custom compression mold for the tibial insert allowing for compression molded components instead of machined.

Tibial components were molded using solely GUR 4150 UHMWPE (Ticona) or GUR 4150 UHMWPE with 2% alendronate sodium (ALN), a bisphosphonate (BP). Each PE and PE-BP specimen was molded using the same methodology previously described in Specific Aim 1.

A 4-station Stanmore/Instron Knee Simulator was used with two stations containing PE and PE-BP for a 2-million cycle experiment. The molded components were machined to lock within the tibial plateau. The bearing surfaces of these components were compression molded; however, to have proper use of the locking mechanism, grooves had to be machined into the anterior and posterior non-weight bearing surfaces of the components.

Lubricant used was 50% defined calf bovine serum (Hyclone, Logan, UT) diluted with deionized water + 0.2% w/v sodium azide (NaN_3, Sigma) as an anti-microbial agent per station. Approximately 0.5L of the lubricant was cycled through each station throughout each segment of the trial. Each station had its own lubricant reservoir to minimize potential contamination. Lubricant containers were maintained at the base of the knee simulator with a sensor at the tibial cup to ensure that the stations always had lubricant. Additionally, the simulator was set to 'automatic pumping mode' so that lubricant was circulated every 10 minutes for the duration of the experiment. Due to evaporation, lubricant levels were checked and topped off twice a day to ensure that a 50% concentration of bovine serum was maintained.

For 0 to 1 million cycles, the samples were removed and cleaned at every 250,000 cycles to assess if early failure occurred. From 1-2 million cycles, segments of 500,000 cycles will be used. The testing environment was maintained at 35°±2°C to mimic physiological conditions. To supply and track the actual waveforms, an external computer interface was used (General Robotics Ltd., Milton Keynes, England) to ensure that the input waveforms were performing adequately. ISO standard 14243 for force controlled-simulators was used as a guideline for this experiment to determining appropriate waveform inputs with cycles occurring at 1Hz. Waveforms inputs were determined through an iterative process prior to the start of the experiment; they were considered acceptable if the average deviation over the gait cycle was less than 10% of the ISO 14243 standard. Deviation from the ISO standard was monitored throughout the experiment.

The duration for the study was two million cycles, which represents approximately one year of use in patients. This experiment was aimed at elucidating whether PE-BP does in fact wear at a similar rate to UHMWPE using a more rigorous test. Every 250,000 cycles (0-1M) or 500,000 million cycles (1-2M), the simulator was stopped to weigh the tibial inserts following cleaning and drying. All the test specimens were cycled between stations every 250,000 or 500,000 million cycles depending on which segment of the test was occurring. This was done to minimize the effects of inter-station variability on resulting wear rates as there were slight differences in the roughnesses of each of the four femurs.

Kinematic and kinetic data were recorded by logging files from the simulator approximately every 12 hours. Each file included 15 seconds of data measured at 50Hz. Logged files were assessed daily to ensure that simulator operation was maintained within 10% of the ISO standard. Files included information such as flexion angle, axial load, anterior/posterior displacement, internal/external tibial rotation, anterior/posterior implant shear reaction force, and internal/external implant reaction torque.

Two specimens of each material (PE and PE-BP) were maintained as non-loaded soak controls in 50% bovine serum with 0.2% sodium azide within a $35° \pm 2°C$ environmental chamber to allow for calculation of fluid absorbed into the specimens. The tibial inserts (both experimental and soak) were cleaned using ASTM F1715 method at the end of each interval (1/4 or 1/2M cycles). After cleaning, the tibial inserts were allowed to dry for 24 hours in a desiccator under vacuum prior to weighing (Mettler

Toledo, d=.01mg). Tibial components, cups holding the components and the tubing in the knee simulator were cleaned with a bleach and detergent mixture at each time point.

Finally, non-contact profilometery and stereomicroscopy were conducted at 0 and 2 million cycles to analyze the surface for microscopic changes in wear that may not be apparent via the gravimetric weights. Non-contact profilometery (NT-2000 Non-Contacting Surface Profilometer; Wyko, Tucson, AZ) was performed on 8 points per insert (4 points/condyle) at the prior to and after the experiment. The gross images of the tibial inserts were recorded using stereomicroscopy (Model K400P, Motic Inc, Xiamen, China) at 6X & 12X magnification to view the center of medial and lateral bearing surfaces at the beginning and end of the study (0 and 2M cycles). Stereomicroscope used attachments for image acquisition including a fluorescent ring lamp illuminator and a color digital camera (Model Inifinity 2-1C, Lumenera Corp., Ottawa, Ontario, Canada) with 1392x1040 pixel resolution.

 The femurs were analyzed using non-contact profilometry (6 points per condyle (12 points/femur)) and stereomicroscopy (12X, 6 points/femur) before and after the experiment.

Further, two tibial plateaus were imaged using a Hitachi S-3400N SEM after experimentation had finished to compare the surfaces within the wear condylar wear path. Variable pressure (30Pa) SEM at 100X and 250X was used to investigate the primary modes of wear. It was expected that these would be polishing and burnishing, however, as this is a composite material other modes may be seen such as abrasion if the drug is harder than the polyethylene and scratches its surface. Additionally, we used

Energy-dispersive X-ray spectroscopy (abbreviated EDX or EDS) to analyze the surface to evaluate whether there was ALN on the surface of the tibial inserts. For analysis of the EDX spectrogram, it is important to know that the k-line for phosphorus appears at 2.0.

Finally, calculation of wear for this experiment was soak control-corrected using the gravimetric weights from the 4 specimens in the environmental chamber. Two-tailed t-tests (α=.05) will be used to analyze the results for significance.

4.3 Results
Simulator Performance

Figure 4.1 shows that the ISO standard for walking was followed during the trial. Further, Figure 4.2 shows the results of the maintenance of the waveform within 10% of the ISO standards. Flexion, axial, and internal/external torque were maintained within the "good"0-5% error) throughout the experiment while A/P actuation force was maintained within the acceptable region (5-7.5%) as shown in Figure 4.2).
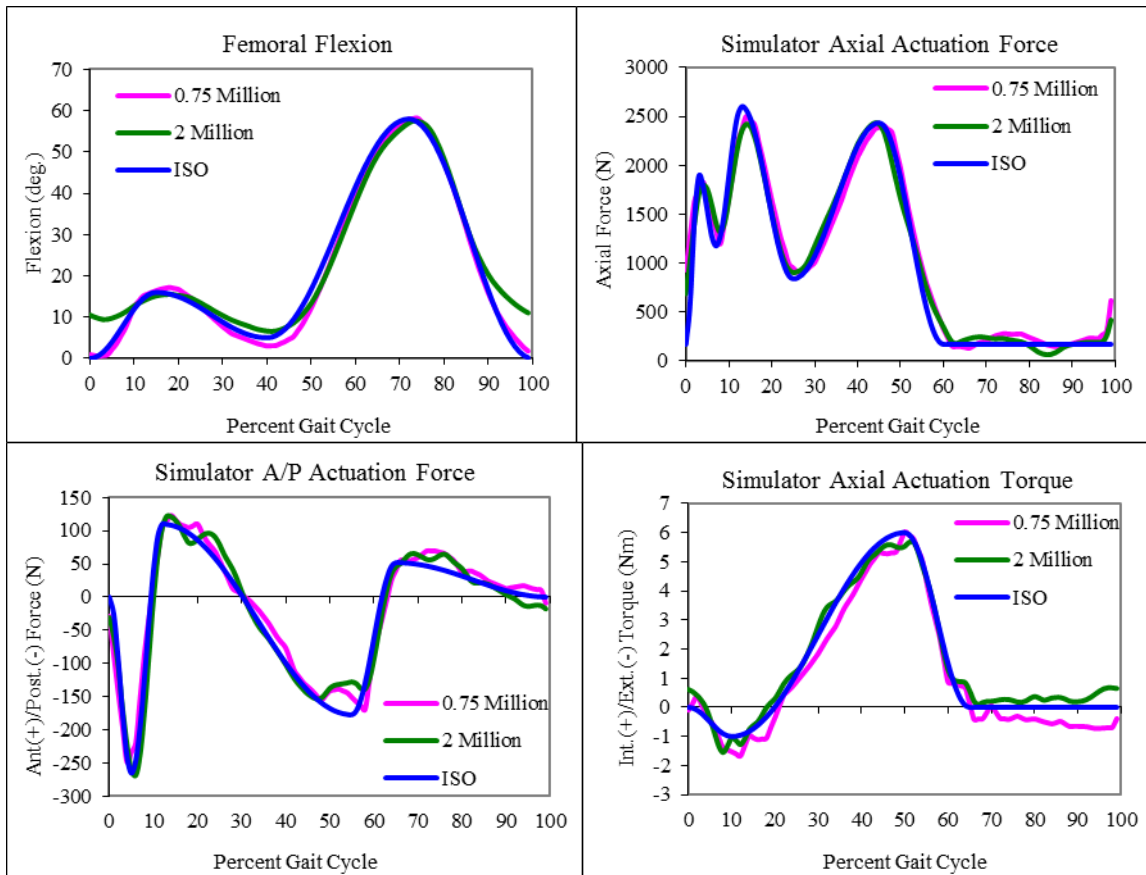
Figure 4.1: Simulator performance from beginning of trial (0.75M cycles, pink) to end of trial (2M cycles, green) superimposed over the ISO Standard
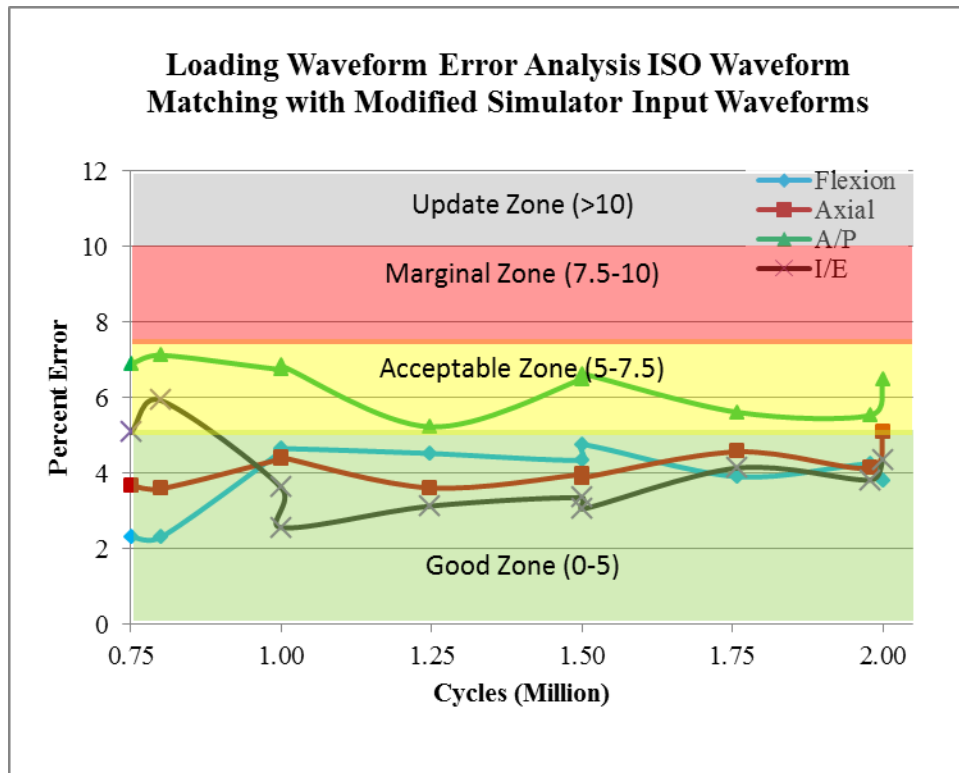
Figure 4.2: Loading waveform error analysis ISO waveform matching with modified simulator input waveforms

TKR Kinetic and Kinematic Results

All stations performed similarly in kinetic and kinematic performance. Figure 4.3 and

Figure 4.4 illustrate a comparison of the averaged 4-station values for 0.75M and 2M

cycles. The shift in tibial global A/P motion is attributed to replacement of the axial

bearing during the experiment.
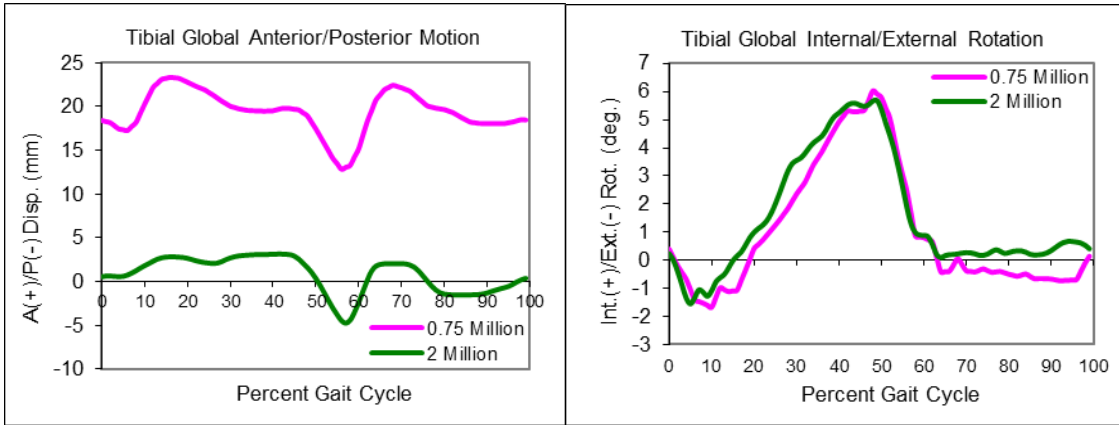
Figure 4.3: TKR kinematics over the gait cycle (0.75M – 2M cycles)
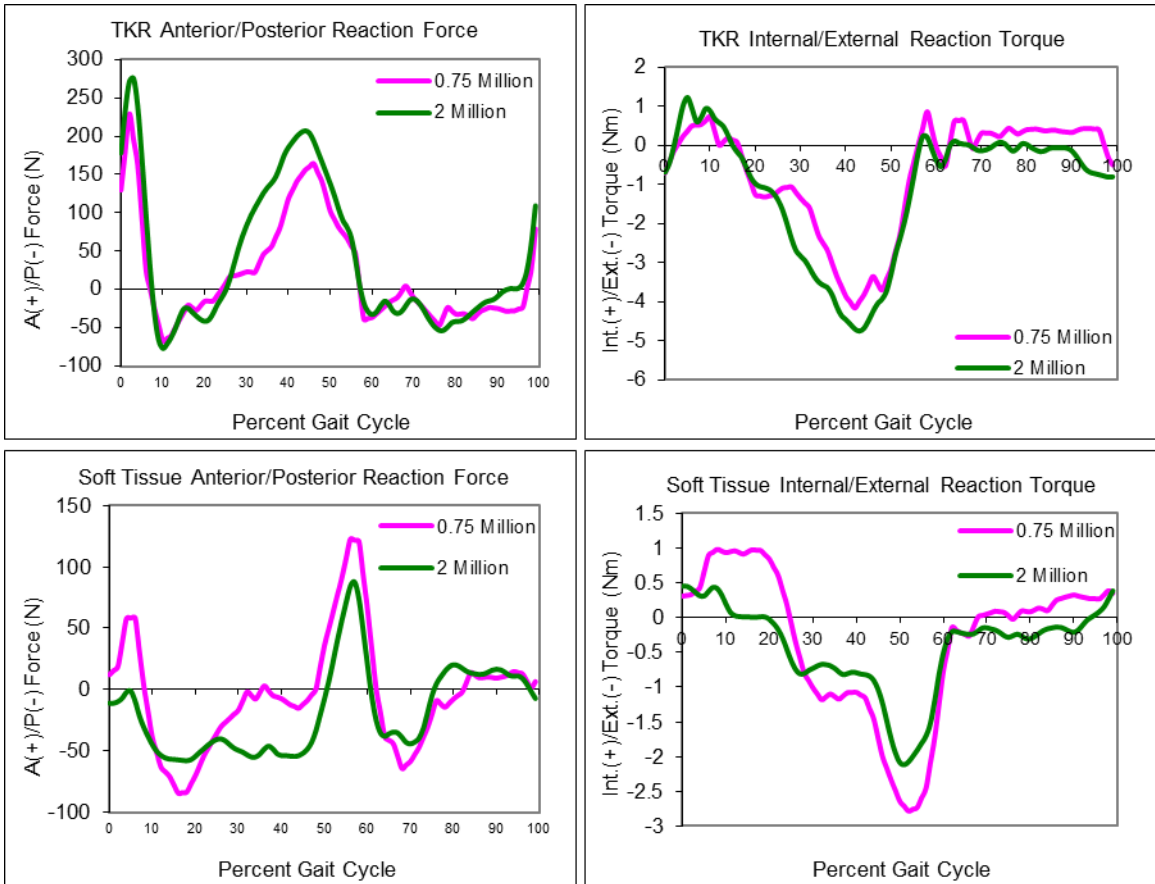
Figure 4.4: TKR implant and soft tissue forces over the gait cycle (0.75M – 2M cycles)

Femoral Countersurface

Using non-contact profilometery, it was found that the 4 femurs had an average roughness of 43.5 ± 23.4nm at the beginning of the TKR experiment. Representative images are shown in Figure 4.5.

Stereomicroscopy was also completed of the femurs (12X) prior to starting the test to have a better visualization of the differences in roughness among the femoral components. It can clearly be seen that the femurs have abrasion along the wear track. All images in Figure 4.6 are from the medial side of the femur along the wear track (Lateral images were similar, but are not shown below).
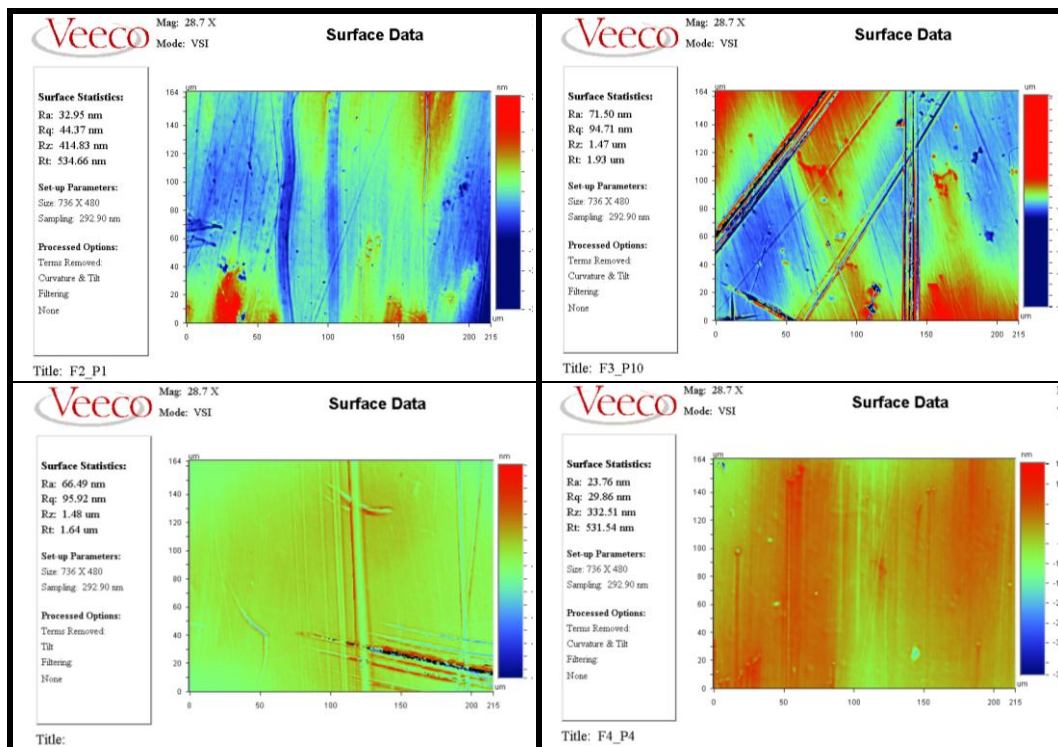
Figure 4.5: Representative images of non-contact profilometry scans of femurs at 0M cycles (28.7X)

	Femur 1	Femur 2	Femur 3	Femur 4
0°				
45°				
90°				
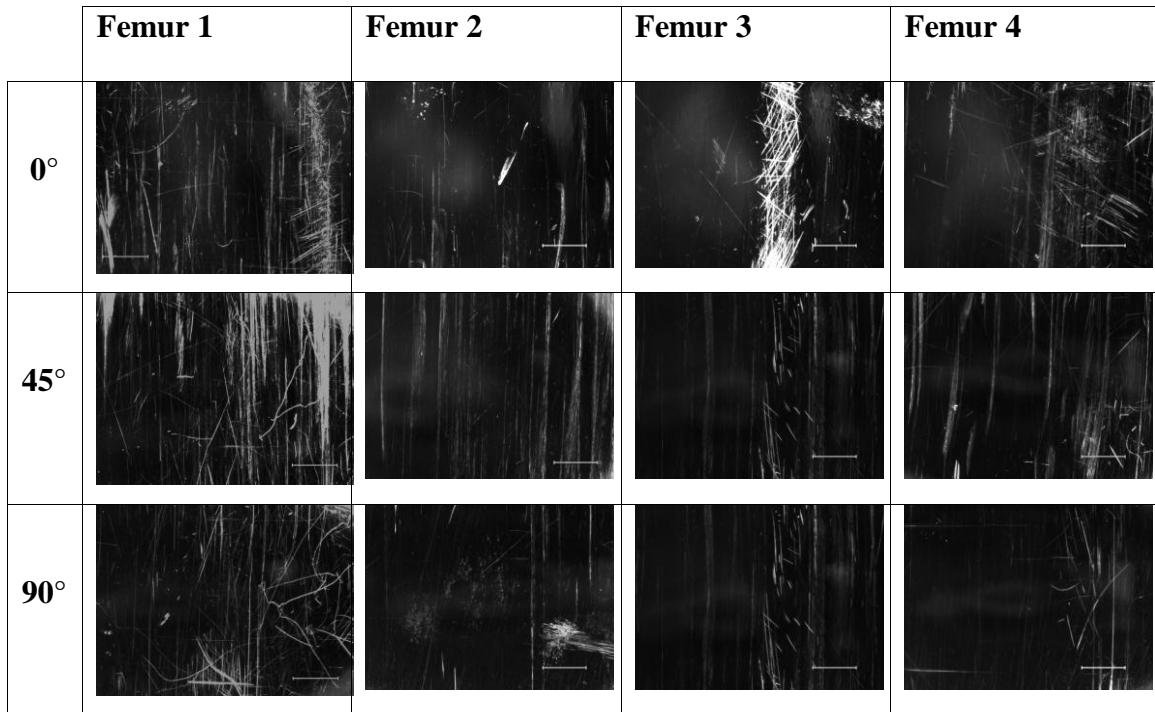
Figure 4.6: Stereomicroscopic images (12X) of femurs at 0°, 45°, and 90° prior to TKR study (Note: each measurement bar represents 1000μm)

Material Performance

The roughnesses of the PE and PE-ALN components decreased by 31.6% and 56.4% respectively (See Table 4.1). There was not a significant difference in the Ra (p=0.51) or Rq (0.57) values at 0M between the two materials. At 2 million cycles, PE-ALN was significantly rougher than the PE only, both for Ra (Ra, p=0.002) and Rq (0.01). Representative images for PE and PE-ALN at 0M and 2M cycles are shown in Figure 4.7.

	PE Only	PE - ALN
0M		
0M		
2M		
2M		
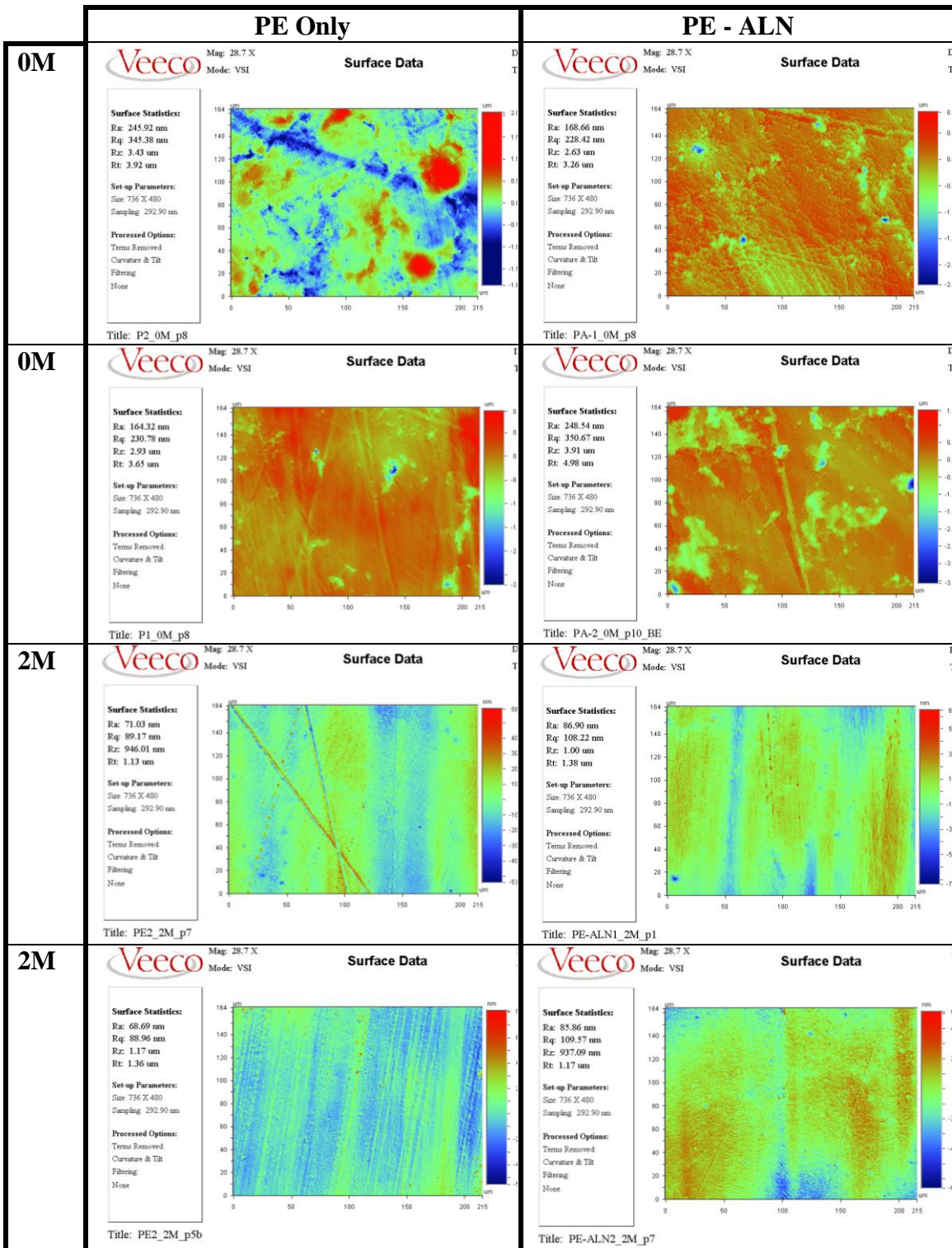
Figure 4.7: Representative images of non-contact profilometry scans of PE and PE-ALN at 0M and 2M cycles (28.7X)

Table 4.1: Summary of mean roughness (nm) and root mean squared roughness (Rq) of PE bearing surfaces cycled against roughened CoCrMo femurs over 2 million cycles

	Ra (nm)		Rq (nm)	
	PE	**PE-ALN**	**PE**	**PE-ALN**
0M	156.8 ± 53.7	276.4 ± 127.5	221.3 ± 66.1	388.6 ± 176.3
2M	$107.3 \pm 46.6^{*}$	$120.5 \pm 30.6^{*}$	$138.8 \pm 56.9^{\dagger}$	$154.3 \pm 41.0^{\dagger}$
	$^{*}p = 0.002$		$^{\dagger}p = 0.01$	

Stereomicroscopy was also completed before and after the experiment. Images from the beginning of the experiment showed uniform compression molded surfaces for both materials with a few scratches from the molding process (Figure 4.8). Images at 2M cycles exhibited the expected wear track on both condyles (Figure 4.9 and Figure 4.10). Images from the center of the wear track show burnishing and scratching. It is evident at the anterior and posterior of the tibial insert the delineation between the wear path and the unworn compression molded surfaces. Additionally, bisphosphonate is apparent in the surfaces of the PE-ALN samples at both timepoints (Figure 4.8 - 4.10).

	PE Only	PE - ALN
0M (6X)	1000 µm	1000 µm
0M (12X)	1000 µm	1000 µm
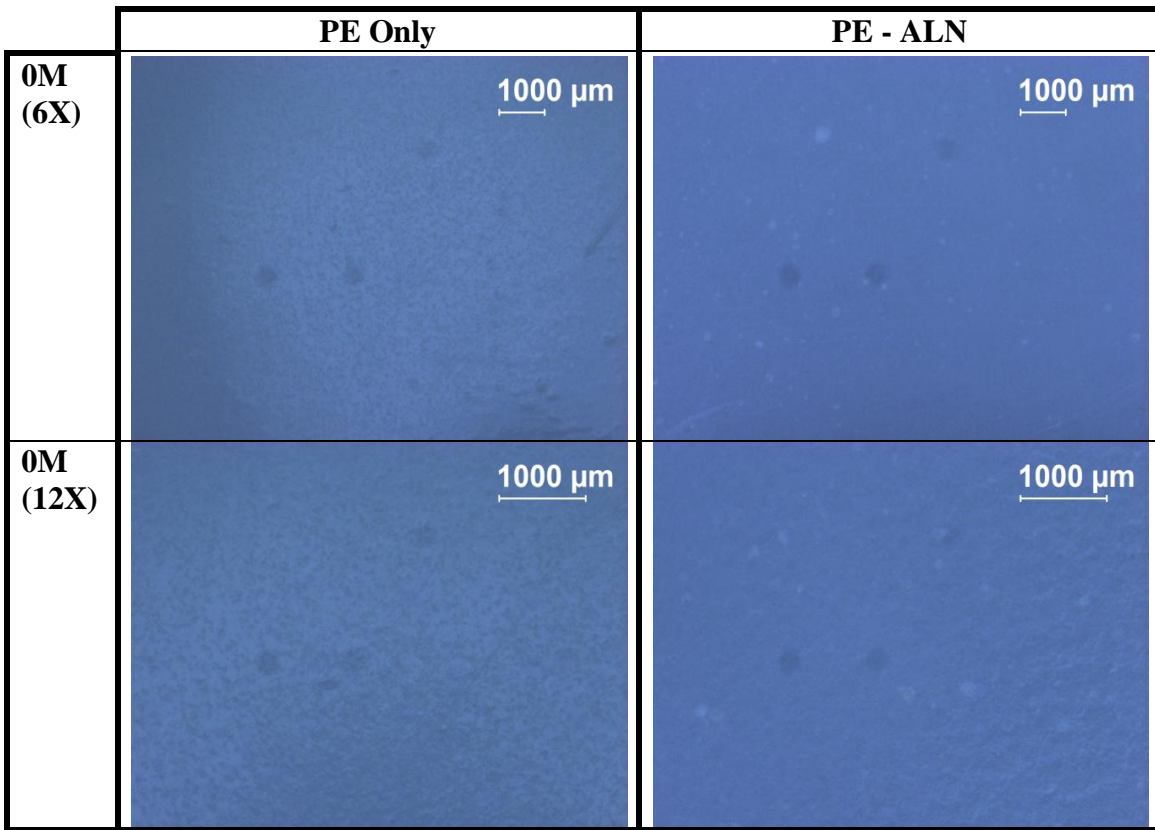
Figure 4.8: Representative stereomicroscopic images of PE and PE-ALN at 6X & 12X magnification
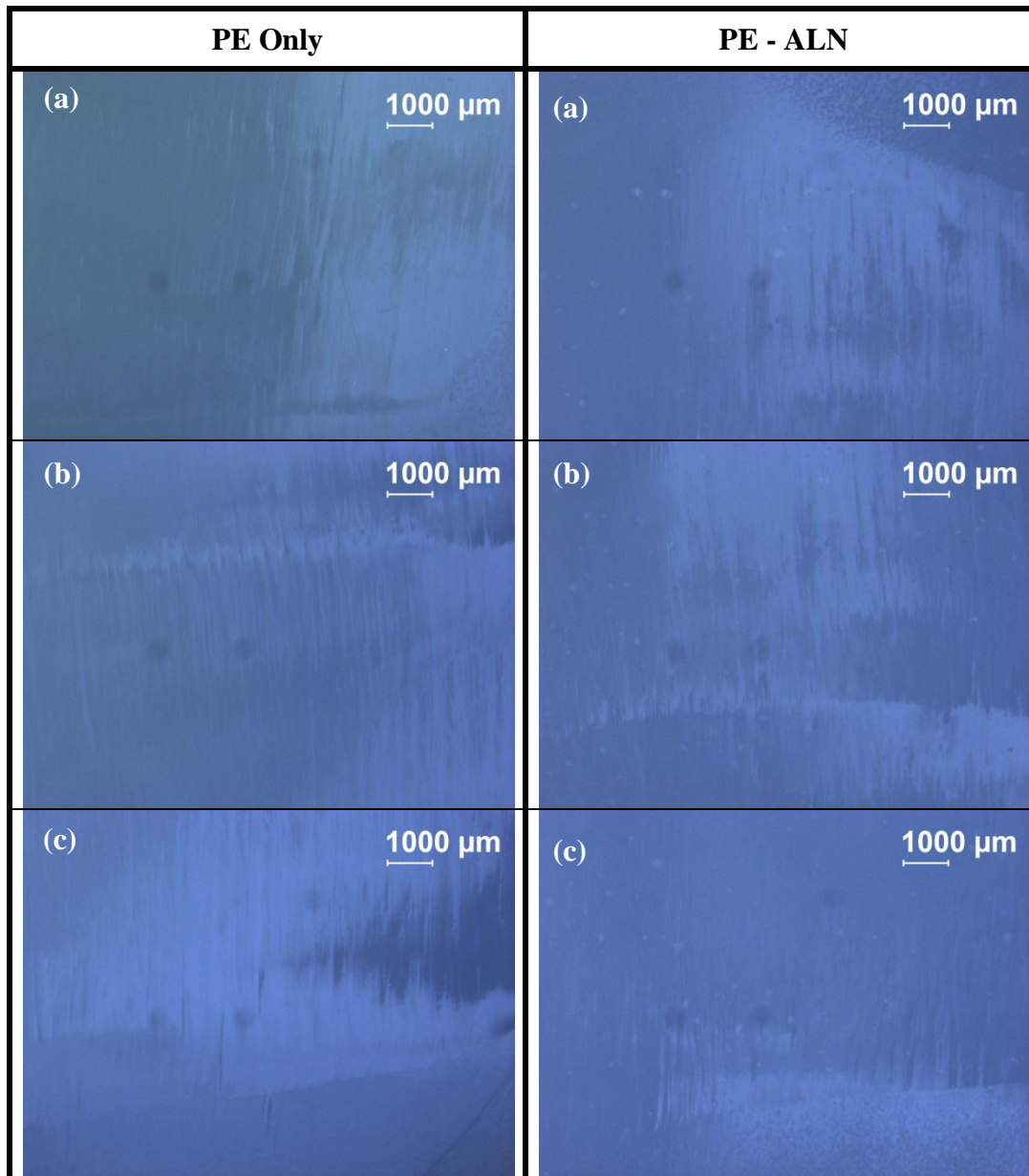
Figure 4.9: Representative stereomicroscopic images of (a) anterior, (b) center, and (c) posterior of wear track at 6X magnification

PE Only	PE - ALN
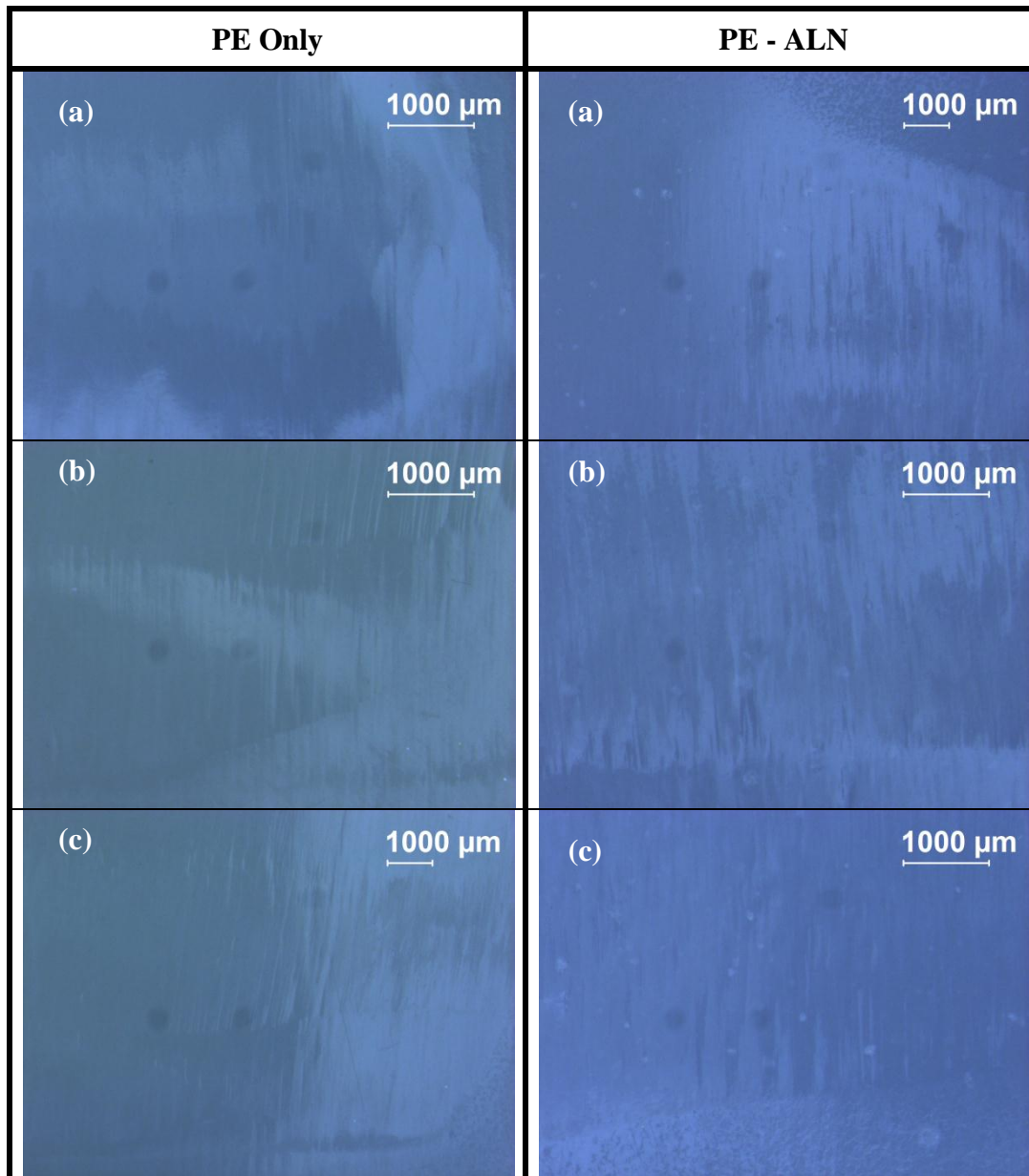
Figure 4.10: Representative stereomicroscopic images of (a) anterior, (b) center, and (c) posterior of wear track at 12X magnification

The SEM images show non-worn specimens at 0M (Figure 4.11 and Figure 4.12). These specimens show residual Teflon in the outer surface of the implant as evidenced by the white spots on the SEM images. This was confirmed using EDX. The only peaks shown in the EDX spectra were carbon (C) and Fluorine (F) (Figure 4.13). UHMWPE is comprised of carbon and hydrogen while Teflon is comprised of carbon and fluorine. No ALN (specifically the phosphorus) was found using EDX. The primary modes of wear that can be observed in these images are scratching and burnishing.
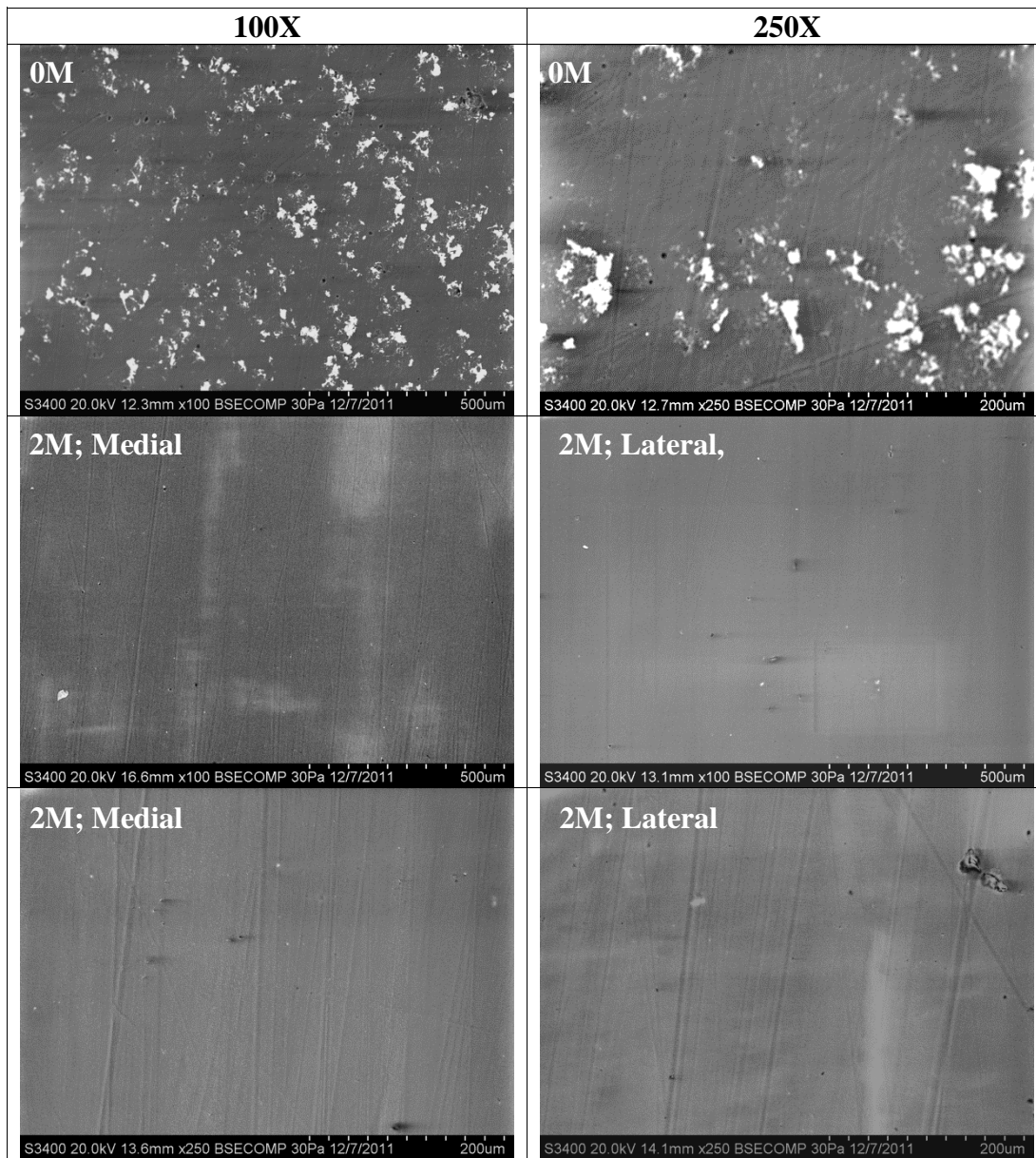
Figure 4.11: Representative SEM images of PE-ALN at 0M and 2M cycles (100X & 250X magnification)
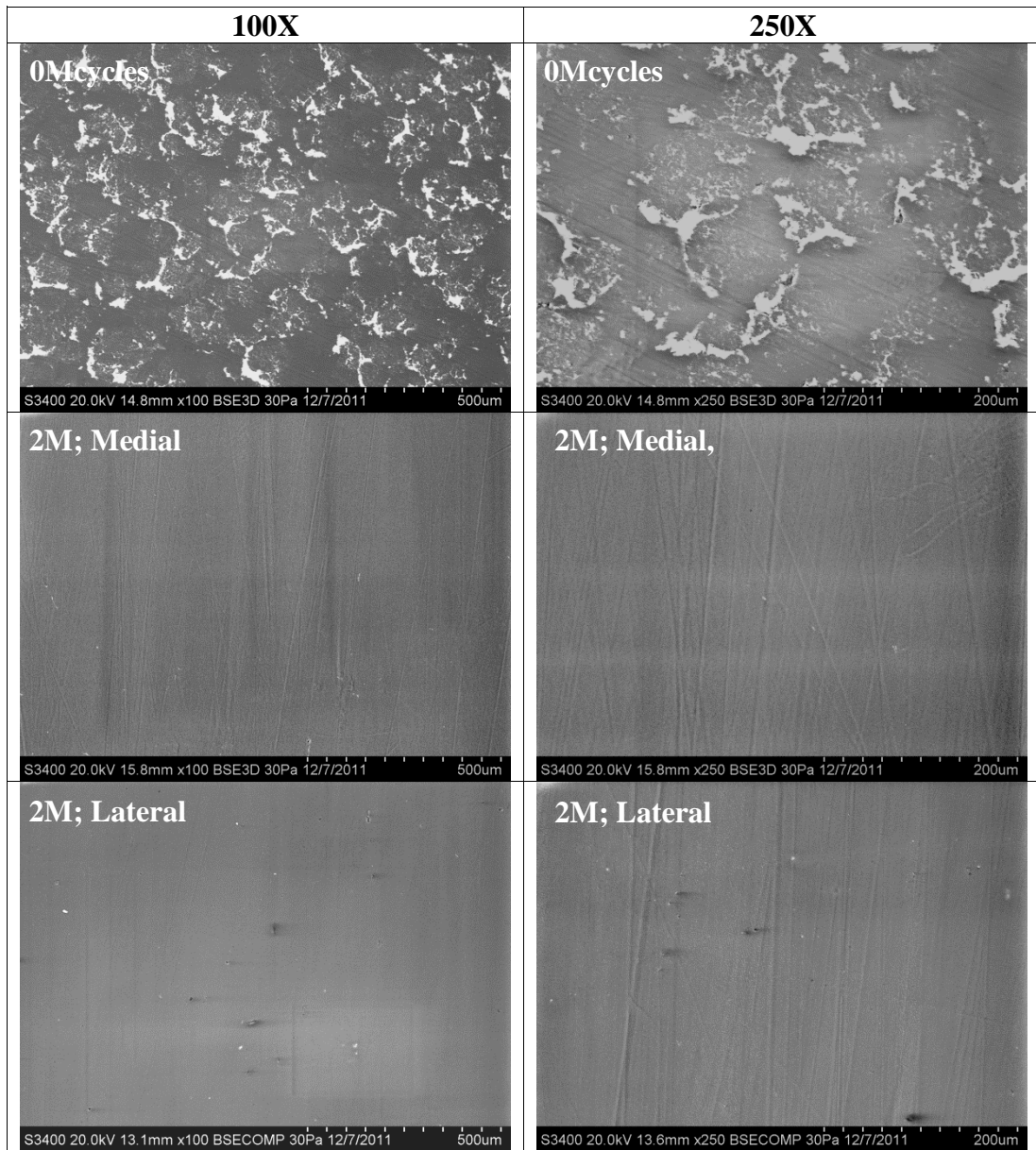
100X	250X

Figure 4.12: Representative SEM images of PE at 0M and 2M cycles (100X & 250X magnification)

Spectrum processing :
No peaks omitted

Processing option : All elements analyzed
(Normalised)
Number of iterations = 5

Standard :
C   CaCO3   1-Jun-1999 12:00 AM
F   MgF2   1-Jun-1999 12:00 AM

Element	Weight%	Atomic%
C K	89.15	92.86
F K	10.85	7.14
Totals	100.00	
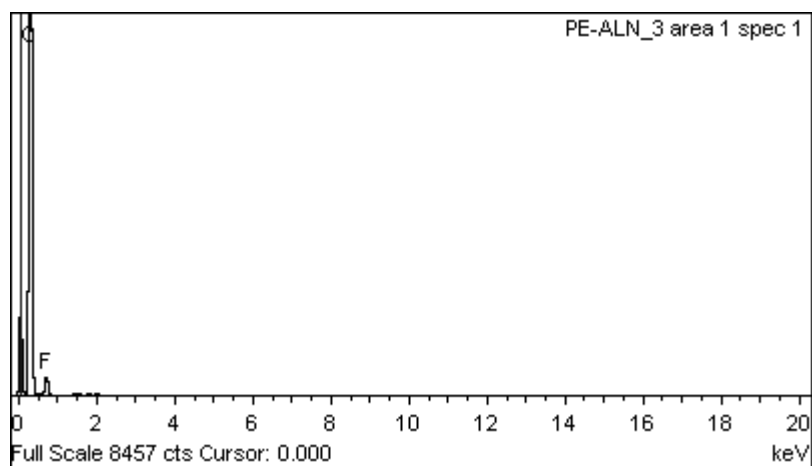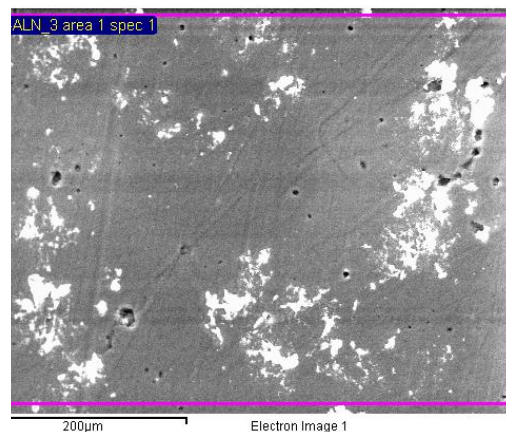
Figure 4.13: Representative EDX spectra

Gravimeteric Weight Loss Results

All specimens showed steady raw weight loss over the 2M cycle trial (Figure 4.14). Further, the soak control specimens continued to gain weight over the course of the trial (Figure 4.16).

From the graphs it can be observed that over the 2 million cycles, the tibial components showed similar gravitational loss (Figure 4.15). The lines diverged more at 2M. The average weight loss per million cycles was not statistically different between the two materials (p=0.14) with 37.2 ± 14.2mg for PE and 47.3 ± 16.9mg for PE-ALN (Figure 4.17).
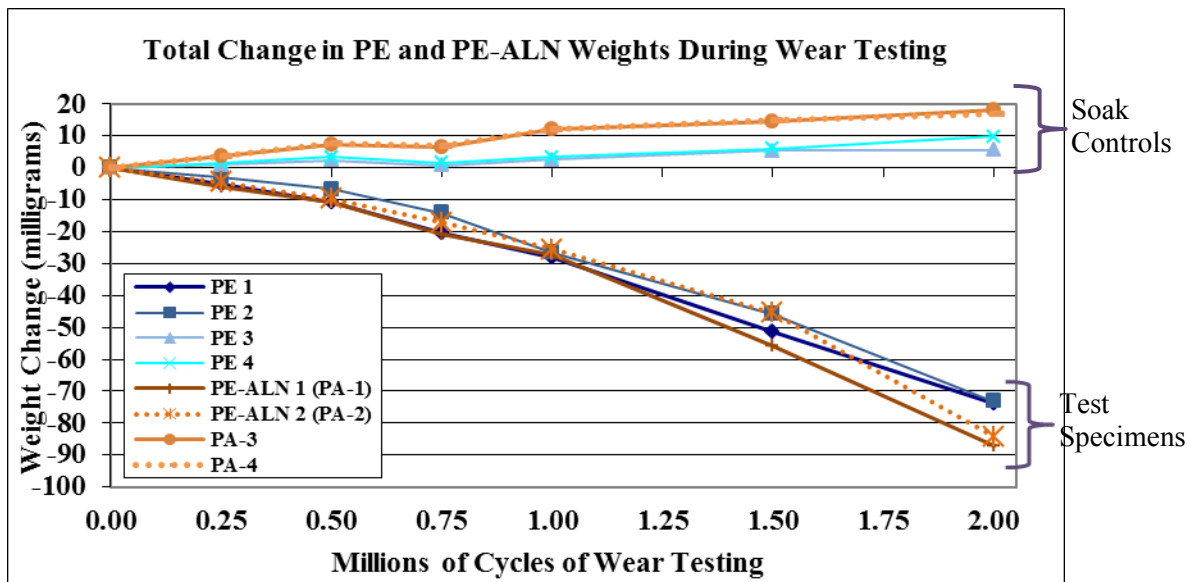
Figure 4.14: Summary of the total change in weight of PE and PE-ALN over 2M cycles
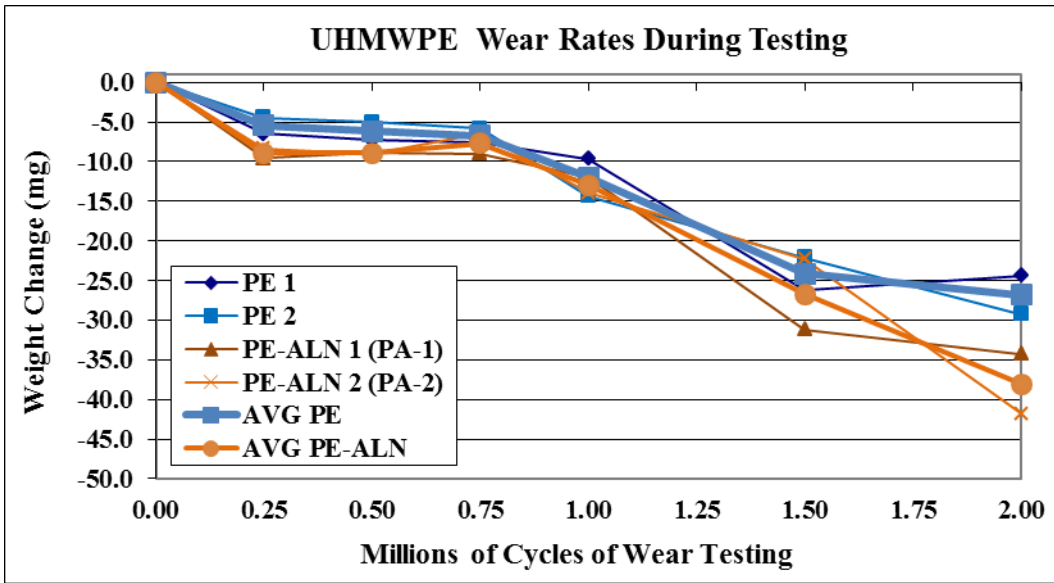
Figure 4.15: Summary of the soak control corrected total change in weight of PE and PE-ALN over 2M cycles
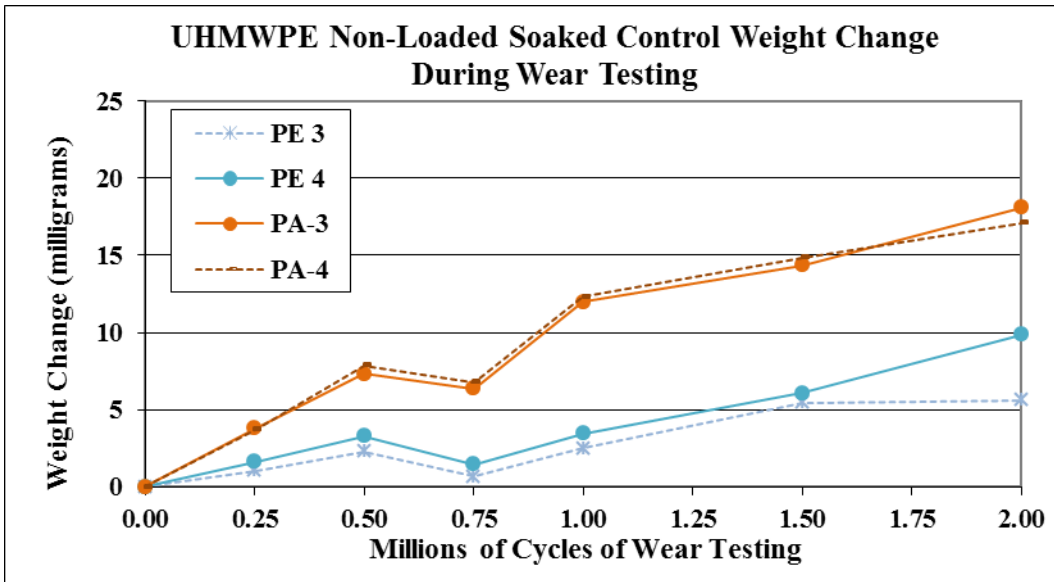
Figure 4.16: Expanded view of non-loaded soak control specimens over 2 million cycles
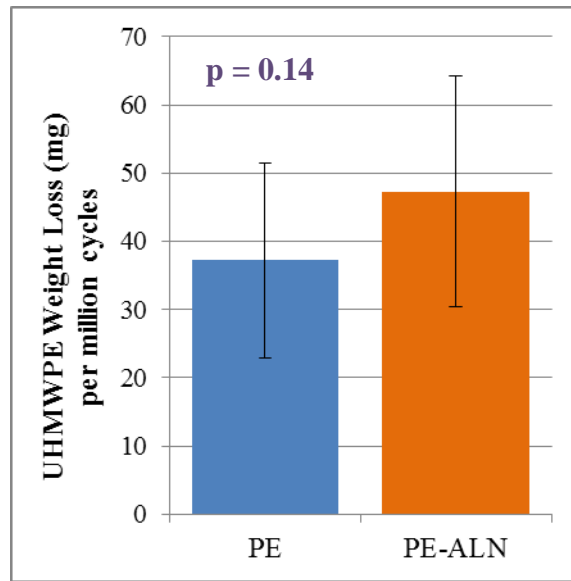
Figure 4.17: Average per-million weight loss of PE and PE-ALN over 2M cycle trial

4.4 Discussion

The results of this test show that there is a non-significant difference between the two materials. This is an aggressive test due to the higher Ra of the femoral components that is run over a short number of cycles (2M instead of 5M). It is unknown whether the divergence seen at 2M cycles is an anomaly or an actual increase in wear rate (and thus decrease in gravitational weight) of the PE-ALN. It should be noted that there exists much more variability in a total knee simulator test than a pin-on-disk test as there are many more moving components and more variables that can affect the outcome. A 5M cycle test would help elucidate this issue.

One additional concern is the shelf life of bisphosphonate. From the manufacturers, the shelf life of bisphosphonate is two years. Bisphosphonate released will bind to the exposed hydroxyapatite, where it will remain bound until osteoclasts attempt to resorb that section of bone. The drug does not become active until both the drug and a small amount of the bone (specifically the hydroxyapatite) have been ingested by an osteoclast. Merck has reported in its prescribing information that alendronate has a terminal half-life of more than 10 years in the human skeleton if it can become bound before being excreted. However, while the drug is bound to bone, it is inactive. At a minimum, if using the shelf life only, the drug will be relased for the first two years. However, the drug is likely to be active longer than its shelf life, the first two years. Further, there is already precedent on the market for drug loaded materials that are left in place after the drug would expire, namely the antibiotic-doped polymethylmethacrylate (bone cement) products used in orthopaedics that remain in the body until revision or the patient expires. There are several currently on the market but some examples are Simplex P with Tobramycin (Stryker) and Palacos R+G (includes Gentamicin; Zimmer).

4.5 Conclusion

The overall wear rates of PE-ALN in comparison to standard PE was not significantly different and therefore this material does have the potential to be a new enriched UHMWPE for future use *in vivo*.

— CHAPTER FIVE —

CONCLUSIONS

The objective of this investigation was to develop and characterize a bisphosphonate-enriched ultra-high molecular weight polyethylene (UHMWPE) for biomedical applications. The mechanical and tribological properties of the novel material were evaluated using standard tests such as tensile testing, pin-on-disk tests, and total knee simulator experimentation. The main hypothetical question was whether a BP-enriched UHMWPE that would wear similarly to the current gold standard of UHMWPE could be developed.   It has been shown through tensile testing that a material with similar yield strength can be generated. Further, pin-on-disk and total knee simulator tests showed no significant differences in the gravitational weight loss during the process. The other main concern with this material was whether or not the drug would release. High pressure liquid chromatography (HPLC) experiments have shown that there is very little migration of the drug over 28 days and functional wear tests have shown a continued release of drug over a 40km wear regime. Based on comparisons with virgin UHMWPE, this material possesses sufficient mechanical and tribological properties to merit consideration for use in the orthopaedic bearing applications.

— CHAPTER SIX —

PROJECT RECOMMENDATIONS

Future project recommendations:

- Repeat the HPLC for the OrthoPOD pin-on-disk test as there is still 10mL of frozen serum. This time, however, run 3 groups of deproteinated bovine serum: PE-ALN, PE only, and new filtered serum. The reason to this would be to elucidate what the small peaks in the range of ALN are; whether they are resultant of the degrading bovine serum, if they are degraded drug, or a combination of both.

- A 5 million cycle test to ensure the two materials have similar wear rates.

- A long-term animal model in order to look at 4-6 month performance of this material compared to a standard PE model. The recommendation would be to do a canine model. This would require either a large grant or industry support. But, prior to *in vivo* tests, a large animal model is necessary. As both materials have already been tested *in vitro* and *in vivo* a small animal model may not be necessary.

- Determine whether the PE-ALN can be cleaned and gamma sterilized at the higher doses used for crosslinking. It is known that the ALN can be sterilized at normal sterilization doses from previous PMMA-ALN studies performed in other labs. This would allow for secondary material, XLPE-ALN, for applications that prefer the highly crosslinked polyethylene. If ALN is still viable after the high

doses of gamma sterilization, then do tensile testing, OrthoPOD testing, and a 5M cycle knee simulator test.

- Once patenting has been completed and if XLPE-ALN is viable, create a new blend using 0.2% vitamin E or other antioxidant in conjunction with a lower dose (e.g. 1%) ALN. If this blend can be made, then do tensile testing, OrthoPOD testing, and a 5M cycle knee simulator test.

APPENDICES

APPENDIX A

Additional Results from Specific Aim 1

Additional graph of uniaxial tensile test data for UHMWPE and UHMWPE + tag specimens.
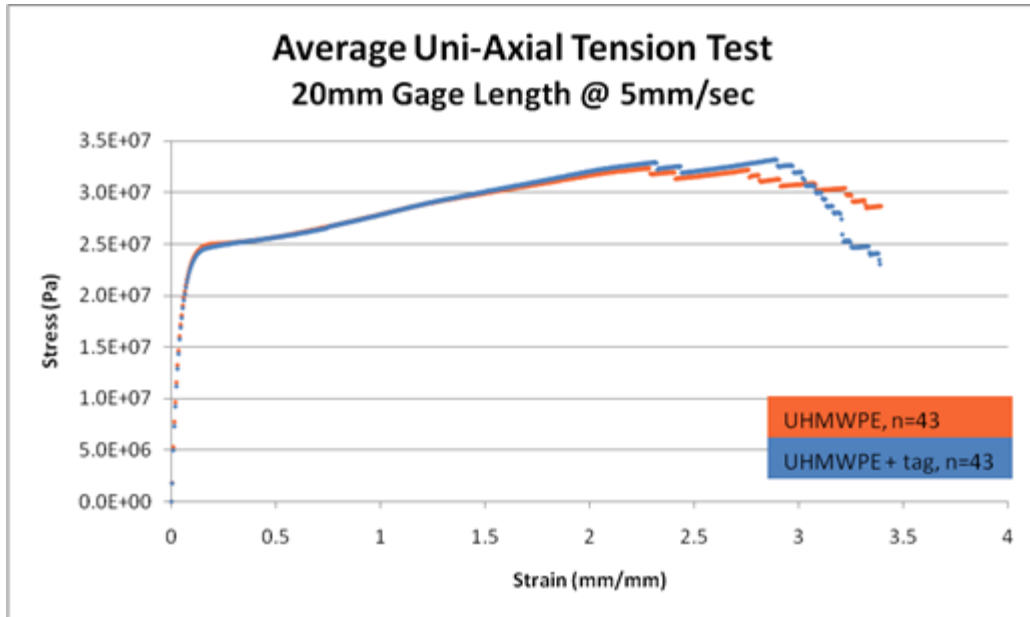
Figure A-1: Uniaxial Tensile Test Data for UHMWPE and UHMWPE + tag
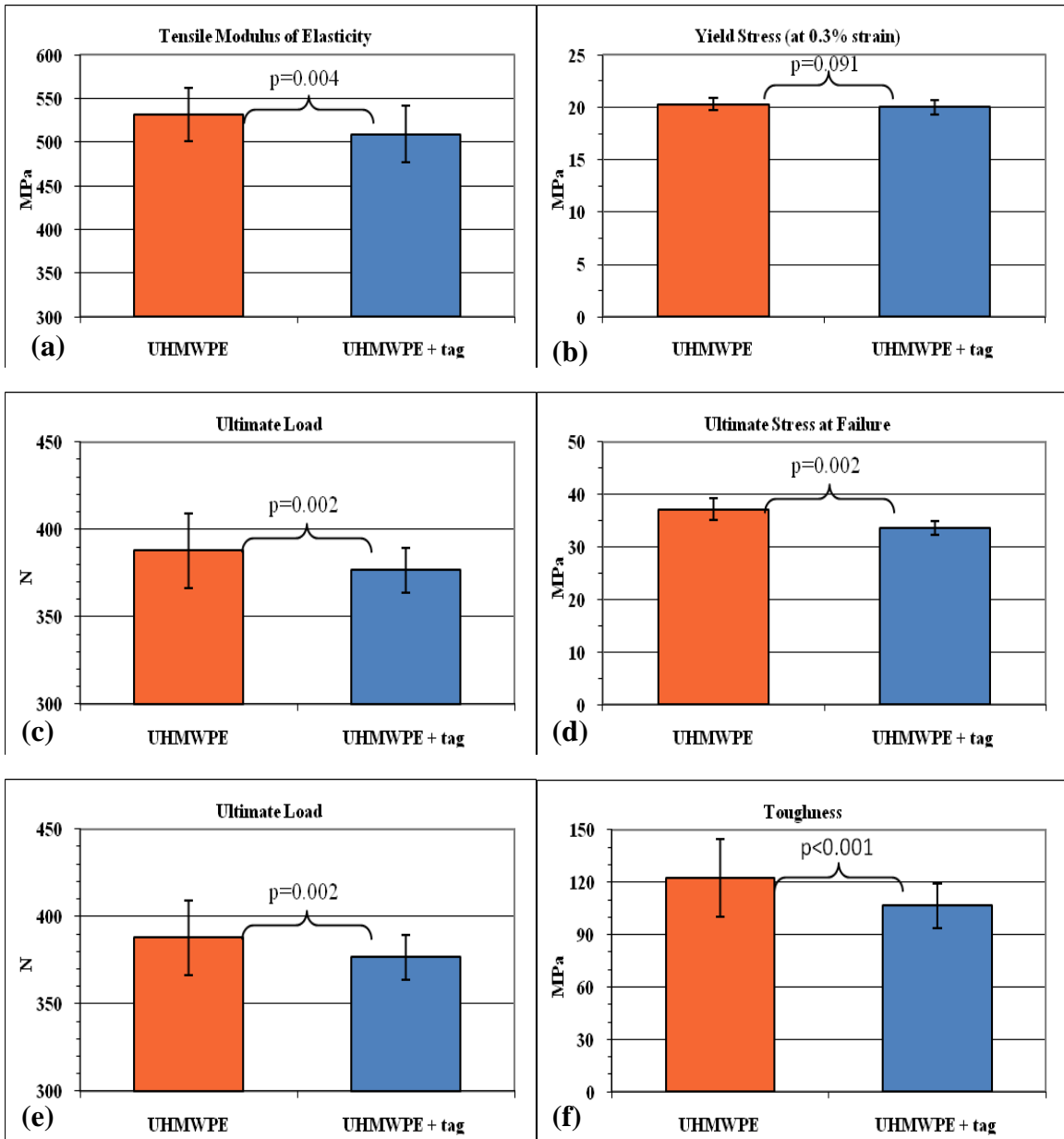
Figure A-2: Results of tensile test (a) Modulus of Elasticity [MPa] (b) Yield Stress at 3% Strain [MPa], (c) Ultimate Stress at Failure [MPa], (d) Ultimate Strain (%), (e) Ultimate Load [N], and (f) Toughness [MPa]
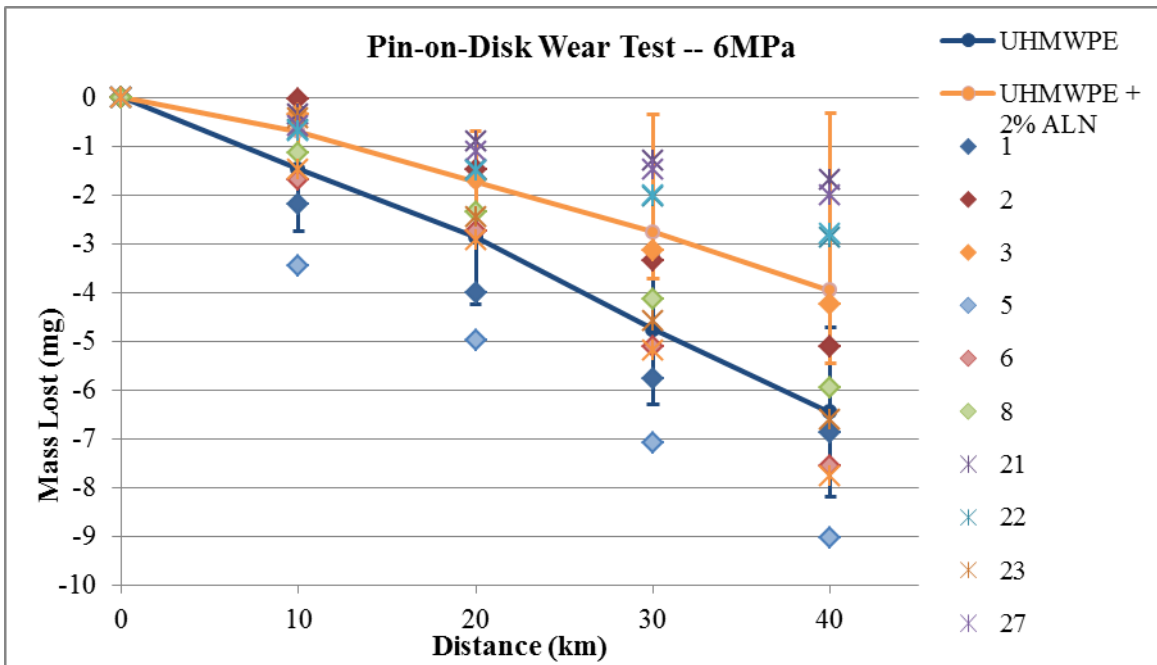
Figure A-3: Average change in gravimetric weights over 40km OrthoPod trial (6MPa contact pressure) with all individual points superimposed

Additional Images of OrthoPOD pins from Functional Drug Elution Experiment
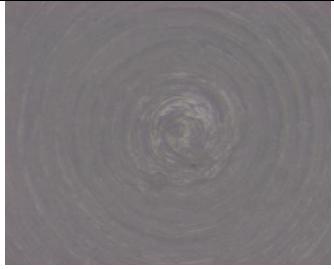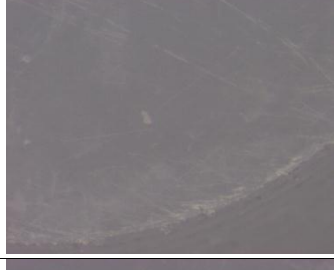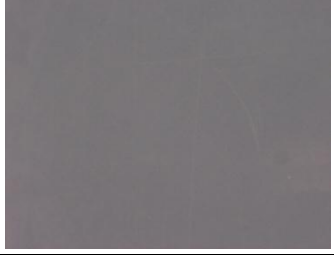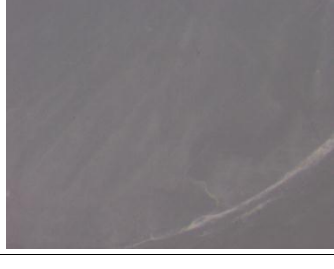
Included in this appendix are the additional images of the OrthoPOD pins (PE or PE-BP) and the diamond-coated CoCrMo countersurfaces used in the 40km OrthoPOD test of Aim 2. Pins 1, 2, 3, 5, 6, and 8 are PE-only pins (PE). Pins 21, 22, 23, 27, 28, and 29 are PE-BP pins.
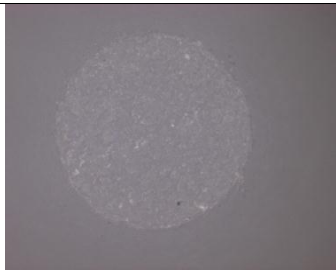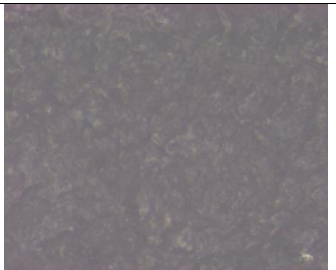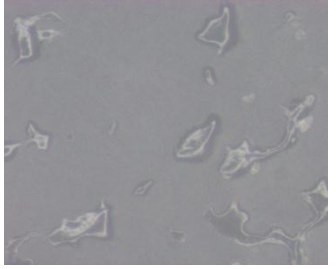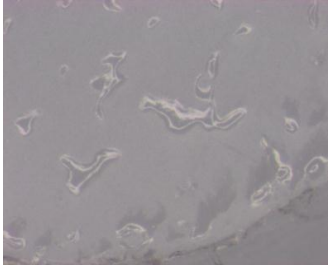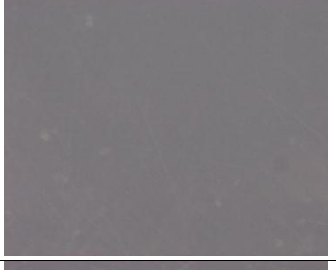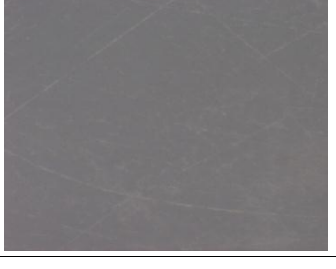
Figure B-1: Representative Images (4) of Diamond-like Coated CoCrMo disks used as the countersurface of the OrthoPOD experiment (Aim 2)

Table B-1: Microscope Images of each pin from the OrthoPOD 40km wear test presented in Aim 2
Pin 1 (PE)
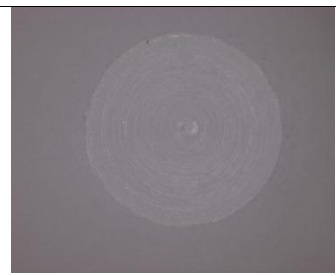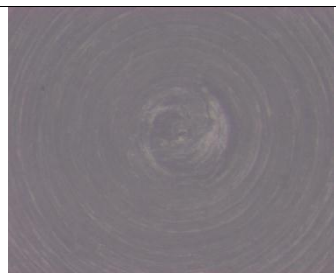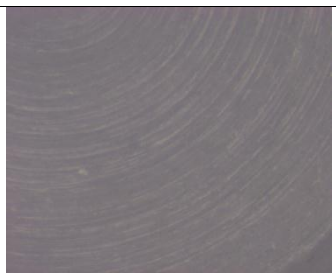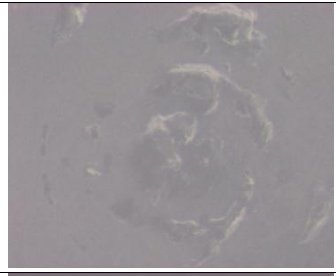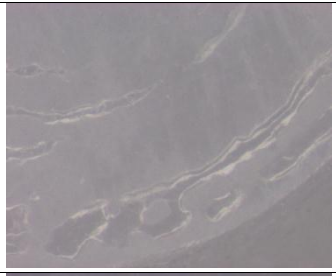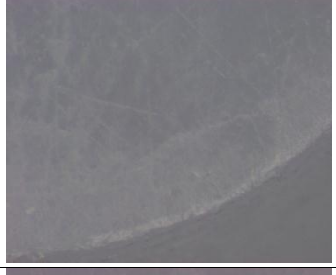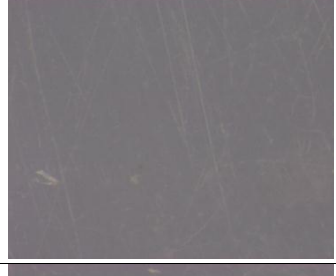
	12X	50X	50X
0km			
10km			
20km			
30km			
40km			

Pin 2 (PE)
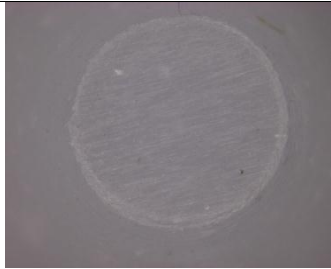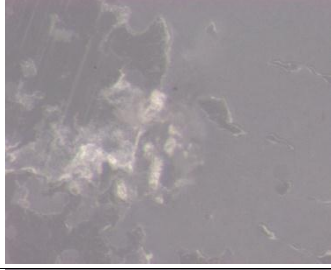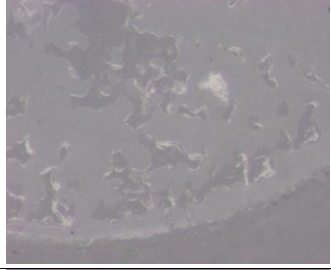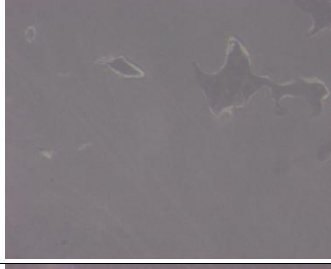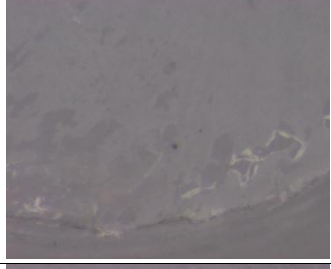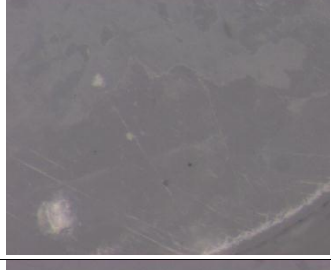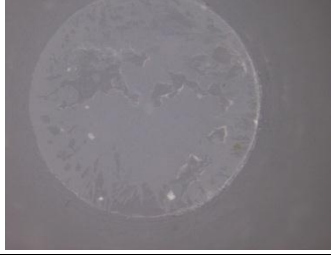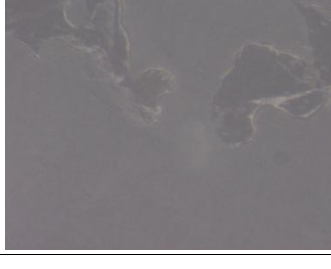
	12X	50X	50X
0km			
10km			
20km			
30km			
40km			

Pin 3 (PE)

	12X	50X	50X
0km			
10km			
20km			
30km			
40km			
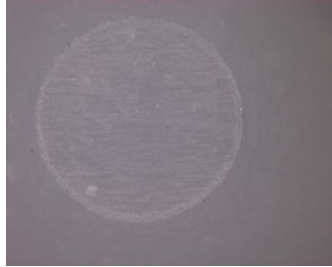
Pin 21 (PE-BP)
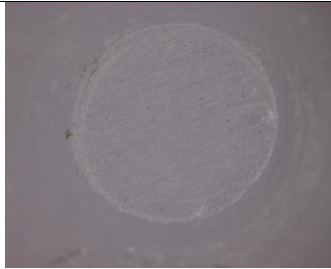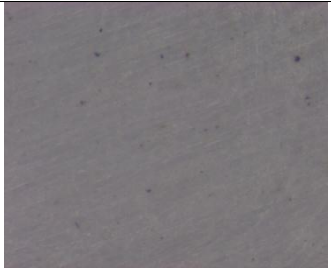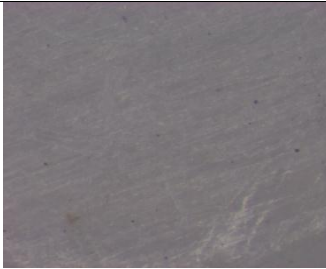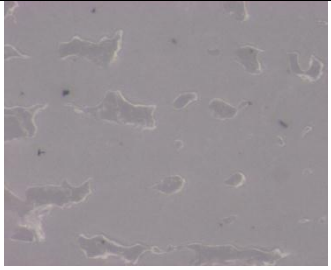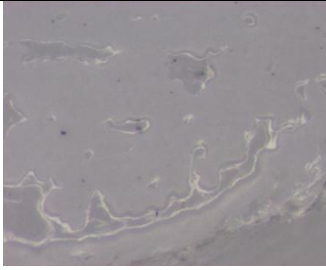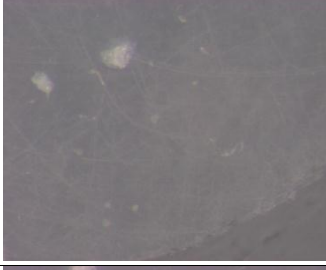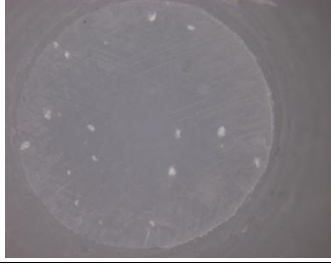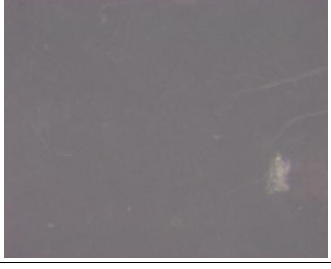
	12X	50X	50X
0km			
10km			
20km			
30km			
40km			
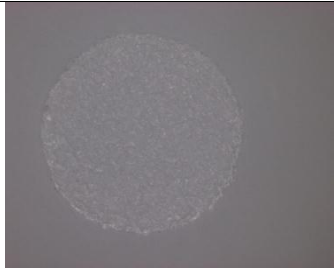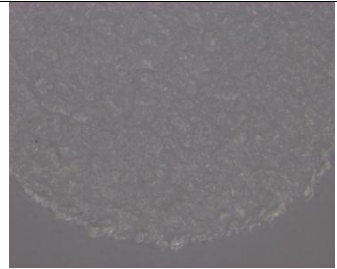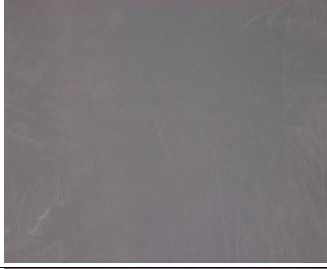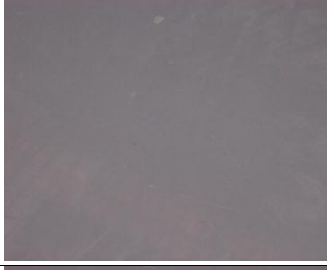
Pin 22 (PE-BP)

	12X	50X	50X
0km			
10km			
20km			
30km			
40km			
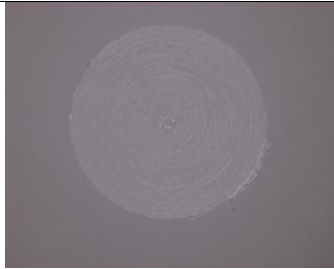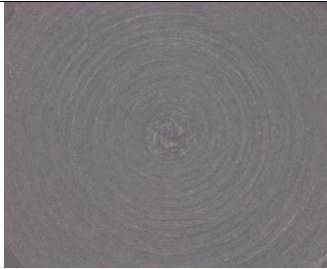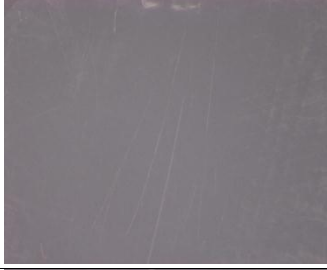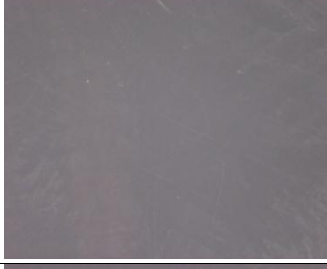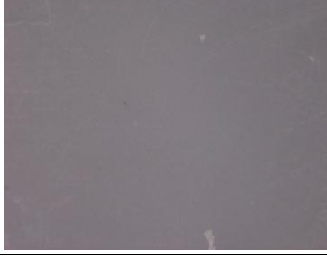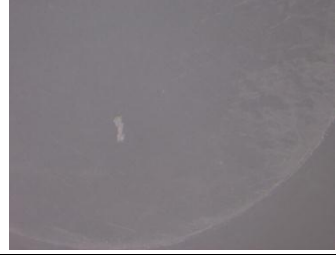
Pin 23 (PE-BP)

	12X	50X	50X
0km			
10km			
20km			
30km			
40km			
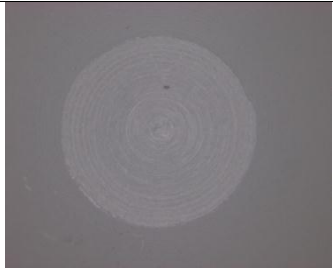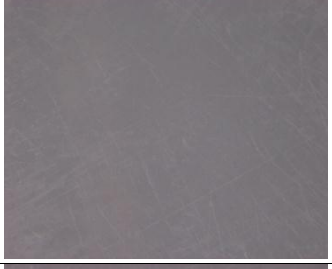
Pin 5 (PE)

	12X	25X	25X
0km			
10km			
20km			
30km			
40km			
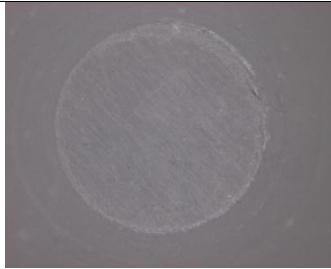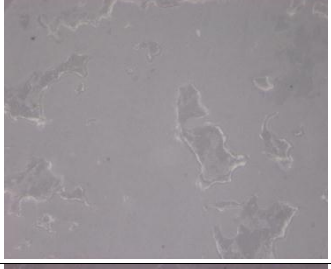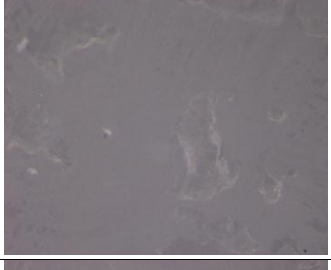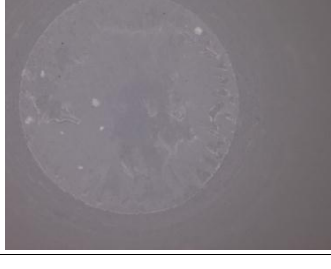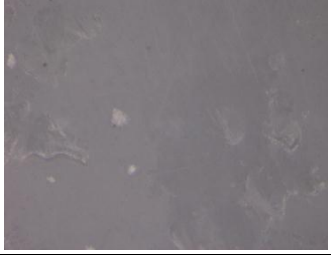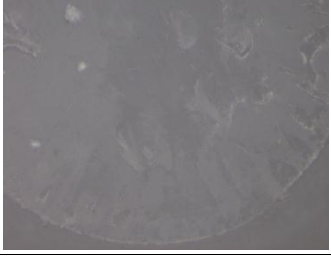
Pin 6 (PE)

	12X	25X	25X
0km			
10km			
20km			
30km			
40km			

Pin 8 (PE)
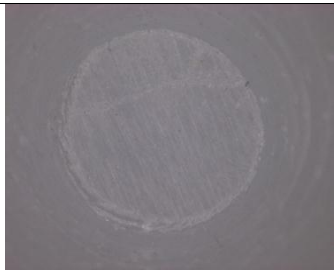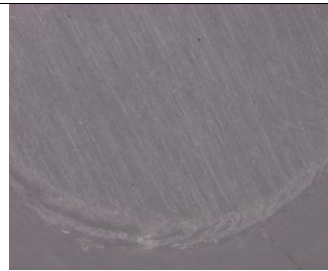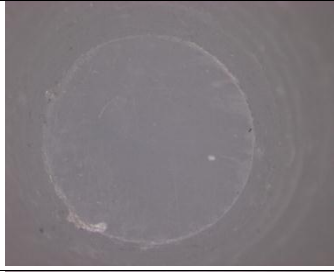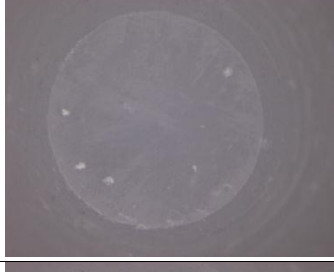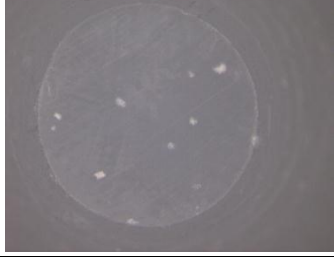
	12X	25X	25X
0km			
10km			
20km			
30km			
40km			

Pin 27 (PE-BP)
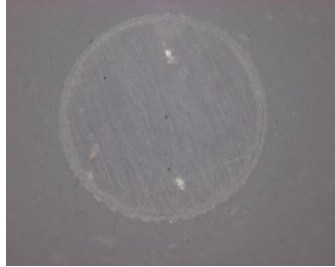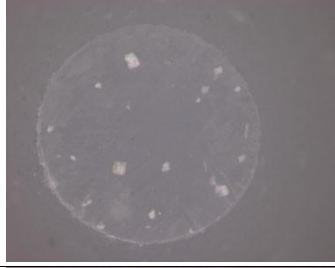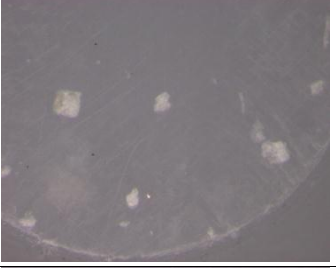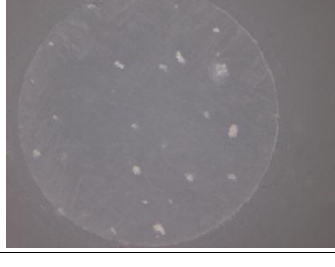
	12X	25X	25X
0km			
10km			
20km			
30km			
40km			

Pin 28 (PE-BP)

	12X	25X	25X
0km			
10km			
20km			
30km			
40km			

Pin 29 (PE-BP)

	12X	25X	25X
0km			
10km			
20km			
30km			
40km			

REFERENCES

1. Kurtz S, Ong K, Lau E, Mowat F, Halpern M. 2007. Projections of primary and revision hip and knee arthroplasty in the united states from 2005 to 2030. Journal of Bone and Joint Surgery-American Volume 89A: 780-785.

2. Fischer KJ, Vikoren THH, Ney S, et al. 2006. Mechanical evaluation of bone samples following alendronate thehrapy in healthy male dogs. Journal of Biomedical Materials Research - Part B Applied Biomaterials 76B: 143-48.

3. von Knoch F, Eckhardt C, Alabre CI, et al. 2007. Anabolic effects of bisphosphonates on peri-implant bone stock. Biomaterials 28: 3549-3559.

4. DeFrances CJ, Podgornik MN. 2006. 2004 National Hospital Discharge Survey. Advance Data . May 4;(371):1-19.

5. National Institute of Health. 2003. Total Knee Replacement. NIH Consensus and State-of-the-Science Statements. 20(1): 1-40.

6. Shanbhag AS, Rubash HE, Jacobs JJ. 2006. Joint Replacement and Bone Resorption, Taylor & Francis Group; 783 p.

7. Cook SD, Thomas KA, Haddad,R J,Jr. 1988. Histologic analysis of retrieved human porous-coated total joint components. Clinical Orthopaedics and Related Research. 234(1)90-101.

8. Oonishi H, Kadoya Y. 2000. Wear of high-dose gamma-irradiated polyethylene in total hip replacements. Journal of Orthopaedic Science: Official Journal of the Japanese Orthopaedic Association 5: 223-228.

9. Muratoglu OK, Bragdon CR, Jasty M, et al. 2004. Knee-simulator testing of conventional and cross-linked polyethylene tibial inserts. The Journal of Arthroplasty 19: 887-897.

10. Rand JA, Trousdale RT, Ilstrup DM, Harmsen WS. 2003. Factors affecting the durability of primary total knee prostheses. The Journal of Bone and Joint Surgery - American Volume 85-A: 259-265.

11. Vessely MB, Whaley AL, Harmsen WS, Schleck CD, Berry DJ. 2006. The Chitranjan Ranawat Award: Long-term survivorship and failure modes of 1000 cemented condylar total knee arthroplasties. Clinical Orthopaedics and Related Research 452: 28-34.

12. Mahoney OM, Kinsey TL. 2008. 5- to 9-year survivorship of single-radius, posterior-stabilized TKA. Clinical Orthopaedics and Related Research 466: 436-442.

13. Aglietti P, Buzzi R, De Felice R, Giron F. 1999. The insall-burstein total knee replacement in osteoarthritis: A 10-year minimum follow-up. The Journal of Arthroplasty 14: 560-565.

14. Oliver MC, Keast-Butler OD, Hinves BL, Shepperd JAN. 2005. A hydroxyapatite-coated insall-burstein II total knee replacement: 11-year results. The Journal Of Bone And Joint Surgery - British Volume 87: 478-482.

15. Attar FG, Khaw F, Kirk LMG, Gregg PJ. 2008. Survivorship analysis at 15 years of cemented press-fit condylar total knee arthroplasty. The Journal of Arthroplasty 23: 344-349.

16. Duffy GP, Murray BE, Trousdale RR. 2007. Hybrid total knee arthroplasty analysis of component failures at an average of 15 years. The Journal of Arthroplasty 22: 1112-1115.

17. Granchi D, Cenni E, Tigani D, et al. 2008. Sensitivity to implant materials in patients with total knee arthroplasties. Biomaterials 29: 1494-1500.

18. Chesney D, Sales J, Elton R, Brenkel IJ. 2008. Infection after knee arthroplasty a prospective study of 1509 cases. The Journal of Arthroplasty 23: 355-359.

19. Charnley J. 1975. Fracture of femoral prostheses in total hip replacement. A clinical study. Clinical Orthopaedics and Related Research 105-120.

20. Harris WH, Schiller AL, Scholler JM, Freiberg RA, Scott R. 1976. Extensive localized bone resorption in the femur following total hip replacement. The Journal of Bone and Joint Surgery - American Volume 58: 612-618.

21. Willert HG. 1977. Reactions of the articular capsule to wear products of artificial joint prostheses. Journal Of Biomedical Materials Research 11: 157-164.

22. Howie DW, Vernon-Roberts B, Oakeshott R, Manthey B. 1988. A rat model of resorption of bone at the cement-bone interface in the presence of polyethylene wear particles. Journal of Bone and Joint Surgery - American Volume 70: 257-63.

23. Goodman SB, Fornasier VL, Kei J. 1991. Quantitative comparison of the histological effects of particulate polymethylmethacrylate versus polyethylene in the rabbit tibia. Archives of Orthopaedic and Trauma Surgery 110: 123-126.

24. Pizzoferrato A, Ciapetti G, Stea S, Toni A. 1991. Cellular events in the mechanisms of prosthesis loosening. Clinical Materials 7: 51-81.

25. Bullough PG, DiCarlo EF, Hansraj KK, Neves MC. 1988. Pathologic studies of total joint replacement. The Orthopedic Clinics of North America 19: 611-625.

26. Al-Saffar N, Kadoya Y, Revell P. 1994. Role of newly formed vessels and cell adhesion molecules in the tissue response to wear products from orthopaedic implants. Journal of Materials Science - Materials in Medicine 5: 813-818.

27. Ingham E, Fisher J. 2005. The role of macrophages in osteolysis of total joint replacement. Biomaterials 26: 1271-1286.

28. Xu JW, Konttinen YT, Lassus J, et al. 1996. Tumor necrosis factor-alpha (TNF-alpha) in loosening of total hip replacement (THR). Clinical and Experimental Rheumatology 14: 643-648.

29. Kim KJ, Rubash HE, Wilson SC, D'Antonio JA, McClain EJ. 1993. A histologic and biochemical comparison of the interface tissues in cementless and cemented hip prostheses. Clinical Orthopaedics and Related Research 142-152.

30. Sabokbar A, Rushton N. 1995. Role of inflammatory mediators and adhesion molecules in the pathogenesis of aseptic loosening in total hip arthroplasties. The Journal of Arthroplasty 10: 810-816.

31. Xu JW, Li TF, Partsch G, et al. 1998. Interleukin-11 (IL-11) in aseptic loosening of total hip replacement (THR). Scandinavian Journal of Rheumatology 27: 363-367.

32. Al-Saffar N, Khwaja HA, Kadoya Y, Revell PA. 1996. Assessment of the role of GM-CSF in the cellular transformation and the development of erosive lesions around orthopaedic implants. American Journal of Clinical Pathology 105: 628-639.

33. Schmalzried TP, Callaghan JJ. 1999. Wear in total hip and knee replacements. The Journal of Bone and Joint Surgery - American Volume 81: 115-136.

34. Parasnis NC, Ramani K. 1998. Analysis of the effect of pressure on compression moulding of UHMWPE. Journal of Materials Science - Materials in Medicine 9: 165-172.

35. Komistek RD, Kane TR, Mahfouz M, Ochoa JA, Dennis DA. 2005. Knee mechanics: A review of past and present techniques to determine in vivo loads. Journal of Biomechanics 38: 215-228.

36. Burny F, Donkerwolcke M, Moulart F, et al. 2000. Concept, design and fabrication of smart orthopedic implants. Medical Engineering & Physics 22: 469-479.

37. Komistek RD, Stiehl JB, Dennis DA, Paxson RD, Soutas-Little RW. 1998. Mathematical model of the lower extremity joint reaction forces using kane's method of dynamics. Journal of Biomechanics 31: 185-189.

38. Morrison JB. 1970. Mechanics of knee joint in relation to normal walking. Journal of Biomechanics 3(1): 51-64.

39. Wimmer MA, Andriacchi TP. 1997. Tractive forces during rolling motion of the knee: Implications for wear in total knee replacement. Journal of Biomechanics 30: 131-137.

40. Seireg A, Arvikar RJ. 1973. Mathematical model for evaluation of forces in lower extremities of musculoskeletal system. Journal of Biomechanics 6(3): 323-326.

41. Taylor SJG, Walker PS, Perry JS, Cannon SR, Woledge R. 1998. The forces in the distal femur and the knee during walking and other activities measured by telemetry. Journal of Arthroplasty 13: 428-437.

42. Taylor SJG, Walker PS. 2001. Forces and moments telemetered from two distal femoral replacements during various activities. Journal of Biomechanics 34: 839-848.

43. Seireg A, Arvikar RJ. 1975. Prediction of muscular load sharing and joint forces in lower-extremities during walking. Journal of Biomechanics 8: 89-102.

44. Anderson FC, Pandy MG. 2001. Dynamic optimization of human walking. Journal of Biomechanical Engineering-Transactions of the ASME 123: 381-390.

45. Stewart T, Jin ZM, Shaw D, et al. 1995. Experimental and theoretical study of the contact mechanics of five total knee joint replacements. Proceedings of the Institution of Mechanical Engineers - Part H, Journal of Engineering in Medicine 209: 225-231.

46. Collier MB, Engh Jr. CA, McAuley JP, Engh GA. 2007. Factors associated with the loss of thickness of polyethylene tibial bearings after knee arthroplasty. Journal of Bone and Joint Surgery - American Volume 89: 1306-1314.

47. Argenson JN, O'Connor JJ. 1992. Polyethylene wear in meniscal knee replacement. A one to nine-year retrieval analysis of the oxford knee. The Journal of Bone and Joint Surgery - British Volume 74: 228-232.

48. Cornwall GB, Bryant JT, Hansson CM. 2001. The effect of kinematic conditions on the wear of ultra-high molecular weight polyethylene (UHMWPE) in orthopaedic bearing applications. Proceedings of the Institution of Mechanical Engineers - Part H, Journal of Engineering in Medicine 215: 95-106.

49. McGloughlin TM, Kavanagh AG. 2000. Wear of ultra-high molecular weight polyethylene (UHMWPE) in total knee prostheses: A review of key influences. Proceedings of the Institution of Mechanical Engineers - Part H, Journal of Engineering in Medicine 214: 349-359.

50. Saikko V, Calonius O, Keränen J. 2001. Effect of counterface roughness on the wear of conventional and crosslinked ultrahigh molecular weight polyethylene studied with a multi-directional motion pin-on-disk device. Journal of Biomedical Materials Research 57: 506-512.

51. Cooper JR, Dowson D, Fisher J. 1993. Effect of transfer film and surface roughness on the wear of lubricated ultra-high molecular weight polyethylene. Clinical Materials 14: 295-302.

52. Cooper JR, Dowson D, Fisher J. 1993. Macroscopic and microscopic wear mechanisms in ultra-high molecular weight polyethylene. Wear 162-64: 378-384.

53. Kernick M, Allen C. 1997. Sliding wear of UHMWPE against zirconia in saline containing proteins. Wear 203-204: 537-543.

54. Besong AA, Tipper JL, Mathews BJ, et al. 1999. The influence of lubricant on the morphology of ultra-high molecular weight polyethylene wear debris generated in laboratory tests. Proceedings of the Institution of Mechanical Engineers - Part H, Journal of Engineering in Medicine 213: 155-158.

55. Ahlroos T, Saikko V. 1997. Wear of prosthetic joint materials in various lubricants. Wear 211: 113-119.

56. Bell J, Besong AA, Tipper JL, et al. 2000. Influence of gelatin and bovine serum lubricants on ultra-high molecular weight polyethylene wear debris generated in in vitro simulations. Proceedings of the Institution of Mechanical Engineers - Part H, Journal of Engineering in Medicine 214: 513-18.

57. International Organization for Standardization. 1997. Implants for surgery – Wear of total knee joint prostheses – Part 1: Loading and displacement parameters for wear testing machines with load control and corresponding environmental conditions for tests. ISO 14243-1.

58. International Organization for Standardization. 2000. Implants for surgery – Wear of total knee joint prostheses – Part 3: Loading and displacement parameters for wear testing machines with displacement control and corresponding environmental conditions for tests. ISO 14243-3.

59. Bigsby RJA, Hardaker CS, Fisher J. 1997. Wear of ultra-high molecular weight polyethylene acetabular cups in a physiological hip joint simulator in the anatomical position using bovine serum as a lubricant. Proceedings of the Institution of Mechanical Engineers - Part H, Journal of Engineering in Medicine 211: 265-269.

60. Joyce TJ, Vandelli C, Cartwright T, Unsworth A. 2001. A comparison of the wear of cross-linked polyethylene against itself under reciprocating and multi-directional motion with different lubricants. Wear 250: 206-211.

61. Benson LC, DesJardins JD, LaBerge M. 2001. Effects of in vitro wear of machined and molded UHMWPE tibial inserts on TKR kinematics. Journal of Biomedical Materials Research 58: 496-504.

62. Gevaert MR, LaBerge M, Gordon JM, DesJardins JD. 2005. The quantification of physiologically relevant cross-shear wear phenomena on orthopedic bearing materials using the MAX-shear wear testing system. Journal of Tribology - Transactions of the ASME 127: 740-749.

63. Aurora A, DesJardins JD, Joseph PF, LaBerge M. 2006. Effect of lubricant composition on the fatigue properties of ultra-high molecular weight polyethylene for total knee replacement. Proceedings of the Institution of Mechanical Engineers - Part H, Journal of Engineering in Medicine 220: 541-551.

64. DesJardins J, Aurora A, Tanner SL, et al. 2006. Increased total knee arthroplasty ultra-high molecular weight polyethylene wear using a clinically relevant hyaluronic acid simulator lubricant. Proceedings of the Institution of Mechanical Engineers - Part H,- Journal of Engineering in Medicine 220: 609-623.

65. Wasielewski RC, Galante JO, Leighty RM, Natarajan RN, Rosenberg AG. 1994. Wear patterns on retrieved polyethylene tibial inserts and their relationship to technical considerations during total knee arthroplasty. Clinical Orthopaedics and Related Research 299: 31-43.

66. Sauer WL, Anthony ME. 1998. Predicting the clinical wear performance of orthopaedic bearing surfaces. In: Jacobs JJ, Craig TL editors. Alternative bearing surfaces in total joint replacement, ASTM STP 1346, American Society for Testing and Materials; p 1-29.

67. Kurtz SM, Muratoglu OK, Evans M, Edidin AA. 1999. Advances in the processing, sterilization, and crosslinking of ultra-high molecular weight polyethylene for total joint arthroplasty. Biomaterials 20: 1659-1688.

68. McKellop H, Clarke I, Markolf K, Amstutz H. 1981. Friction and wear properties of polymer, metal, and ceramic prosthetic joint materials evaluated on a multichannel screening device. Journal of Biomedical Materials Research 15: 619-653.

69. Wright TM, Bartel DL. 1986. The problem of surface damage in polyethylene total knee components. Clinical Orthopaedics and Related Research 205: 67-74.

70. Wright TM, Rimnac CM, Faris PM, Bansal M. 1988. Analysis of surface damage in retrieved carbon fiber-reinforced and plain polyethylene tibial components from posterior stabilized total knee replacements. Journal of Bone and Joint Surgery - American Volume 70A: 1312-1319.

71. Wright TM, Astion DJ, Bansal M, et al. 1988. Failure of carbon fiber-reinforced polyethylene total knee-replacement components - a report of 2 cases. Journal of Bone and Joint Surgery - American Volume 70A: 926-932.

72. Chowdhury SKR, Mishra A, Pradhan B, Saha D. 2004. Wear characteristic and biocompatibility of some polymer composite acetabular cups. Wear 256: 1026-1036.

73. Galetz MC, Blass T, Ruckdaschel H, et al. 2007. Carbon nanofibre-reinforced ultrahigh molecular weight polyethylene for tribological applications. Journal of Applied Polymer Science 104: 4173-4181.

74. Mosleh M, Suh NP, Arinez J. 1998. Manufacture and properties of a polyethylene homocomposite. Composites Part A - Applied Science and Manufacturing 29: 611-617.

75. Suh NP, Mosleh M, Arinez J. 1998. Tribology of polyethylene homocomposites. Wear 214: 231-236.

76. Marais C, Feillard P. 1992. Manufacturing and mechanical characterization of unidirectional polyethylene-fiber polyethylene-matrix composites. Composites Science and Technology 45: 247-255.

77. Alei PE, Suh NP. 1986. Ultra tough plastic material. U.S. Patent 4,600,631. filed May 1, 1984, and issued July 15, 1986.

78. Deng M, Shalaby SW. 1997. Properties of self-reinforced ultra-high-molecular-weight polyethylene composites. Biomaterials 18: 645-655.

79. Ries MD, Weaver K, Rose RM, et al. 1996. Fatigue strength of polyethylene after sterilization by gamma irradiation or ethylene oxide. Clinical Orthopaedics and Related Research 333: 87-95.

80. Sauer WL, Weaver KD, Beals NB. 1996. Fatigue performance of ultra-high-molecular-weight polyethylene: Effect of gamma radiation sterilization. Biomaterials 17: 1929-1935.

81. Shibata N, Tomita N, Onmori N, Kato K, Ikeuchi K. 2003. Defect initiation at subsurface grain boundary as a precursor of delamination in ultrahigh molecular weight polyethylene. Journal of Biomedical Materials Research - Part A 67: 276-284.

82. Oral E, Christensen SD, Malhi AS, Wannomae KK, Muratoglu OK. 2006. Wear resistance and mechanical properties of highly cross-linked, ultrahigh-molecular weight polyethylene doped with vitamin E. The Journal of Arthroplasty 21: 580-591.

83. Oral E, Wannomae KK, Rowell SL, Muratoglu OK. 2006. Migration stability of alpha-tocopherol in irradiated UHMWPE. Biomaterials 27: 2434-2439.

84. Oral E, Rowell SL, Muratoglu OK. 2006. The effect of alpha-tocopherol on the oxidation and free radical decay in irradiated UHMWPE. Biomaterials 27: 5580-5587.

85. Renò F, Bracco P, Lombardi F, et al. 2004. The induction of MMP-9 release from granulocytes by vitamin E in UHMWPE. Biomaterials 25: 995.

86. Renò F, Cannas M. 2006. UHMWPE and vitamin E bioactivity: An emerging perspective. Biomaterials 27: 3039-3043.

87. Bracco P, Oral E. 2011. Vitamin E-stabilized UHMWPE for total joint implants: A review. Clinical Orthopaedics and Related Research 469: 2286-2293.

88. Pesakova V, Klezl Z, Balik K, Adam M. 2000. Biomechanical and biological properties of the implant material carbon-carbon composite covered with pyrolytic carbon. Journal of Materials Science - Materials in Medicine 11: 793-798.

89. Howling GI, Sakoda H, Antonarulrajah A, et al. 2003. Biological response to wear debris generated in carbon based composites as potential bearing surfaces for artificial hip joints. Journal of Biomedical Materials Research - Part B, Applied Biomaterials 67B: 758-764.

90. Green TR, Fisher J, Stone M, Wroblewski BM, Ingham E. 1998. Polyethylene particles of a 'critical size' are necessary for the induction of cytokines by macrophages in vitro. Biomaterials 19: 2297-2302.

91. Matthews JB, Besong AA, Green TR, et al. 2000. Evaluation of the response of primary human peripheral blood mononuclear phagocytes to challenge with in vitro generated clinically relevant UHMWPE particles of known size and dose. Journal of Biomedical Materials Research 52: 296-307.

92. Howling GI, Ingham E, Sakoda H, et al. 2004. Carbon-carbon composite bearing materials in hip arthroplasty: Analysis of wear and biological response to wear debris. Journal of Materials Science - Materials in Medicine 15: 91-98.

93. Teoh SH, Tang ZG, Ramakrishna S. 1999. Development of thin elastomeric composite membranes for biomedical applications. Journal of Materials Science - Materials in Medicine 10: 343-352.

94. Tang ZG, Teoh SH, McFarlane W, Poole-Warren LA, Umezu M. 2002. In vitro calcification of UHMWPE/PU composite membrane. Materials Science & Engineering - Part C, Biomimetic and Supramolecular Systems 20: 149-152.

95. Wang M, Joseph R, Bonfield W. 1998. Hydroxyapatite-polyethylene composites for bone substitution: Effects of ceramic particle size and morphology. Biomaterials 19: 2357-2366.

96. Wang M, Bonfield W. 2001. Chemically coupled hydroxyapatite-polyethylene composites: Structure and properties. Biomaterials 22: 1311-1320.

97. Wang M, Chandrasekaran M, Bonfield W. 2002. Friction and wear of hydroxyapatite reinforced high density polyethylene against the stainless steel counterface. Journal of Materials Science - Materials in Medicine 13: 607-611.

98. Roeder RK, Sproul MM, Turner CH. 2003. Hydroxyapatite whiskers provide improved mechanical properties in reinforced polymer composites. Journal of Biomedical Materials Research - Part A 67A: 801-812.

99. Fang LM, Leng Y, Gao P. 2005. Processing of hydroxyapatite reinforced ultrahigh molecular weight polyethylene for biomedical applications. Biomaterials 26: 3471-3478.

100. Fang LM, Leng Y, Gao P. 2006. Processing and mechanical properties of HA/UHMWPE nanocomposites. Biomaterials 27: 3701-3707.

101. Fang LM, Gao P, Leng Y. 2007. High strength and bioactive hydroxyapatite nano-particles reinforced ultrahigh molecular weight polyethylene. Composites - Part B, Engineering 38: 345-351.

102. Premnath V, Harris WH, Jasty M, Merrill EW. 1996. Gamma sterilization of UHMWPE articular implants: An analysis of the oxidation problem. Biomaterials 17: 1741-1753.

103. Reeves EA, Barton DC, FitzPatrick DP, Fisher J. 2000. Comparison of gas plasma and gamma irradiation in air sterilization on the delamination wear of the ultra-high molecular weight polyethylene used in knee replacements. Proceedings of the Institution of Mechanical Engineers - Part H, Journal of Engineering in Medicine 214: 249-255.

104. Fisher J, McEwen HMJ, Barnett PI, et al. 2004. Influences of sterilizing techniques on polyethylene wear. Knee 11: 173-176.

105. Fisher J, Reeves EA, Isaac GH, Saum KA, Sanford WM. 1997. Comparison of the wear of aged and non-aged ultrahigh molecular weight polyethylene sterilized by gamma irradiation and by gas plasma. Journal of Materials Science - Materials in Medicine 8: 375-378.

106. Urban JA, Collier MB, Engh CA, Engh GA. 2006. Relationship between product demand, tibial polyethylene insert shelf age, and total knee arthroplasty survival - retrospective review of total knees of one design. Journal of Arthroplasty 21: 330-337.

107. Shen FW, McKellop HA. 2002. Interaction of oxidation and crosslinking in gamma-irradiated ultrahigh molecular-weight polyethylene. Journal of Biomedical Materials Research 61: 430-439.

108. Talmo CT, Shanbhag AS, Rubash HE. 2006. Nonsurgical management of osteolysis: Challenges and opportunities. Clinical Orthopaedics and Related Research 453: 254-264.

109. Schmalzried TP, Campbell P, Schmitt AK, Brown IC, Asmtutz HC. 1997. Shape and dimensional characteristics of polyethylene wear particles generated in vivo by total knee replacements compared to total hip replacements. Journal of Biomedical Materials Research - Part B, Applied Biomaterials 38: 203-10.

110. Shanbhag AS, Jacobs JJ, Glant TT, et al. 1994. Composition and morphology of wear debris in failed uncemented total hip replacement. The Journal of Bone and Joint Surgery - British Volume 76: 60-67.

111. Jacobs JJ, Roebuck KA, Archibeck M, Hallab NJ, Glant TT. 2001. Osteolysis: Basic science. Clinical Orthopaedics and Related Research 393: 71-77.

112. Shi Wei, Kitaura H, Ping Zhou, Ross FP, Teitelbaum SL. 2005. IL-1 mediates TNF-induced osteoclastogenesis. Journal of Clinical Investigation 115: 282-290.

113. Goodman SB, Song Y, Chun L, Regula D, Aspenberg P. 1999. Effects of TGFbeta on bone ingrowth in the presence of polyethylene particles. The Journal of Bone and Joint Surgery - British Volume 81: 1069-1075.

114. Sumner DR, Turner TM, Purchio AF, et al. 1995. Enhancement of bone ingrowth by transforming growth factor-beta. The Journal of Bone and Joint Surgery - American Volume 77: 1135-1147.

115. Childs L.M., Paschalis E.P., Xing L., et al. 2002. In vivo RANK signaling blockade using the receptor activator of NF-kappaB:Fc effectively prevents and ameliorates wear debris-induced osteolysis via osteoclast depletion without inhibiting osteogenesis. Journal of Bone and Mineral Research 17: 192-9.

116. von Knoch F, Heckelei A, Wedemeyer C, et al. 2005. Suppression of polyethylene particle-induced osteolysis by exogenous osteoprotegerin. Journal of Biomedical Materials Research - Part A 75: 288-294.

117. Childs LM, Goater JJ, O'Keefe RJ, Schwarz EM. 2001. Efficacy of etanercept for wear debris-induced osteolysis. Journal Of Bone And Mineral Research: The Official Journal of the American Society for Bone and Mineral Research 16: 338-347.

118. Schwarz EM, Campbell D, Totterman S, et al. 2003. Use of volumetric computerized tomography as a primary outcome measure to evaluate drug efficacy in the prevention of peri-prosthetic osteolysis: A 1-year clinical pilot of etanercept vs. placebo. Journal of Orthopaedic Research 21: 1049.

119. Francis MD, Graham R, Russell G, Fleisch H. 1969. Diphosphonates inhibit hydroxyapatite dissolution in vitro and bone resorption in tissue culture and in vivo. Science 165: 1262-64.

120. Francis MD. 1969. The inhibition of calcium hydroxyapatite crystal growth by polyphosphonates and polyphosphates. Calcified Tissue International 3: 151-62.

121. Fleisch H, Graham R, Russell G, Francis MD. 1969. Diphosphonates inhibit hydroxyapatite dissolution in vitro and bone. Science 165: 1262-64.

122. Ralston SH, Hacking L, Willocks L, Bruce F, Pitkeathly DA. 1989. Clinical, biochemical, and radiographic effects of aminohydroxypropylidene bisphosphonate treatment in rheumatoid arthritis. Annals of the Rheumatic Diseases 48: 396-399.

123. Eggelmeijer F, Papapoulos SE, van Paassen HC, Dijkmans BA, Breedveld FC. 1994. Clinical and biochemical response to single infusion of pamidronate in patients with active rheumatoid arthritis: A double blind placebo controlled study. The Journal of Rheumatology 21: 2016-2020.

124. Lala R, Matarazzo P, Bertelloni S, et al. 2000. Pamidronate treatment of bone fibrous dysplasia in nine children with McCune-albright syndrome. Acta Paediatrica 89: 188-193.

125. Lane JM, Khan SN, O'Connor WJ, et al. 2001. Bisphosphonate therapy in fibrous dysplasia. Clinical Orthopaedics and Related Research 6-12.

126. Bembi B, Parma A, Bottega M, et al. 1997. Intravenous pamidronate treatment in osteogenesis imperfecta. The Journal of Pediatrics 131: 622-625.

127. Fujiwara I, Ogawa E, Igarashi Y, Ohba M, Asanuma A. 1998. Intravenous pamidronate treatment in osteogenesis imperfecta. European Journal of Pediatrics 157: 261.

128. Åström E, Söderhäll S. 1998. Beneficial effect of bisphosphonate during five years of treatment of severe osteogenesis imperfecta. Acta Paediatrica 87: 64-68.

129. Lehmann HJ, Mouritzen U, Christgau S, Cloos PAC, Christiansen C. 2002. Effect of bisphosphonates on cartilage turnover assessed with a newly developed assay for collagen type II degradation products. Annals of the Rheumatic Diseases 61: 530-533.

130. Maksymowych WP. 2003. Bisphosphonates for arthritis--a confusing rationale. The Journal of Rheumatology 30: 430-434.

131. Merck & Co, Inc. 2011. Fosamax prescribing information: http://www.merck.com/product/usa/pi_circulars/f/fosamax/fosamax_pi.pdf. Accessed December 1, 2011.

132. Shanbhag AS, Hasselman CT, Rubash HE. 1997. The John Charnley Award. Inhibition of wear debris mediated osteolysis in a canine total hip arthroplasty model. Clinical Orthopaedics and Related Research 344: 33-43.

133. Yamakawa I, Kawahara M, Watanabe S, Miyake Y. 1990. Sustained release of insulin by double-layered implant using poly(D,L-lactic acid). Journal of Pharmaceutical Sciences 79: 505-509.

134. Pistel KF, Bittner B, Koll H, Winter G, Kissel T. 1999. Biodegradable recombinant human erythropoietin loaded microspheres prepared from linear and star-branched block copolymers: Influence of encapsulation technique and polymer composition on particle characteristics. Journal of Controlled Release: Official Journal of the Controlled Release Society 59: 309-325.

135. Jones DH, Corris S, McDonald S, Clegg JC, Farrar GH. 1997. Poly(DL-lactide-co-glycolide)-encapsulated plasmid DNA elicits systemic and mucosal antibody responses to encoded protein after oral administration. Vaccine 15: 814-817.

136. Bodmeier R, McGinity JW. 1987. The preparation and evaluation of drug-containing poly(dl-lactide) microspheres formed by the solvent evaporation method. Pharmaceutical Research 4: 465-471.

137. Alex R, Bodmeier R. 1990. Encapsulation of water-soluble drugs by a modified solvent evaporation method. I. effect of process and formulation variables on drug entrapment. Journal of Microencapsulation 7: 347-355.

138. Weidenauer U, Bodmer D, Kissel T. 2003. Microencapsulation of hydrophilic drug substances using biodegradable polyesters. part I: Evaluation of different techniques for the encapsulation of pamidronate di-sodium salt. Journal of Microencapsulation 20: 509.

139. Weidenauer U, Bodmer D, Kissel T. 2004. Microencapsulation of hydrophilic drug substances using biodegradable polyesters. part II: Implants allowing controlled drug release -- a feasibility study using bisphosphonates. Journal of Microencapsulation 21: 137-149.

140. Kurtz S, Gawel H, Patel J. 2011. History and systematic review of wear and osteolysis outcomes for first-generation highly crosslinked polyethylene. Clinical Orthopaedics & Related Research 469: 2262-2277.

141. Im G, Sheeraz A, Qureshi JK, Rubash HE, AS Shanbhag. 2004. Osteoblast proliferation and maturation by bisphosphonates. Biomaterials 25: 4105-15.

142. Merck Index. 2006. Alendronic acid. Merck Index, 14th ed. John Wiley & Sons; p 42.

143. Bartel DL, Bicknell VL, Wright TM. 1986. The effect of conformity, thickness, and material on stresses in ultra-high molecular weight components for total joint replacement. The Journal of Bone and Joint Surgery - American Volume 68: 1041-1051.

144. Moreau MF, Guillet C, Massin P, et al. 2007. Comparative effects of five bisphosphonates on apoptosis of macrophage cells in vitro. Biochemical Pharmacology 73: 718-723.

145. Crossett L. 2006. Evolution of the low contact stress (LCS) complete knee system. Orthopedics 29: S17-S22.

146. Szivek JA, Anderson PL, Benjamin JB. 1996. Average and peak contact stress distribution evaluation of total knee arthroplasties. The Journal of Arthroplasty 11: 952-963.

147. Jalali-Vahid D, Jagatia M, Jin ZM, Dowson D. 2001. Prediction of lubricating film thickness in a ball-in-socket model with a soft lining representing human natural and artificial hip joints. Proceedings of the Institution of Mechanical Engineers - Part J, Journal of Engineering Tribology 215: 363-372.

148. Di Paolo J, Berli ME. 2006. Numerical analysis of the effects of material parameters on the lubrication mechanism for knee prosthesis. Computer Methods in Biomechanics & Biomedical Engineering 9: 79-89.

149. von Knoch F, Jaquiery C, Kowalsky M, et al. 2005. Effects of bisphosphonates on proliferation and osteoblast differentiation of human bone marrow stromal cells. Biomaterials 26: 6941-6949.

150. Rogers MJ. 2003. New insights into the molecular mechanisms of action of bisphosphonates. Current Pharmaceutical Design 9: 2643-2658.

151. Huk OL, Zukor DJ, Antoniou J, Petit A. 2003. Effect of pamidronate on the stimulation of macrophage TNF-α release by ultra-high-molecular-weight polyethylene particles: A role for apoptosis. Journal of Orthopaedic Research 21: 81.

152. Petit A, Mwale F, Antoniou J, Zukor DJ, Huk OL. 2006. Effect of bisphosphonates on the stimulation of macrophages by alumina ceramic particles: A comparison with ultra-high-molecular-weight polyethylene. Journal of Materials Science - Materials in Medicine 17: 667-673.

153. von Knoch M, Wedemeyer C, Pingsmann A, et al. 2005. The decrease of particle-induced osteolysis after a single dose of bisphosphonate. Biomaterials 26: 1803-1808.

154. Iwase M, Kim KJ, Kobayashi Y, Itoh M, Itoh T. 2002. A novel bisphosphonate inhibits inflammatory bone resorption in a rat osteolysis model with continuous infusion of polyethylene particles. Journal of Orthopaedic Research 20: 499-505.

155. Shanbhag A, Hasselman C, Rubash H. 1997. Inhibition of wear debris mediated osteolysis in a canine total hip arthroplasty model. Clinical Orthopaedics and Related Research 344: 33-43.

156. Han YHR, Qin XZ. 1996. Determination of alendronate sodium by ion chromatography with refractive index detection. Journal of Chromatography 719A: 345-352.

157. Cornelio RB, Pavei C, Verza SG, et al. 2009. Quantification of sodium alendronate by LC anion exchange using in line complexation. Journal of Liquid Chromatography & Related Technologies 32: 2857-2865.

158. Mabrey JD, Afar-Keshmiri A, Engh GA, et al. 2002. Standardized analysis of UHMWPE wear particles from failed total joint arthroplasties. Journal of Biomedical Materials Research - Part B, Applied Biomaterials 63: 475-83.

159. Kurtz SM editor. 2009. UHMWPE biomaterials handbook: Ultra high molecular weight polyethylene in total joint replacement and medical devices, 2nd ed. London: Academic Press; 568 p.

160. Kurtz SM. 2004. The UHMWPE handbook, Boston: Academic Press; 379 p.

161. Marcus R, Feldman, D, Kelsey J. 1996. Osteoporosis, San Diego: Academic Press; 1373p.